

เอ็นเอดีโคเนสจากข้าว *Oryza sativa* L. และเอนไซม์รีคอมบิแนนท์



นางสาวรัชชนก ดำริห์สุข

ศูนย์วิทยทรัพยากร
จุฬาลงกรณ์มหาวิทยาลัย

วิทยานิพนธ์นี้เป็นส่วนหนึ่งของการศึกษาคตามหลักสูตรปริญญาวิทยาศาสตรมหาบัณฑิต

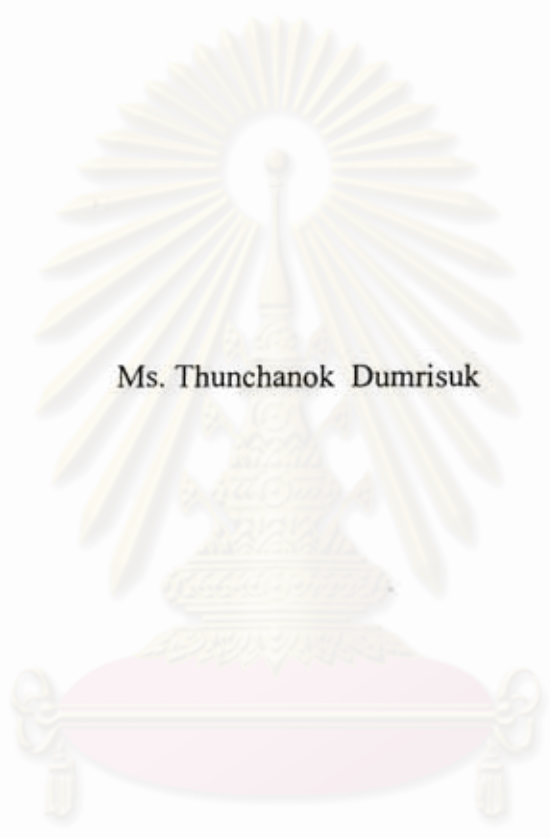
สาขาวิชาชีวเคมี ภาควิชาชีวเคมี

คณะวิทยาศาสตร์ จุฬาลงกรณ์มหาวิทยาลัย

ปีการศึกษา 2552

ลิขสิทธิ์ของจุฬาลงกรณ์มหาวิทยาลัย

NAD KINASE FROM RICE *Oryza sativa* L. AND RECOMBINANT ENZYMES



Ms. Thunchanok Dumrisuk

ศูนย์วิทยทรัพยากร
จุฬาลงกรณ์มหาวิทยาลัย

A Thesis Submitted in Partial Fulfillment of the Requirements
for the Degree of Master of Science Program in Biochemistry
Department of Biochemistry

Faculty of Science

Chulalongkorn University


Academic Year 2009

Copyright of Chulalongkorn University

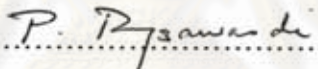
521763

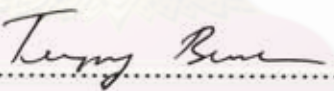
Thesis Title NAD KINASE FROM RICE *Oryza sativa* L. AND
RECOMBINANT ENZYMES
By Miss Thunchanok Dumrisuk
Field of Study Biochemistry
Thesis Advisor Assistant Professor Teerapong Buaboocha, Ph.D.
Thesis Co-advisor Assistant Professor Kanoktip Packdibamrung, Ph.D.


Accepted by the Faculty of Science, Chulalongkorn University in Partial
Fulfillment of the Requirements for the Master's Degree


..... Dean of the Faculty of Science
(Professor Supot Hannongbua, Dr.rer.nat.)

THESIS COMMITTEE


..... Chairman
(Associate Professor Piamsook Pongsawasdi, Ph.D.)


..... Thesis Advisor
(Assistant Professor Teerapong Buaboocha, Ph.D.)


..... Thesis Co-advisor
(Assistant Professor Kanoktip Packdibamrung, Ph.D.)


..... Examiner
(Associate Professor Tipaporn Limpaseni, Ph.D.)


..... External Examiner
(Ratre Wongpanya, Ph.D.)

4972322923: MAJOR OF BIOCHEMISTRY

KEYWORDS: NAD kinase / rice (*Oryza sativa* L.) / *Escherichia coli*

THUNCHANOK DUMRISUK: NAD KINASE FROM RICE *Oryza sativa* L.
AND RECOMBINANT ENZYMES. THESIS ADVISOR: ASST. PROF.
TEERAPONG BUABOOCHA, Ph.D. THESIS CO- ADVISOR: ASST. PROF.
KANOKTIP PACKDIBAMRUNG, Ph.D., 136 pp.

NAD kinase is found in both prokaryotic cells and eukaryotic cells. It catalyzes the phosphorylation of NAD⁺ to NADP⁺ using ATP. NAD⁺ and NADP⁺ act as important electron acceptors in numerous metabolic pathways. They maintain redox homeostasis and prevent cells from reactive oxygen species (ROS). In this study, *NAD kinase 1* (*OsNADK 1*) and *NAD kinase 2* (*OsNADK2*) from the rice *Oryza sativa* L. genome were identified and cloned into the expression vector pET21a(+). The resulting recombinant plasmids were introduced into *Escherichia coli* strain Rosetta (DE3) pLysS for *OsNADK1* and Rosetta-gami for *OsNADK2*. As a result, the recombinant protein OsNADK1 of approximately 60 kDa was detected in the inclusion bodies by SDS-PAGE and western blot analysis. The insoluble protein was then solubilized with 8 M urea, purified by Ni-column chromatography and refolded but no NAD kinase activity could be found. However, NAD kinase activity was detected in the soluble protein fraction for both *OsNADK1* and *OsNADK2* by in-gel activity staining. The soluble OsNADK1 was then purified by Ni-column chromatography, detected by SDS-PAGE and its NAD kinase specific activity determined in reactions involved DCIP reduction was 31.33 $\mu\text{mol NADP}/\text{min}/\text{mg}$ with a 23-purification fold. The calculated V_{max} (unit $\text{mg}^{-1}\text{protein}$) and K_m (mM) are 0.35 and 0.79 for NAD⁺ and 2.32 and 0.29 for ATP, respectively. Then activity of native NADKs was assayed in the crude extracts from leaves of KDML105 rice seedlings grown under salt stress. NAD kinase activity decreased after 6 hours of salt stress treatment, and continued to decline until after 24 hours of salt stress. When NAD kinase was partially purified from rice crude protein extract using DEAE-Toyopearl and Butyl-Toyopearl column chromatography, NADK activity (0.7 $\mu\text{mol NADP}/\text{min}/\text{mg}$) was obtained with a 12-purification fold. Finally, ³⁵S-recombinant CaM binding assay showed that OsCaM1-1 specifically interacted with the protein from crude extract of the recombinant protein NADK2 suggesting that NADK2 might be a target protein of OsCaM1-1.

Department.....Biochemistry...

Field of Study....Biochemistry.....

Academic Year2009.....

Student's Signature.....*Thunchanok*.....

Advisor's Signature.....*Teerapong Buaboocha*.....

Co-advisor's Signature.....*Kanoktip Packdibamrung*.....

ACKNOWLEDGEMENTS

This study was carried out during four years at the Department of Biochemistry, Faculty of Science, Chulalongkorn university. I am very grateful to my advisor Assistant Professor Dr. Teerapong Buaboocha, and my co-advisor Assistant Professor Dr. Kanoktip Packdibamrung for their excellent guidance and support from the very beginning to the very end of my thesis. Both, your enthusiasm and your biochemical knowledge have been invaluable for the completion of this thesis. Working with you was inspiring and an extraordinary pleasure.

My gratitude is also extended to Associate Professor Dr. Piamsook Pongsawasdi, Associate Professor Dr. Tipaporn Limpaseni and Dr. Ratre Wongpanya for serving as thesis committees, for their valuable comments and also useful suggestions.

My appreciation is also expressed to all members in Dr. Teerapong's laboratory, Biochemistry department for their warm support and positive working atmosphere that help me enjoy and happy throughout my study encouragement, especially Srivilai Phean-o-pas, for her patience and guidance in carrying out various experiment. Thanks also to Santhana Nakapong and Bongkoj Boonburapong for their constant support and advice.

Many thanks to all my friends of the Department of Biochemistry, for their instruction, lending helping, interesting discussion and friendships in the laboratory.

Finally, I wish to thank my deepest gratitude to my parents and my family for their love, care, understanding and encouragement extended throughout my study.

CONTENTS

	Page
ABSTRACT (Thai).....	iv
ABSTRACT (English).....	v
ACKNOWLEDGEMENTS.....	vi
CONTENTS.....	vii
LIST OF TABLES.....	xii
LIST OF FIGURES.....	xiii
LIST OF ABBREVIATIONS.....	xvii
CHAPTER I INTRODUCTION.....	1
Metabolic roles of NAD ⁺ and NADP ⁺	1
NAD(P) ⁺ - mediated signaling	3
NADK - the essential enzyme for NADP ⁺ biosynthesis	5
Subcellular localization and physiological roles of eukaryotic NADKs	6
Redox-reactions generating NADPH	11
Modulation of NADK activity	11
Calcium signaling	12
Calmodulin.....	14
Rice as a model monocot system.....	24
Objectives of the thesis	27
CHAPTER II MATERIALS AND METHODS.....	28
2.1 Materials.....	28
2.1.1 Rice seed	28

	Page
2.1.2 Instruments.....	28
2.1.3 Materials.....	29
2.1.4 Chemicals and reagent.....	30
2.1.5 Enzymes.....	32
2.1.6 Kit and plasmids.....	33
2.1.7 Radioactive.....	33
2.1.8 Antibiotics.....	33
2.1.9 Oligonucleotide primers.....	33
2.1.10 Microorganisms.....	34
2.1.11 Software.....	34
2.2 Bacterial growth medium.....	34
2.3 Methods.....	34
2.3.1 Quantitative method for determination of DNA concentration.....	34
2.3.2 Sequence analysis.....	35
2.3.3 Cloning of the NAD kinase genes into cloning vector (pTZ57R/T)	35
2.3.3.1) Primer design.....	35
2.3.3.2) PCR amplification.....	36
2.3.3.3) Agarose gel electrophoresis.....	37
2.3.3.4) Extraction of DNA fragment from agarose gel.....	38
2.3.3.5) Ligation of PCR products to pTZ57R/T.....	38
2.3.3.6) Transformation of ligated products to <i>E. coli</i> host cell by CaCl ₂ method.....	39

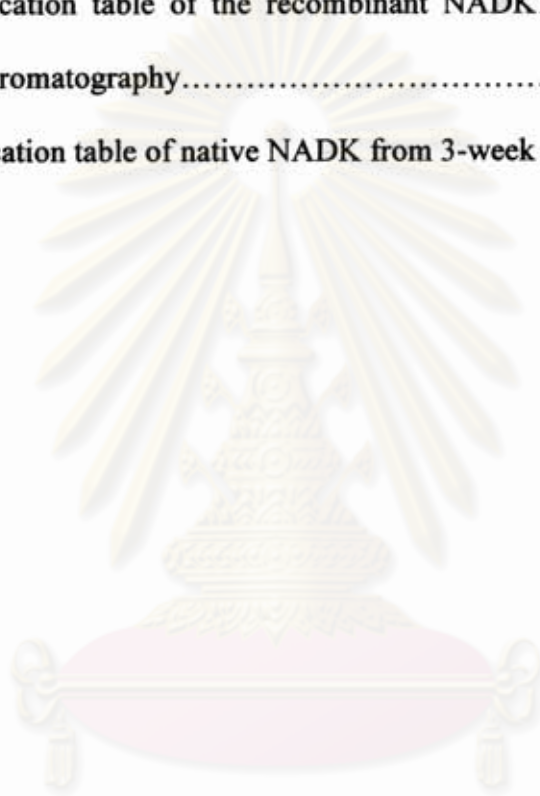
	Page
a) Preparation of <i>E. coli</i> competent cells.....	39
b) Transformation by CaCl ₂ method.....	40
2.3.3.7) Analysis of recombinant plasmids.....	40
a) Plasmid DNA isolation by alkaline lysis method	41
b) Restriction enzyme analysis.....	42
2.3.4 Cloning of <i>NADK</i> genes into expression vector pET21a(+).	42
2.3.4.1) Vector DNA preparation.....	42
2.3.4.2) Preparation of <i>NADK</i> gene fragments	42
2.3.4.3) Ligation of <i>NADK</i> gene fragments to pET21a(+).	43
2.3.4.4) Transformation of <i>E. coli</i> XL-1Blue cell by CaCl ₂ method.....	43
2.3.4.5) Analysis of recombinant plasmids.....	44
2.3.5 Sequence analysis.....	44
2.4 Expression of the <i>NADK1</i> and <i>NADK2</i> genes.....	44
2.4.1 Preparation of cell expression.....	45
2.4.2 Optimization for <i>NADK</i> genes expression	45
2.4.3 Determination of protein concentration.....	46
2.4.4 SDS-polyacrylamide gel electrophoresis.....	46
2.4.5 Protein staining	47
2.5 Purification of the <i>NADK1</i> proteins.....	47
2.5.1 Crude extract preparation.....	47
2.5.2 <i>NADK1</i> protein purification by Nickel Sepharose column.....	48

	Page
2.6 Western blot detection of the His-tagged protein.....	49
2.7 NAD kinase assay.....	51
2.7.1 In-gel activity staining.....	51
2.7.2 Measurement of NAD kinase activity.....	52
2.8 Partial purification of NAD kinase from rice <i>Oryza sativa</i> L. cultivar Khao Dok Ma Li 105 (KDML105).....	53
2.8.1 Preparation of rice seedlings	53
2.8.2 Preparation of soluble extract.....	53
2.8.3 Partial purification of NAD kinase.....	54
2.9 ³⁵ S-recombinant CaM binding assay.....	54
CHAPTER III RESULTS	56
3.1 NAD kinase sequence analysis	56
3.2 Molecular cloning of the NAD kinase genes	59
3.3 Expression of the recombinant NADK1 and NADK2.....	61
3.4 NAD kinase assay of the recombinant NADK1 and NADK2.....	70
3.4.1 Measurement of NAD Kinase Activity.....	70
3.4.2 In-gel activity staining.....	71
3.5 Purification and characterization of the recombinant NADK1 protein..	77
3.6 NAD kinase activity of rice <i>Oryza sativa</i> L. cultivar Khao Dok Ma Li 105 (KDML105).....	85
3.6.1 Measurement of NAD kinase activity in rice under salt stress.....	85

	Page
3.6.2 Partial purification of NAD kinase from rice <i>Oryza sativa</i> L. cultivar Khao Dok Ma Li 105 (KDML105).....	85
3.7 Regulation by calmodulin.....	94
3.7.1 Effect of CaM on NAD kinase activity.....	94
3.7.2 ³⁵ S-recombinant CaM binding assay.....	94
CHAPTER IV DISCUSSION.....	100
4.1 Amino acid sequences of NAD kinase from rice <i>Oryza sativa</i> L.....	100
4.2 Cloning and expression of NAD kinase genes.....	101
4.3 Purification and characterization of recombinant NAD kinase.....	104
4.4 NAD kinase activity of rice <i>Oryza sativa</i> L. cultivar Khao Dok Ma Li 105 (KDML105).....	105
4.5 Regulation by calmodulin.....	108
CHAPTER V CONCLUSION.....	110
REFERENCES.....	112
APPENDICES.....	121
APPENDIX A.....	122
APPENDIX B.....	123
BIOGRAPHY.....	136

LIST OF TABLES

Table		Page
2.1	The sequences and the length of oligonucleotide primers used for cloning of the NAD kinase genes	36
3.1	The purification table of the recombinant NADK1 by Ni-Sepharose column chromatography.....	82
3.2	The purification table of native NADK from 3-week old rice seedlings...	93



ศูนย์วิทยทรัพยากร
 จุฬาลงกรณ์มหาวิทยาลัย

LIST OF FIGURES

Figure	Page
1.1 NAD(P) ⁺ as electron carrier and in regulatory reactions.....	2
1.2 Structures of Ca ²⁺ -mobilizing derivatives of NAD(P) ⁺	4
1.3 Partial multiple alignment of NADKs from several organisms.....	9
1.4 Crystal structures of prokaryotic NADKs.	10
1.5 Generation of NADP in eukaryotic cells.....	13
1.6 Calmodulin acts as a multifunctional protein.....	15
1.7 The Ca ²⁺ -bound-calmodulin-mediated signal transduction in plants.....	18
1.8 Ribbon presentations of calmodulin.....	20
1.9 Neighbor-joining tree based on amino acid similarities among OsCaM and OsCML proteins.....	23
1.10 Structural features of <i>Oryza sativa</i> L.....	26
2.1 Exploded view of the Trans-Blot [®] SD (Bio-Rad).....	50
3.1 Sequence comparison of rice <i>Oryza sativa</i> L. NADK1 (OsNADK1) and NADK2 (OsNADK2) with NADK1 (AtNADK1) and NADK2 (AtNADK2) from Arabidopsis.....	57
3.2 Sequence comparison of the N-terminal region containing a predicted CaM-binding domain from OsNADK2 and AtNADK2.....	58
3.3 Ethidium-bromide stained 1% agarose gels of the PCR products amplified from the <i>NADK1</i> and <i>NADK2</i> cDNAs.....	60

Figure	Page
3.4 Analyses of the recombinant plasmid pTZ57R/T with <i>NADK1</i> or <i>NADK2</i> inserted by digesting with restriction enzymes followed by separation by 1% agarose gel electrophoresis.....	62
3.5 Restriction analysis of the recombinant pET21a/ <i>NADK1</i> on 1.0 % agarose gel.....	63
3.6 Restriction analysis of the recombinant pET21a/ <i>NADK2</i> on 1.0 % agarose gel.....	64
3.7 Nucleotide and deduced amino acid sequences of <i>NADK1</i> gene in the recombinant plasmid.....	66
3.8 Nucleotide and deduced amino acid sequences of <i>NADK2</i> gene in the recombinant plasmid.....	69
3.9 SDS-PAGE analysis of the soluble protein fractions from <i>E. coli</i> Rosetta (DE3) pLysS harboring pET21a/ <i>NADK1</i> and Rosetta-gami harboring pET21a/ <i>NADK2</i> after induction by various IPTG concentrations.....	72
3.10 SDS-PAGE analysis of the inclusion bodies from <i>E. coli</i> Rosetta (DE3) pLysS harboring <i>NADK1</i> and Rosetta-gami harboring <i>NADK2</i> after induction by various IPTG concentrations.....	73
3.11 Induction of recombinant <i>NADK1</i> to various IPTG concentrations.	74
3.12 Induction of recombinant <i>NADK2</i> to various IPTG concentrations.....	75
3.13 In-gel activity staining of soluble proteins extracted from <i>E. coli</i> Rosetta (DE3) pLysS harboring <i>NADK1</i> and Rosetta-gami harboring <i>NADK2</i>	76

Figure	Page
3.14 Purification of recombinant NADK1 from the inclusion bodies.....	79
3.15 Purification of recombinant NADK1 from the soluble protein fraction...	80
3.16 Western blot analysis of the recombinant protein from <i>E. coli</i> Rosetta (DE3) pLysS harboring <i>NADK1</i>	81
3.17 Substrate saturation curves of the recombinant NADK1.....	83
3.18 Lineweaver-Burg plots of NAD kinase.....	84
3.19 NAD kinase activity of the crude extracts from 3-week old KDML105 rice seedlings after salt stress.....	86
3.20 SDS-PAGE analysis of the rice protein crude extract precipitated with saturated ammonium sulfate.....	88
3.21 SDS-PAGE analysis of the protein crude extract from <i>E. coli</i> expressing NADK1 and NADK2 precipitated with saturated ammonium sulfate.....	89
3.22 NAD kinase specific activity of rice extracts precipitated in various concentrations of saturated ammonium sulfate.....	90
3.23 NAD kinase specific activity of crude extracts from <i>E. coli</i> expressing NADK1 precipitated in various concentrations of saturated ammonium sulfate.....	90
3.24 NAD kinase specific activity of crude extract from <i>E. coli</i> expressing NADK2 in various concentrations of saturated ammonium sulfate.....	91
3.25 SDS-PAGE analysis of the partially purified native NAD kinase from 3-week old rice seedlings.....	92

Figure	Page
3.26 SDS-PAGE analysis of the purification of recombinant OsCaM1-1 protein by Phenyl-Sepharose.....	96
3.27 NAD kinase specific activity of the purified recombinant NADK1 in the presence of various calcium concentrations and 300nM OsCaM1-1.....	97
3.28 NAD kinase specific activity of the 0-30% saturated ammonium sulfate precipitate from <i>E. coli</i> expressing NADK2 in the presence of various calcium concentrations and 300 nM OsCaM1-1.....	97
3.29 NAD kinase specific activity of the rice protein crude extract in the presence of various calcium concentrations and 300 nM OsCaM1-1.....	98
3.30 ³⁵ S-recombinant CaM binding assay.....	99

LIST OF ABBREVIATIONS

A	absorbance, 2'-deoxyadenosine (in a DNA sequence)
bp	base pair
C	2'-deoxycytidine (in a DNA sequence)
Da	Dalton
DNA	deoxyribonucleic acid
DTT	dithiothreitol
EDTA	ethylene diamine tetraacetic acid
EtBr	ethidium bromide
g	gram
G	2'-deoxyguanosine (in a DNA sequence)
hr	hour
HCl	hydrochloric acid
IPTG	isopropyl-thiogalactoside
kb	kilobase
LB	Luria-Bertani
M	mole per liter (molar)
Mg ²⁺	magnesium ion
mA	milliampere
mg	milligram
min	minute
ng	nanogram
nm	nanometer
O.D.	optical density

°C	degree celcius
µg	microgram
µl	microlitre



ศูนย์วิทยทรัพยากร
จุฬาลงกรณ์มหาวิทยาลัย

CHAPTER I

INTRODUCTION

Metabolic roles of NAD⁺ and NADP⁺

Nicotinamide adenine dinucleotide (NAD⁺) and nicotinamide adenine dinucleotide phosphate (NADP⁺) have become well established as key energy transducers, precursors for the signaling molecules and metabolic regulators (Noctor *et al.* 2006). The structure of NAD⁺ and NADP⁺ differ only in the presence of an extra phosphate on the adenosine (Figure 1.1A). NAD⁺ is used in catabolic reactions and the generated NADH provides reducing power for other metabolic pathways or ATP synthesis. NADP⁺ is an essential cofactor for one of the fundamental processes of life, the photosynthesis in plant chloroplasts. NADPH is considered to be the reductive power of the cell being an indispensable cofactor of reductases maintaining the pool of reduced glutathione and thioredoxin and of detoxifying enzymes such as cytochrome P450. However, NAD(P)⁺ was discovered to be not only an electron carrier but also a precursor for molecules involved in protein modification and signaling pathways (Figure 1.1). The knowledge of the role of “NAD(P)⁺-consuming” enzymes in the regulation of important cellular functions has rapidly increased. Thus, the interest in the biosynthetic routes leading to NAD(P)⁺ formation and maintaining the nucleotide pools is rising. One of the crucial enzymes in the maintenance of the NADP⁺ pool is NAD kinase. It phosphorylates NAD⁺ to NADP⁺ using ATP as a phosphoryl donor. This reaction represents the only known way to generate NADP⁺ in all living organisms.

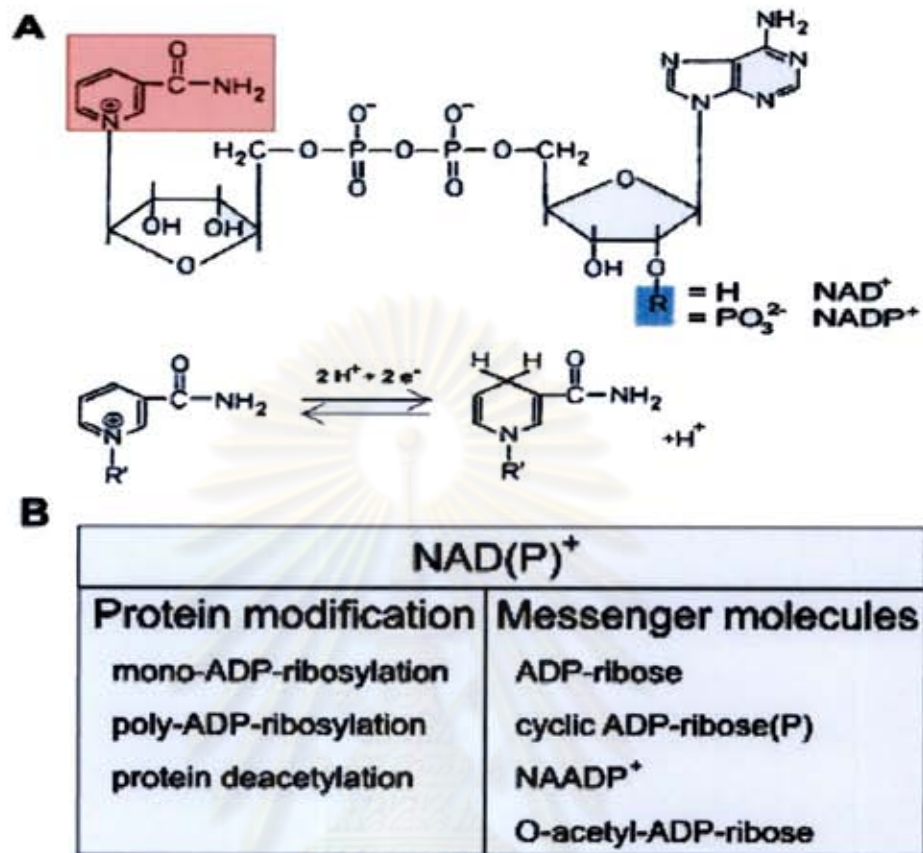


Figure 1.1: NAD(P)⁺ as electron carrier and in regulatory reactions. (A) Structure of NAD(P)⁺. The nicotinamide moiety is boxed in red. The lower part shows the difference in hydrogen atoms in the nicotinamide moiety during reversible conversion between oxidized and reduced forms. (B) NAD(P)⁺ serves as a precursor of messenger molecules and as a substrate for covalent modifications of target molecules.

NAD(P)⁺ - mediated signaling

NAD(P)⁺ is used as a precursor for molecules involved in calcium signaling. The divalent cation calcium (Ca²⁺) is the most common signal transduction element in prokaryotic and eukaryotic cells which controls many processes (Berridge *et al.*, 2000). Unlike other second messenger molecules, Ca²⁺ cannot be metabolized therefore cells have to tightly regulate intracellular Ca²⁺ levels. The cell has two sources of Ca²⁺ entry, either from the external medium or release from internal stores, mainly the endoplasmatic/sarcoplasmatic reticulum (ER/SR). These Ca²⁺ influx mechanisms are balanced by Ca²⁺ pumps to remove the Ca²⁺ signal. Both processes are often organized to produce short spikes and waves of Ca²⁺ to avoid the cytotoxic effects of prolonged high intracellular Ca²⁺ levels (Pollak, 2007). The release of Ca²⁺ from internal stores is stimulated and modulated by Ca²⁺ itself or the second messenger molecules including myo-inositol 1,4,5-trisphosphate (IP3), cyclic ADP-ribose (cADPr; Figure 1.2), and nicotinic acid adenine dinucleotide phosphate (NAADP; Figure 1.2). IP3 releases Ca²⁺ from the ER after binding its receptor (IP3R) (Streb *et al.*, 1983). Ca²⁺ mobilization by the pyridine nucleotide derivatives was discovered shortly after (Clapper *et al.*, 1987; Lee *et al.*, 1989; Lee and Aarhus, 1995) and has been detected in several organisms and cell types (Lee, 2001; Guse, 2004). Cyclic ADPr was shown to be an endogenous activator of Ca²⁺-induced Ca²⁺ release by ryanodine receptor (RyR) in the ER/SR (Galione *et al.*, 1991) while NAADP activates intracellular Ca²⁺ channels distinct from those that are

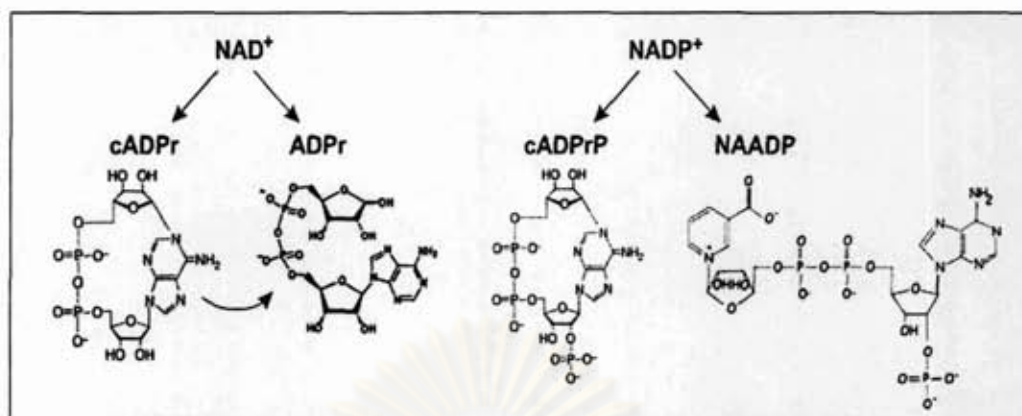


Figure 1.2: Structures of Ca²⁺-mobilizing derivatives of NAD(P)⁺. Cyclic ADPr is formed from NAD⁺ by ADPr cyclase. ADPr is generated directly by NAD⁺ hydrolysis or by cADPr hydrolysis. NAADP formation by a base-exchange reaction, substituting nicotinamide for nicotinic acid, and the same class of enzymes synthesizes cADPrP from NADP⁺. ADPr, ADP-ribose; cADPr, cyclic ADPr; cADPrP, 2'-phosphate cADPr; NAADP, nicotinic acid ADP. (Pollak *et al.*, 2007)

ศูนย์วิทยทรัพยากร
จุฬาลงกรณ์มหาวิทยาลัย

sensitive to IP₃ and cADPr (Clapper *et al.*, 1987; Lee and Aarhus, 1995).

NADK – the essential enzyme for NADP⁺ biosynthesis

NAD kinase (NADK) catalyzes the phosphorylation of NAD⁺ to NADP⁺ using ATP or inorganic polyphosphate as phosphoryl donors. This reaction represents the only known way to generate NADP⁺ in prokaryotic and eukaryotic cells. NADP⁺ synthesis was first reported in yeast homogenates (Vestin, 1937; von Euler and Adler, 1938). Later, the enzyme was partially purified and characterized from yeasts, mammals, plants and sea urchin (McGuinness and Butler, 1985). However, conclusive structural information has only recently become available after identification of the amino acid sequences of *Mycobacterium tuberculosis* and *Micrococcus flavus* NADKs (Kawai *et al.*, 2000). To date, NADKs of *Homo sapiens*, *Saccharomyces cerevisiae*, *Arabidopsis thaliana* and multiple prokaryotes have been characterized (Magni *et al.*, 2006; Pollak *et al.*, 2007). NADK is an essential enzyme as has been demonstrated in *Escherichia coli*, *M. tuberculosis*, *Bacillus subtilis* and *Salmonella enterica* (Gerdes *et al.*, 2002; Kobayashi *et al.*, 2003; Sasseti *et al.*, 2003; Grose *et al.*, 2006) and in the yeast *S. cerevisiae* (Bieganowski *et al.*, 2006; Shianna *et al.*, 2006). The comparison of known NADK amino acid sequences shows a highly conserved region, the catalytic domain, within the C-terminus of the proteins whereas the N-terminal parts vary and are significantly longer in eukaryotic NADKs (Figure 1.3). The catalytic domain (Pfam PF01513) is characterized by two well-conserved motifs, the GGDG motif and a glycine-rich motif. The GGDG motif is also found in diacylglyceride kinase, sphingosine kinase and 6-phosphofructokinase thereby proposed to be a feature of a kinase superfamily including NADK (Labesse *et al.*, 2002). The importance of both motifs for the enzymatic activity was confirmed by

site-directed mutagenesis of amino acid residues within the motifs (Labesse *et al.*, 2002; Raffaelli *et al.*, 2004; Mori *et al.*, 2005b) and was further supported by three-dimensional structures of prokaryotic NADKs (Garavaglia *et al.*, 2004; Liu *et al.*, 2005; Mori *et al.*, 2005b; Oganessian *et al.*, 2005; Poncet-Montange *et al.*, 2007).

While several three-dimensional structures of prokaryotic NADKs have been resolved (Figure 1.4), no eukaryotic one is yet reported. *M. tuberculosis* NADK is a biological tetramer and corresponds to a dimer of dimers (Garavaglia *et al.*, 2004; Mori *et al.*, 2005b). The overall structure is organized into an N-domain, a C-domain and a C-terminal tail. The N-terminal domain resembles a classical Rossmann fold, known to be involved in dinucleotide binding (Rossmann *et al.*, 1974), consisting of a single parallel β -sheet flanked by α -helices. The C-terminal domain adopts a novel fold with structural similarity to the human Ki67 fork-head-associated domain (Garavaglia *et al.*, 2004). The structures of *Archaeoglobus fulgidus* and *Listeria monocytogenes* NADKs show similarities, two dimers assemble into a tetramer (Liu *et al.*, 2005; Poncet-Montange *et al.*, 2007). The substrates NAD^+ and ATP and the product NADP^+ are all bound to a cleft between the N- and C-domains. Subunit interactions are required for ligand binding (see Figure 1.4B; black broken line). Indeed, known NADKs are homo-oligomeric proteins as determined by gel filtration experiments.

Subcellular localization and physiological roles of eukaryotic NADKs

Yeast – The presence of NADK activity in the cytoplasm and mitochondria of yeast is long established (McGuinness and Butler, 1985). Three NADK isoforms in *S. cerevisiae* have been characterized recently. ScNADK-1 and ScNADK-2 are cytosolic proteins and exhibit relaxed substrate specificity with some preference

towards NAD^+ (Kawai *et al.*, 2001b; Shi *et al.*, 2005) whereas ScNADK-3 localizes to the mitochondrial matrix and prefers NADH as substrate (Outten and Culotta, 2003). A global analysis of protein expression in yeast revealed ScNADK-2 to be less present (~300 molecules per cell) compared to ~5000 molecules of isoform 1 and 3 (Ghaemmaghami *et al.*, 2003). In agreement, ScNADK-1 and ScNADK-3 are responsible for almost all NADK activity *in vivo* since the disruption of both is synthetically lethal, with or without the deletion of isoform 2 (Bieganowski *et al.*, 2006; Shianna *et al.*, 2006). The double mutant can be rescued by overexpression of any of the yeast NADK isoforms (Bieganowski *et al.*, 2006) or human NADK (Shianna *et al.*, 2006). Notably, ScNADK-3, the mitochondrial isoform, was established as the most critical generator of NADPH in yeast. Yeast cells deleted for this isoform are highly sensitive towards oxidative stress induced by hydrogen peroxide or hyperoxia (Krems *et al.*, 1995; Outten and Culotta, 2003). ScNADK-3 mutants exhibit increased frameshift mutations in the mitochondrial DNA and increased petite colony formation (Strand *et al.*, 2003). Deletion strains accumulate iron in the mitochondria and are defective in mitochondrial Fe-S cluster-containing enzymes (Outten and Culotta, 2003) leading to upregulation of genes involved in iron transport (Shianna *et al.*, 2006). In contrast, disruption of ScNADK-1 or ScNADK-2 does not result in severe growth defects or in hypersensitivity to high oxygen concentration (Outten and Culotta, 2003). ScNADK-1 is suggested to provide NADP^+ for cytosolic NADP-dependent dehydrogenases and detoxifying systems while the role of isoform 2 remains rather unclear (Bieganowski *et al.*, 2006).

Plants – NADK activity has originally been associated with cytoplasmic (Simon *et al.*, 1982), mitochondrial (Dieter and Marme, 1984) and chloroplastic fractions (Muto and Miyachi, 1981; Jarrett *et al.*, 1982). Based on sequence similarity with NADKs from other organisms, three genes encoding putative NADKs were predicted in the *A. thaliana* genome (Hunt *et al.*, 2004) and subsequently cloned and characterized (Turner *et al.*, 2004; Turner *et al.*, 2005). AtNADK-1 and AtNADK-3 are expressed in most tissues, while isoform 2 is only expressed in leaves (Turner *et al.*, 2004; Berrin *et al.*, 2005). Recent studies on the localization of overexpressed green fluorescent protein-NADK constructs in plant revealed AtNADK-2 to be targeted to the chloroplasts (Chai *et al.*, 2005) while AtNADK-1 and AtNADK-3 are found in the cytoplasm (Chai *et al.*, 2006). Plant NADK isoforms respond differently to stress conditions. Irradiation or treatment with hydrogen peroxide of plant cell suspensions induced AtNADK-1 mRNA and protein levels (Berrin *et al.*, 2005). The transcript of AtNADK-3 is induced by cold, osmotic stress, a superoxide-generating agent and high salinity whereas the transcript levels of AtNADK-1 and AtNADK-2 were not significantly affected by these conditions (Chai *et al.*, 2006). Plants deficient for AtNADK-1 exhibit increased sensitivity to oxidative stress (Berrin *et al.*, 2005). The knockout of NADK-2 in *A. thaliana* delays growth and development, resulting in reduced leaf size and seed production. NADK activity and NADP(H) content was significantly lowered in leaves of the mutant compared to wild-type (Takahashi *et al.*, 2006). AtNADK-2 protects chloroplasts against oxidative stress and plays a vital role in chlorophyll synthesis according to the importance of NADP⁺ in photosynthesis (Chai *et al.*, 2005). Knockout of AtNADK-3 enhanced the plants sensitivity to various stress conditions


```

HsNADK 156 A VYK FQTFRFDYDCISKQIFITLGGGGNTLQASSLFGG-SVPPVMAKELGSSGGFLTESSPNNQSC
AtNADK-2 177 FQQT----FYIQDTSILHERVDFVAGLGGKTLRASSLFGG-AVPPVMSKLSLGGFLTSHFADDFCI
ScNADK-1 158 FQKY----WTKDFINENDVFFDIAMVTLGGGGTLEFVSSLPQR-HVPPVMSKLSLGGFLTSHFADDFCI
ScNADK-2 147 FQKY----WSKEFVVKHDSFFDLMTLGGGGTLEASSLFTK-DVPPVMSKLSLGGFLTSHFADDFCI
AtNADK-1 145 FQQTW-E--DDKEISLHTKVDLITLGGGGTLEWASSLFGG-EVPPVMSKLSLGGFLTSHFADDFCI
ScNADK-3 121 NDPNRPPILYTGPEQDIVNRTDLVTLGGGGTLEKVMHFGNTQVPPVLAHSLLGGFLTSHFADDFCI
AtNADK-3 56 KMPVWEFPISRNDSLHPIRDVAVYITLGGGGTLEASHFIDD--SVVGLVNSDPT---CAHGVDELSDC
EcNADK 57 LAETG-----QLADLRVYGGDDEIIGAARTLAF-YDIKVIKINRSLGGFLTSHFADDFCI
MtNADK 56 MRAMGVEIEVVDAQQAADGSLVIVLGGGGTLEPAAEIARN-ASIVLGLVMSKLSLGGFLTSHFADDAV

HsNADK 214 VQVTEG-NAAVVMSRSLKRVVVEEIRKKTAVHNGLGENGSCAAQLDNDVGRQAMQYQVINEVMDRGG
AtNADK-2 192 LKPVHGNNTLDGVIITLRSLRLECEYRGGKAMFG-----KVFDVINEVMDRGG
ScNADK-1 253 LPRIMNK----KHTNLRLRLECEYRRHPPEVDNPTG-----KKICVVEKLSRHRILNEVMDRGG
ScNADK-2 232 LKHILTD----EVEINLRSLRLECEYRRKPFIDAATG-----RKICYIDFISEHNVINEVMDRGG
AtNADK-1 331 LKADMG----FHSITLRRLRLECEYRDKATHEYEPDE-----TMLINEVMDRGG
ScNADK-3 151 FQEVSS----PACILHNTLRLECEYRGGSSIVT-----KANNDFIRKRN
AtNADK-3 121 FDASRSTGHLCAATVENFEVMDIDIFFEVVPAKVSRIE-----LWLNSETLLSHRANLDAQFC
EcNADK 113 LACVTEG----RYISEKRFLEAGVQDDQDPFIS-----TAINEVVIEHFK
MtNADK 125 LKRVVAQ----DYVEEDRLELAVVPPGGPIVVRG-----WALNEVSLRGG

HsNADK 293 SSYLSNDVYELPH-----LSTVWQDQVLSLPTGSTAYAAARSMIKNVSAKHTIPCPHSLSEK
AtNADK-2 242 NPVLSKDFVEHDF-----LQKVVQDQVLSLPTGSTAYATAAGRWVHINYSOMIETIPCPHSLSEK
ScNADK-1 311 SPFLSNDVYELPH-----LQVVAQDQVLSLPTGSTAYLSAAGSLVSTVVAATIPCPHSLSEK
ScNADK-2 290 APQSLKDFYGNDS-----LQKVVQDQVLSLPTGSTAYLSAAGSLVSAVNAATIPCPHSLSEK
AtNADK-1 375 SSYLSNDVYELPH-----FVSCVQDQVLSLPTGSTAYLSAAGRWVHINYSOMIETIPCPHSLSEK
ScNADK-3 235 SPFLSNDVYELPH-----FLSTTIDQVLSLPTGSTAYLSAAGGIVSILVAATIPCPHSLSEK
AtNADK-3 152 PRAVSRFSFHKKPIKAGASSPKTVNCRSE--RQCTARASTAARSAKQVNFMLSRDQEVVREPEKPGSI
EcNADK 156 VAVLIEEVEYELPH-----FAFSQPSDQVLSLPTGSTAYLSAAGSLVSTVVAATIPCPHSLSEK
MtNADK 148 RLGLQVVEELPH-----FVSAFQDQVLSLPTGSTAYLSAAGSVEVQVVAATIPCPHSLSEK

HsNADK 357 FVWYAGVELKIMTSFEA-----KTAWVSFDGRNDE--EHRGSSISLITSCPEPSTCVRDFVSWVFE
AtNADK-2 306 FVILGSAKLEKIPDEA-----KSNAAVSFDGRNQQ--LSPKDSVRVYNSCHPFTVNSDQGTGDFPS
ScNADK-1 375 FVILFSEINLKVKVSMKS-----KSNAAVAFGRNREE--LQPGGKITCASPAFTVEAS--PKESINS
ScNADK-2 354 FVILFSEINLQKVVDMNS-----KTSWVAFGRNIVE--LQKGDVYVNASPFSPTVESS--ASRFEF
AtNADK-1 443 FVILFSEVTVRVVDFNS-----KSAWVSFDGRDPRQ--LEAGFAVCSNAPFVSTACQVESTNDLPS
ScNADK-3 299 FVILFSEIRIKTGSXLNKQVNVVVKIPQD--LDVSEIYVIVN---EYGVYIDQTLPTTRV
AtNADK-3 252 ASDMHSVFKPDQFVDVNWY--SEKTHYDQCCVQHSVQKQDITIEESTAPVWVFLSHG-----ISC
EcNADK 320 FVINSSTIRLFSHR-----KNDLEISLSCIALP--QKEDVLRCDLHNLHFK--DYSFEN
MtNADK 332 FVWCSPEATLADFEADG-----HDLVFDGRREML--KASRFEVTRCVTSKWARDL--SAPSTF

```

Figure 1.3: Partial multiple alignment of NADKs from several organisms.

Amino acid sequences of *H. sapiens* NADK (protein ID NP_075394); *A. thaliana* NADK-1, NADK-2 and NADK-3 (NP_974347, NP_564145 and NP_177980, respectively); *S. cerevisiae* NADK-1, NADK-2 and NADK-3 (P21373, NP_010873 and NP_015136, respectively); *E. coli* NADK (NP_417105); and *M. tuberculosis* NADK (BAB21478) were compared using Clustal W. Identical and similar residues are highlighted in black and grey respectively. The two conserved NADK motifs are boxed in red. (Pollak *et al.*, 2007).

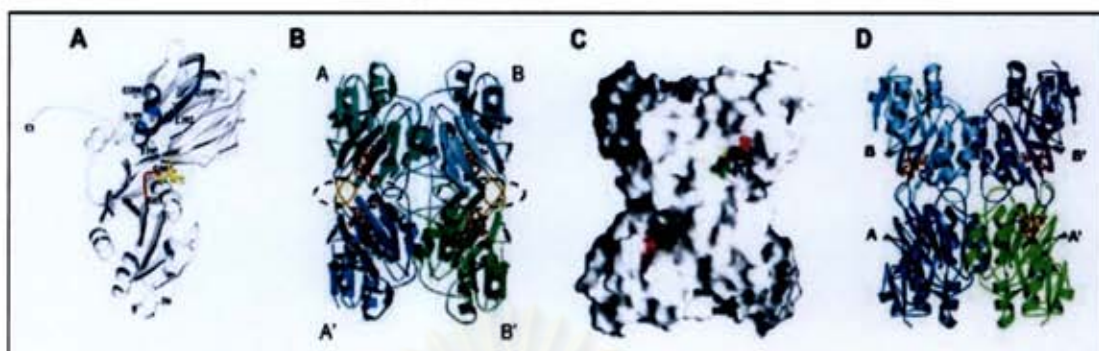


Figure 1.4: Crystal structures of prokaryotic NADKs. (A) Stereo ribbon representation of the MtNADK subunit. Residues of the GGDG sequence fingerprint and of the second conserved region are colored in *red* and *blue*, respectively. Residues proposed to be involved in the NAD binding are drawn in a *ball-and-stick* representation. Ct, C terminus; Nt, N terminus. Modified from (Garavaglia *et al.*, 2004). (B) Ribbon model of quaternary structure of MtNADK-NAD. An asymmetric unit contained 2 subunits (MtNADK-NAD-A/-B, or - A'/B'). NAD⁺ is indicated in *red* (nitrogen, *blue*; phosphorus, *pink*). The A-A' and B-B' contact regions are enclosed by *black broken line*. MtNADK-flexible loops are shown in *yellow* (Mori *et al.*, 2005b). (C) Molecular surface model of quaternary structure of MtNADK-NAD⁺ as shown in (B), but was rotated by 90°C. NAD⁺ is shown in *blue*. Surfaces of residues involved in NAD⁺ binding are colored in *green* (Thr200- Ser205), *yellow* (Asn159, Glu160), and *pink* (Asp85, Gly86). Modified from (Mori *et al.*, 2005b). (D) Ribbon diagram of the AfNADK tetramer in complex with ATP. The individual monomers are labeled as A, A', B and B' (Liu *et al.*, 2005).

(Chai *et al.*, 2006). Under these conditions the mutant plants show significantly decreased NADPH level and GSH/GSSG ratio and increased expression of stress marker genes compared to wild-type plants.

Redox-reactions generating NADPH

Besides a direct phosphorylation of NADH by NADKs several NADP⁺-specific dehydrogenases, as well as nicotinamide nucleotide transhydrogenase have been identified as significant contributors to the cellular NADPH pool (Figure 1.5).

Glucose-6-phosphate dehydrogenase (G6PD), the key regulatory enzyme of the cytosolic pentose phosphate pathway, catalyzes the oxidation of glucose-6-phosphate to 6-phospho-gluconolactone and the production of reducing equivalents in the form of NADPH. Salt stress in plants was reported to increase G6PD activity and protein (Valderrama *et al.*, 2006). This result suggested G6PD to be part of a mechanism to protect cells against oxidative damage. Indeed, G6PD overexpression conferred strong protection against H₂O₂-induced cell death through induction of GSH production (Salvemini *et al.*, 1999; Tian *et al.*, 1999). Conversely, inhibition of G6PD activity potentiated H₂O₂-induced cell death (Tian *et al.*, 1999) confirming that G6PD has an important role in antioxidant defense mechanisms. However NADPH produced by a cytosolic enzyme is unavailable to mitochondria, the major site of superoxide production.

Modulation of NADK activity

A connection between NADK activity and calcium/calmodulin (Ca²⁺/CaM) is well known for decades, at least for the enzymes from sea urchin eggs (Epel *et al.*, 1981), plants (Anderson *et al.*, 1980) and human neutrophils (Williams *et al.*, 1985).

Plants possess both CaM-dependent and -independent NADK isoforms that differ in their subcellular localization (Simon *et al.*, 1982; Dieter and Marme, 1984; Simon *et al.*, 1984; Pou De Crescenzo *et al.*, 2001). However, the activity of the three recombinant NADK isoforms from *A. thaliana* was not influenced by Ca^{2+} /CaM although AtNADK-2 binds CaM in a Ca^{2+} -dependent manner (Turner *et al.*, 2004; Turner *et al.*, 2005).

Calcium signaling

Ca^{2+} serves as an intracellular messenger in many cellular processes including plant responses to environmental stresses such as salinity, drought and cold. These stresses have been shown to induce transient elevation of the cytoplasmic Ca^{2+} concentration level. Because of the cytotoxic effects of calcium, cells pay very particular attention to keeping cytoplasmic calcium levels much lower than the normal extracellular 10^{-3} M level; usually it is in the range 10^{-8} - 10^{-6} M. This is accomplished using a variety of calcium-pumping systems located both in the plasma membrane and organelles and together these operate a very efficient calcium-stat system. But, in addition, cells use the temporary elevation of cytoplasmic calcium to between 10^{-6} and 10^{-5} M that may follow plasma membrane perturbation and alteration of calcium channel activity, as signals, eliciting a variety of predetermined responses. Elevation of the Ca^{2+} concentration is detected by calcium sensor proteins. The classical calcium sensor is calmodulin (CaM), which regulates activity of its protein targets in a calcium-dependent manner. In plants, CaM may play an important role in transducing Ca^{2+} -mediated signals from various environmental stresses into appropriate adaptive cellular responses.

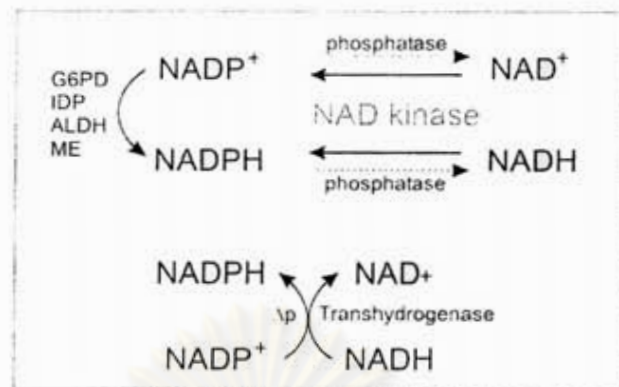


Figure 1.5: Generation of NADP in eukaryotic cells. G6PD, glucose-6-phosphate dehydrogenase; IDP, NADP^+ -dependent isocitrate dehydrogenase; ALDH, NADP^+ -dependent aldehyde dehydrogenase; ME, NADP^+ -dependent malic enzyme; Δp , electrochemical proton gradient.

ศูนย์วิทยทรัพยากร
จุฬาลงกรณ์มหาวิทยาลัย

Calmodulin

Calmodulin (CaM) is probably the most well characterized Ca^{2+} sensors among major groups of Ca^{2+} -binding proteins. It is a small (148 residues, 17 kDa), highly conserved, soluble, intracellular Ca^{2+} -binding protein ubiquitously found in animals, plants, fungi and protozoa, and is regarded as a major transducer of Ca^{2+} signals in mammalian cells. It has four EF-hands that function in pairs. Many proteins involved in Ca^{2+} signal transduction alter their activity in response to changes in free Ca^{2+} levels, but are themselves not able to bind Ca^{2+} ions. Some of these proteins utilize CaM as a sensor and mediator of the initial Ca^{2+} signal. CaM is a multifunctional protein because of its ability to interact and regulate the activity of a number of other proteins as shown in Figure 1.6. CaM relays the Ca^{2+} signal by binding free Ca^{2+} ions to its C- and N-terminal EF-hand pairs, which causes a conformational change and enables Ca^{2+} /CaM to bind to specific CaM-binding domains. The binding of Ca^{2+} /CaM to its target proteins alters their activity in a calcium dependent manner.

Ca^{2+} -bound-calmodulin-mediated signal transduction in plants is shown in Figure 1.7. Biotic and abiotic signals are perceived by receptors, resulting, in some cases, in transient changes in Ca^{2+} concentrations in the cytosol and/or organelles (e.g. nucleus). Increases in free Ca^{2+} concentrations originating from either extracellular pools or intracellular stores are capable of binding to Ca^{2+} -modulated proteins including calmodulin and calmodulin-related proteins. Structural modulations of these proteins enable them to interact with numerous cellular targets that control a multitude of cellular functions, such as metabolism, ion balance, cytoskeleton and protein modifications. In addition, Ca^{2+} and calmodulin might also regulate the expression of

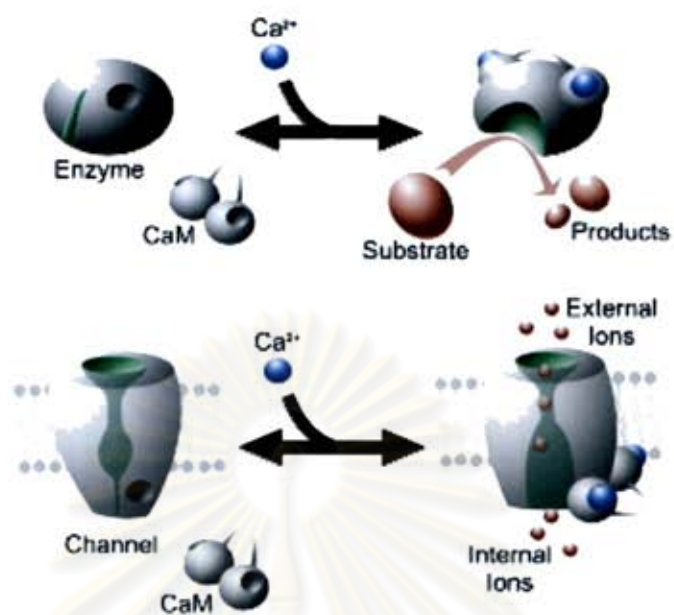


Figure 1.6: Calmodulin acts as a multifunctional protein.

ศูนย์วิทยทรัพยากร
จุฬาลงกรณ์มหาวิทยาลัย

genes by complex signaling cascades or by direct binding to transcription factors. Rapid changes in cellular functions result from direct interactions of calmodulin and calmodulin-related proteins with their targets (within seconds to minutes) while slower responses require gene transcription, RNA processing and protein synthesis (variable times from minutes to days).

The EF hands in CaM are organized into two distinct globular domains, each of which contains one pair of EF hands. Each pair of EF hands is considered the basic functional unit. Pairing of EF hands is thought to stabilize the protein and increase its affinity toward Ca^{2+} . Although each globular domain binds Ca^{2+} and undergoes conformational changes independently, the two domains act in concert to bind target proteins. Upon increase of Ca^{2+} concentration to submicromolar or low micromolar levels, all CaM molecules are activated. Cooperative binding is required for this “on/off” mechanism to function efficiently. The cooperativity of Ca^{2+} binding ensures that full activation of the CaM occurs in a narrow region of calcium concentration during a signaling event.

The selectivity of CaM toward Ca^{2+} also is an important factor in effective transduction of the Ca^{2+} signal. CaMs bind Ca^{2+} selectively in the presence of high concentrations of Mg^{2+} and monovalent cations in the cell. The cation selectivity is achieved by optimizations in the structure folds of the binding loop. For example, discrimination between Ca^{2+} and Mg^{2+} is accomplished through reduction in the size of the binding loop. Binding of Mg^{2+} ions would collapse the EF-hand loop, thereby reducing the distance between negatively charged side chains and destabilizing the CaM- Mg^{2+} complex. Even small changes in the chemical properties of the Ca^{2+} binding loop (e.g., Glu-12→Gln) can drastically reduce the binding affinity to Ca^{2+}

(Beckingham, 1991; Haiech *et al.*, 1991). The Glu-12→Gln mutation changes the carboxylate side chain into carboxylamide, which removes the oxygen ligand for Ca^{2+} . Together, structural analyses in combination with site-directed mutagenesis established that CaMs (and other EF hand-containing proteins, including CBLs) have evolved as highly specific Ca^{2+} sensors (Luan *et al.*, 2002).

The overall structure of Ca^{2+} /CaM is dominated by two EF-hand pairs forming the C- and N- terminal lobes and a long α -helix connecting the two lobes. In vertebrate CaM, the two EF-hand pairs share 48% sequence identity and 75% sequence similarity and the peptide backbone of the two lobes can be superimposed with a mean square derivation of $\sim 0.7 \text{ \AA}^2$ (Vetter and Leclerc, 2003). Structural analysis of the Ca^{2+} -free and Ca^{2+} -bound states of CaM proteins reveals the conformational changes induced by Ca^{2+} binding as shown in Figure 1.8. In the Ca^{2+} -free state, CaM adopts a closed conformation. Ca^{2+} binding triggers a conformational change, and the protein adopts an open conformation with nearly perpendicular interhelical angles between the globular domains. This open conformation exposes a hydrophobic surface within each globular domain and permits the binding of protein targets (Babu *et al.*, 1988; Kuboniwa *et al.*, 1995, Zhang *et al.*, 1995).

Ca^{2+} -CaM binds and regulates the activity of a wide range of proteins that are not necessarily related in structure. How can Ca^{2+} -CaMs bind to so many different proteins? More specifically, the plasticity of the Ca^{2+} -CaM structure must accommodate the variation in both the molecular size and the composition of the target proteins. This issue has been addressed by structural analyses of Ca^{2+} -CaM and target-bound Ca^{2+} -CaM.

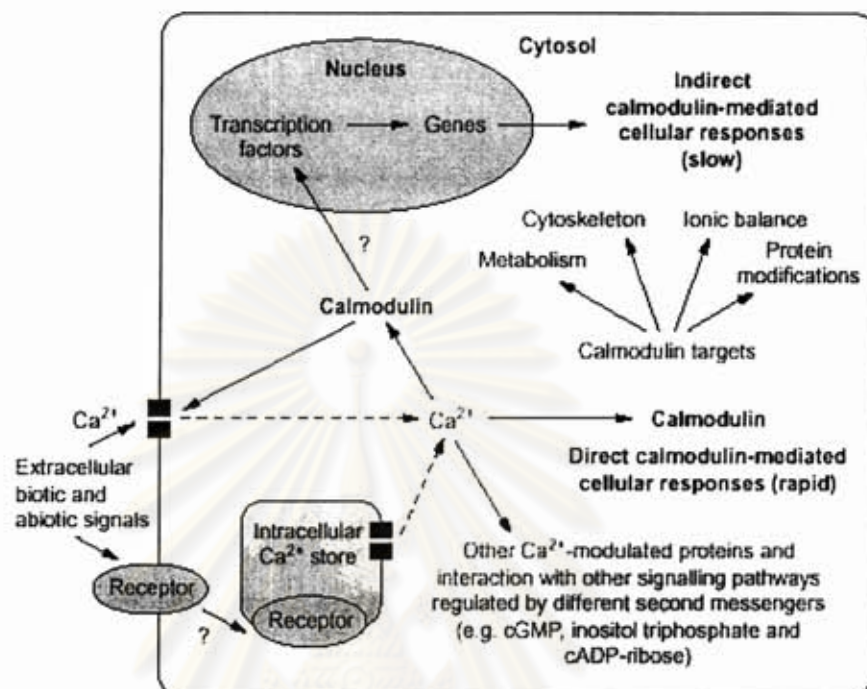


Figure 1.7: The Ca^{2+} -bound-calmodulin-mediated signal transduction in plants. Broken arrows denote Ca^{2+} fluxes from extracellular or intracellular stores, and question marks signify unknown signal transduction intermediates.

ศูนย์วิทยทรัพยากร
จุฬาลงกรณ์มหาวิทยาลัย

Figure 8C shows that the two globular domains of Ca^{2+} -CaM are connected by a flexible tether that can accommodate peptides of varying sizes. The binding of CaM-binding peptides is largely driven by hydrophobic interactions between hydrophobic anchor residues of the peptide with the hydrophobic surface cavities of CaM. Methionine residues, unusually abundant in CaM, play a particularly important role in the binding of target peptides. The methionine side chains are very flexible and the sulfur atom has a larger polarizability than carbon, resulting in stronger van der Waals interactions. The hydrophobic patches of each lobe are surrounded by several charged residues, creating charged binding channel outlets. The C-terminal end of the peptide-binding channel has a negatively charged rim, whereas the N-terminal hydrophobic patch has clusters of negatively and positively charged residues. This charge distribution on the molecular surface contributes to peptide binding via electrostatic interactions and determines the relative binding orientation of CaM-binding peptides. Basic residues at the N-terminus of the peptide form salt bridges with acidic residues surrounding the peptide-binding channel of the C-terminal lobe of CaM. Together, the structures of CaM illustrate how this class of proteins can function as extremely efficient Ca^{2+} sensors and on/off switches, allowing them to transduce Ca^{2+} signals with high efficiency and accuracy.

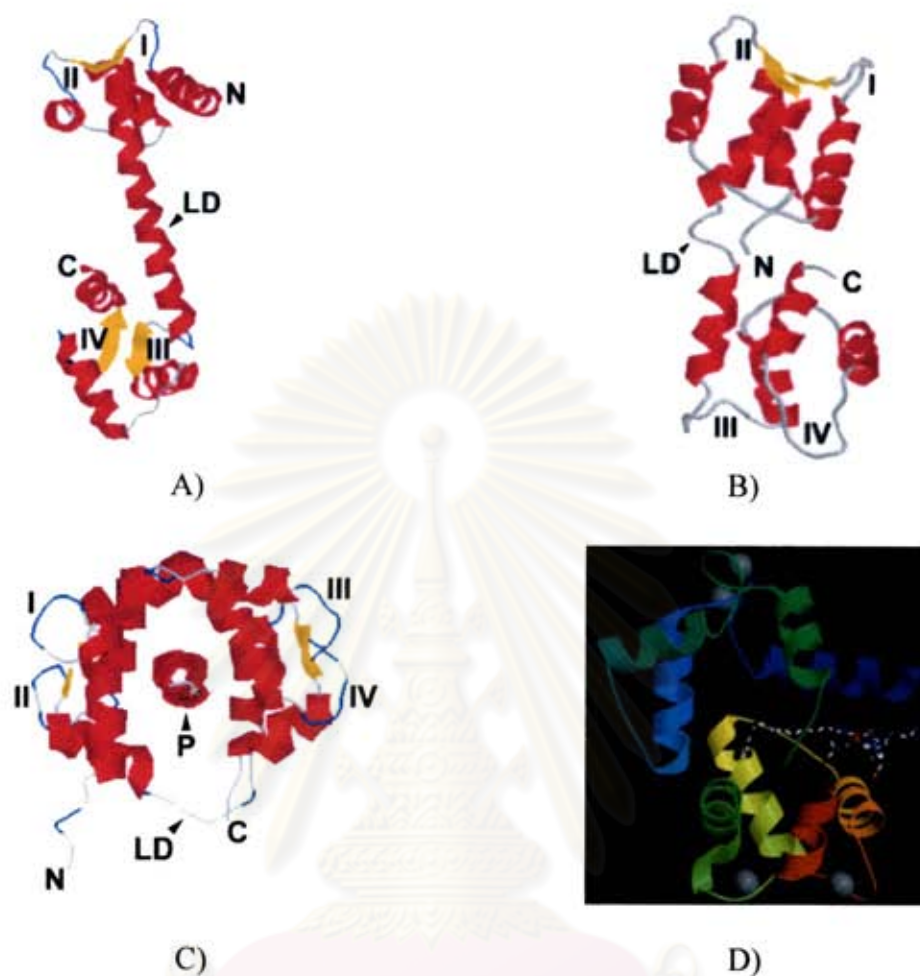


Figure 1.8: Ribbon presentations of calmodulin. (A) Ca^{2+} /CaM determined by X-ray crystallography, (B) globular domain of CaM (apo-CaM) determined by NMR spectroscopy, (C) and (D) Ca^{2+} /CaM-target peptide interaction; Peptide binding causes disruption of the flexible tether, bringing the globular domains closer to form a channel around the peptide. The majority of contacts between Ca^{2+} -CaM and target peptide are nonspecific van der Waals bonds made by residues in the hydrophobic surfaces. For (A) to (C), I-IV, Ca^{2+} -binding loops in the EF-hands; N, amino-termini of the CaM; C, carboxy-termini of the CaM; LD, central linker domain and P, target peptide. The α helix, loop and β -sheet are colored in red, blue and yellow respectively.

In plants, there are multiple *Cam* genes that code for either identical proteins or proteins containing a few conservative changes. These small changes in amino acid composition of CaM isoforms may contribute to differential interaction of each CaM isoform with target proteins. The striking example for differential regulation of CaMs comes from the studies with soybean CaM isoforms. In soybean there are five CaM isoforms (SCaM1 to -5). SCaM1, -2 and -3 are highly conserved compared to other plant CaM isoforms including Arabidopsis CaM isoforms whereas SCaM4 and -5 are divergent and show differences in 32 amino acids with the conserved group (Lee *et al.*, 1995). Soybean isoforms show differences in their relative abundance *in vivo*. The conserved isoforms are relatively abundant in their expression compared to divergent forms. Surprisingly, these divergent CaM isoforms are specifically induced by fungal elicitors or pathogen. These results provide evidence for the differential regulation of CaM isoforms in plants. All CaM isoforms activate phosphodiesterase (PDE) but differ in their activation of NAD kinase, calcineurin and nitricoxide synthase indicating Ca²⁺/CaM specificity between CaM isoforms and target proteins (Lee *et al.*, 1997). Differential regulation of enzymes by soybean divergent and conserved CaM isoforms has also been reported (Lee *et al.*, 2000). Although SCaM isoforms show similar patterns in protein blot overlay assays, they differ in their relative affinity in interacting with CaM binding proteins (Lee *et al.*, 1999). In another samples, two divergent CaM isoforms that are found in Arabidopsis do not interact with proteins that bind to conserved CaM isoforms (Kohler *et al.*, 2000). These studies suggest that conserved and divergent CaM isoforms may interact with different target proteins. There is considerable evidence to indicate that CaM genes are differentially expressed in response to different stimuli indicating that different CaM isoforms are

involved in mediating a specific signal. Three of the six Arabidopsis Cam genes (Cam1, -2 and -3) are inducible by touch stimulation indicating the presence of different cis-regulatory elements in their promoters. In potato, only one of the eight CaM isoforms (PCaM1) is inducible by touch (Takezawa *et al.*, 1995). The presence of multiple CaM isoforms adds further complexity to the Ca²⁺ mediated network. Even though a large family of genes encoding CaM and closely related proteins from several plants has been identified, with the exception of Arabidopsis and, families of genes encoding CaM and related proteins have not been extensively conducted in a whole-genome scale. In Rice CaM proteins, The full-length amino acid sequences were subjected to phylogenetic analysis. Tree construction using the neighbor-joining method and bootstrap analysis performed with ClustalX generated a consensus tree which is depicted in Figure 1.9. This analysis led to separate these proteins into six groups: 1-6. What defines a “true” CaM and distinguishes it from a CaM-like protein that serves a distinct role in vivo is still an open question. Different experimental approaches including biochemical and genetic analyses have been taken to address this question (Buaboocha *et al.*, 2002). by phylogenetic analysis based on amino acid sequence similarity, five proteins in group 1 that have the highest degrees of amino acid sequence identity ($\geq 97\%$) to known typical CaMs from other plant species were identified. Because of these high degrees of amino acid identity, and classified them as “true” CaMs that probably function as typical CaMs. They were named OsCaM1-1, OsCaM1-2, OsCaM1-3, OsCaM2 and OsCaM3. The *OsCam1-1* gene strongly increased under salt stress as early as 30 min and peaked at 1 hour after treatment. In expression pattern of genes encoding OsCaM1-1, OsCam1-2, OsCam1-3, OsCam2 and OsCam3 was evidently different under salt stress treatment. The stimuli that

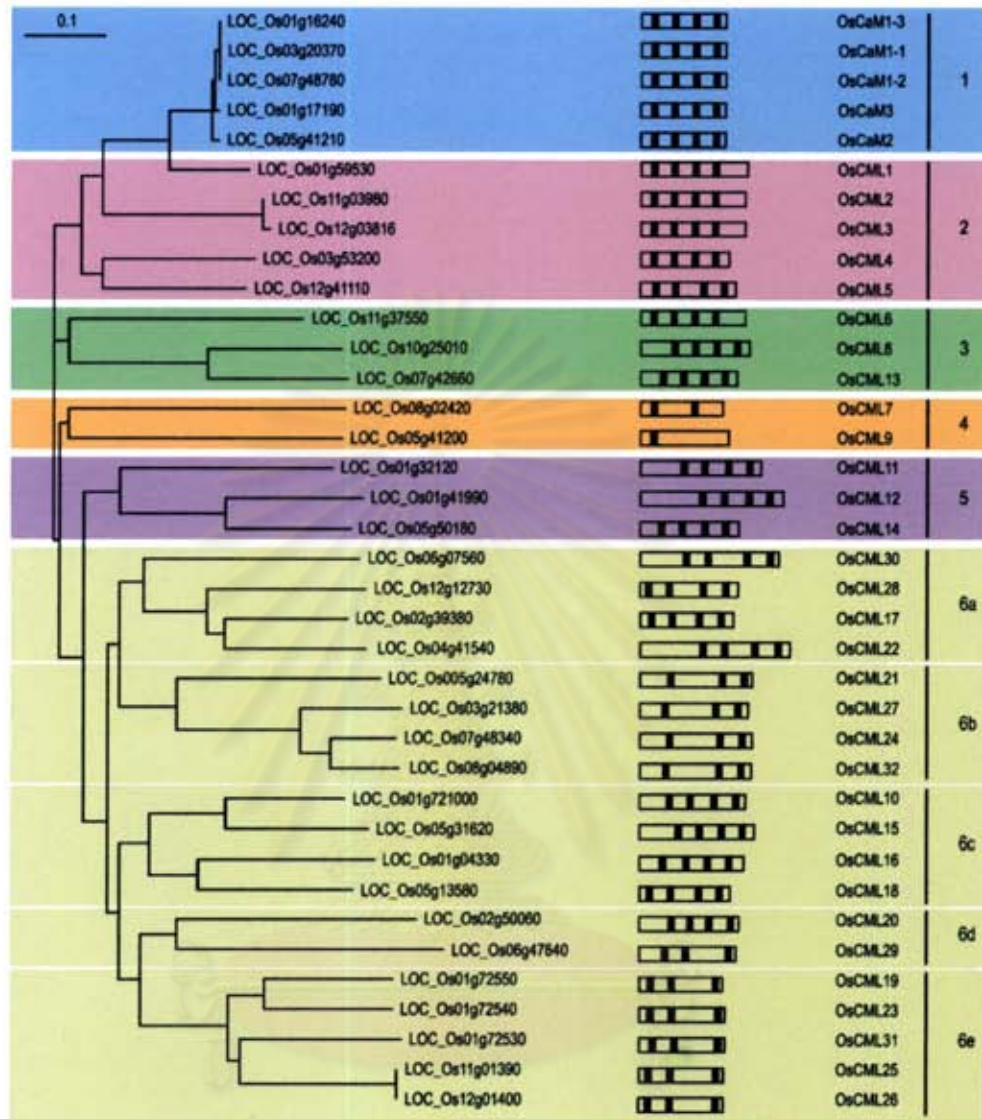


Figure 1.9: Neighbor-joining tree based on amino acid similarities among OsCaM and OsCML proteins. Tree construction using the neighbor-joining method and bootstrap analysis was performed with ClustalX. The TIGR gene identifier numbers are shown and the resulting groupings of CaM and CaM-like proteins designated as 1-6 are indicated on the right. Schematic diagrams of the OsCaM and OsCML open reading frames show their EF hand motif distribution. (Boonpurapong and Buaboocha, 2007).

strongly increased the level of steady state mRNA corresponding to *OsCam1-1* did not affect that of other *OsCam* genes. (Boonpurapong and Buaboocha, 2007).

Rice as a model monocot system

Rice is the world's single most important food crop and a primary food for more than a third of the world's population. Rice refers to two species which are *Oryza sativa* and *Oryza glaberrima*, native to tropical and subtropical southern and southeastern Asia and to Africa, respectively. Among the Asia domesticated rices, *Oryza sativa*, three sub-species are commonly distinguished based on geographic conditions, japonica (also called senica), indica and javanica, all of which include glutinous and non-glutinous varieties. The japonica varieties have narrow dark green leaves, medium-height tillers, and short to intermediate plant height. It is usually grown in cooler subtropics and temperate climates, such as Japan, Portugal, Spain, USSR, Italy, and France. The traditional indica rice varieties, widely grown throughout the tropics and subtropics, are tall and have heavy tillering with long, narrow, light green leaves. The Javanicas have flourished in the equatorial region of Indonesia.

In addition to their adaptation to climate, the three races differ in characteristics of the grain, including the content of amylose, the elongation of the grain, the temperature at which the grain becomes gelatinous and the aroma in cooking. The contrasts which most immediately strike the non-specialist are that indica rices have longer, more slender grains which usually separate when cooked, while japonica rices have shorter, rounder and more translucent grains which quickly become slightly sticky when cooked.

Oryza sativa is an annual grass as shown in Figure 1.10, which grows best when submerged in water. It grows in upland areas, irrigated areas, rainfed lowland areas, and flood-prone areas. Rice is highly adaptable and can be grown in diverse environments. It resembles a weed, 2 to 5 feet tall, depending on the variety and depth of submersion. Rice is constantly bombarded with environmental signals, both biotic and abiotic, some of which cause stress and limit the growth and development and affect the yield and quality. *Oryza sativa* was the cereal selected to be sequenced as a priority and has gained the status of the "model organism". Rice with its relatively small genome size (~430 Mb), ease of transformation, well developed genetics, availability of a dense physical map and molecular markers (Chen *et al.*, 2002), high degree of chromosomal co-linearity with other major cereal such as maize, wheat, barley and sorghum (Ohyanagi *et al.*, 2006) and together with its complete genome sequence is considered a model monocot system. It is being used to understand several fundamental problems of plant physiology, growth and developmental processes ranging from elucidation of a single gene function to whole metabolic pathway engineering. In addition, rice shares extensive synteny among other cereals thereby increasing the utility of this system. These, together with availability of ~28,000 full length cDNAs, a large number of expressed sequence tags, yeast artificial chromosomes, bacterial artificial chromosomes, P1-derived artificial chromosomes, libraries and rich forward and reverse genetics resources have made rice a worthy forerunner among the plants especially among the cereals.



Figure 1.10: Structural features of *Oryza sativa* L. (wikipedia, 2010 : online)

ศูนย์วิทยทรัพยากร
จุฬาลงกรณ์มหาวิทยาลัย

Relatively little is known about NAD kinase activity and its regulation in plant cells. Therefore, a major goal of the work presented in this thesis was to examine the activity of NAD kinase of rice *Oryza sativa* L., a model plant for monocots and one of the most economically important crops in Thailand and the world, and determine the regulation of NAD kinase activity by Ca^{2+} /CaM.

Objectives of the thesis

1. To clone and express rice *NADK* genes in *E.coli* and characterize the recombinant proteins.
2. To determine NAD kinase activity and partially purify NAD kinase from rice *Oryza sativa* L. cultivar KDML105 under salt stress.
3. To determine the effect of OsCaM1-1 on NAD kinase.

ศูนย์วิทยทรัพยากร
จุฬาลงกรณ์มหาวิทยาลัย

CHAPTER II

MATERIALS AND METHODS

2.1 Materials

2.1.1 Rice seeds

Rice *Oryza sativa* L. cultivar Khao Dok Ma Li 105 (KDML105)

2.1.2 Instruments

Autoclave: Labo Autoclave MLS-3020 (Sanyo Electric Co., Ltd., Japan)

Automatic micropipette: Pipetman P2, P20, P100, P1000 (Gilson Medical Electronics S.A., France)

Balance: Sartorius CP423s (Scientific Promotion Co. USA)

Biophotometer (Eppendorf, Germany)

-20 °C Freezer (Sharp, Japan)

Gel documentation apparatus: Gel Doc™ (Syngene, England)

Gel electrophoresis apparatus: Gel mate 2000 (Toyobo, Japan)

Incubator: BM-600 (Mettler GmbH, Germany)

Incubator shaker: Innova™ 4000 (New Brunswick Scientific, UK)

Laminar flow: HS-124 (International Scientific Supply Co., Ltd., USA)

Magnetic stirrer: Fisherbrand (Fisher Scientific, USA)

Magnetic stirrer and heater: Cerastir (Clifton, USA)

Mastercycler gradient PCR system (Eppendorf, Germany)
Microcentrifuge: PMC-880 (Tomy Kogyo Co., Ltd., Japan)
Microtiter plate reader (BMG Labtech)
Microwave oven (Panasonic, Japan)
Orbital shaker (Labinco, Taiwan)
pH meter: pH900 (Precisa, Germany)
PCR workstation Model#P-036 (Scientific Co., USA)
Power supply: Power PAC 1000 (Bio-RAD Laboratories, USA)
Refrigerated centrifuge: 5804R (Eppendorf, Germany)
Refrigerated centrifuge: 5417R (Eppendorf, Germany)
Spectrophotometer: DU[®] 640 (Beckman Coulter, USA)
Vortex mixer: Model K 550-GE (Scientific Inc., USA)

2.1.3 Materials

96-well plate: (NUNC, Denmark)
Butyl-Toyopearl (TOSOH, Japan)
DEAE-Toyopearl (TOSOH, Japan)
Filter paper: Whatman No.1 (Whatman International Ltd., England)
0.6- and 1.5-ml microcentrifuge tube (Axygen Hayward, USA)
0.22 μ m Millipore membrane filter (Millipore, USA)
Nipro disposable syringe (Nissho, Japan)
Nitrocellulose membrane: Protran (Whatman, USA)
0.2 ml-PCR thin wall microcentrifuge tube (Eppendorf, Germany)
10-, 100-, 1000- μ l pipette tips (Axygen Hayward, USA)

PVDF membranes (Macherey-Nagel, Germany)

Quartz cuvette: Hellma 105.201-QS (sigma-aldrich,USA)

2.1.4 Chemicals and reagents

Absolute ethanol (BDH, England)

Adenosine 5'-triphosphate (ATP) disodium salt hydrate (Sigma Chemical Co., USA)

Agar (Merck, Germany)

Agarose (FMC Bioproducts, USA)

Alkaline phosphatase-conjugated rabbit anti-mouse IgG (Jackson ImmunoResearch Laboratories, Inc.)

Ammonium persulfate: $(\text{NH}_4)_2\text{S}_2\text{O}_8$ (Sigma Chemical Co., USA)

Anti-His antiserum (GE Healthcare, USA)

Bacto tryptone (Difco, USA)

Bacto yeast extract (Difco, USA)

BenchMark™ His-tagged Protein Standard (Invitrogen, USA)

Benzamidine hydrochloride (Sigma Chemical Co., USA)

Beta-mercaptoethanol (Fluka, Switzerland)

Boric acid (Merck, Germany)

Bovine Serum Albumin (Sigma Chemical Co., USA)

5-Bromo-4-chloro-3-indole- β -D-galactopyranoside; X-gal (Sigma Chemical co., USA)

5-Bromo-4-chloro-indolyl phosphate: BCIP (Fermentas, USA)

Bromophenol blue (Merck, Germany)

Calcium chloride (Carlo Erba Reagenti, Italy)

Chloroform (Merck, Germany)

Coomassie brilliant blue R-250 (Bio Basic Inc., USA)

Copper sulfate (Carlo Erba Reagenti, Italy)

dATP, dCTP, dGTP, and dTTP (Fermentas Inc., USA)

2,6-Dichlorobenzene-indophenol sodium salt: DCIP (Sigma Chemical Co., USA)

Dimethyl sulfoxide: DMSO C_6H_6SO (Finnzymes, Finland)

di-Sodium hydrogen orthophosphate anhydrous: Na_2HPO_4 (Carlo Erba Reagenti, Italy)

Dithiothreitol (Sigma Chemical Co., USA)

Ethidium Bromide (Sigma Chemical Co., USA)

Ethylene diamine tetraacetic acid: EDTA (Carlo Erba Reagenti, Italy)

Ethylene glycol-bis (β -aminoethylether)-N,N,N',N'-tetraacetic acid: EGTA (Sigma Chemical Co., USA)

Formaldehyde (Sigma Chemical Co., USA)

D-Glucose 6-phosphate disodium salt hydrate (Fluka, Switzerland)

Glacial acetic acid (Carlo Erba Reagenti, Italy)

Glycerol (BDH, England)

Glycine (Sigma Chemical Co., USA)

Hydrochloric acid (Merck, Germany)

Iso-1-thio- β -D-thiogalactopyranoside: IPTG (Serva, Germany)

Isopropanol (Merck, Germany)

Lambda DNA (Promega Co., USA)

Magnesium sulfate (Sigma Chemical Co., USA)

Methanol (Merck, Germany)

Nickel(II) sulfate hexahydrate: NiSO₄ (Sigma Chemical Co., USA)

β-Nicotinamide adenine dinucleotide: NAD (Sigma Chemical Co., USA)

Nitroblue tetrazolium: NBT (Fermentas, Inc., USA)

Phenazine methosulfate: PMS (Sigma Chemical Co., USA)

Phenol crystal (BDH, England)

Phenylmethylsulfonyl fluoride: PMSF (USB, USA)

Potassium chloride (Carlo Erba Reagenti, Italy)

Sodium acetate (Carlo Erba Reagenti, Italy)

Sodium chloride (Carlo Erba Reagenti, Italy)

Sodium dodecyl sulfate (Sigma Chemical Co., USA)

Sodium dihydrogen orthophosphate (Carlo Erba Reagenti, Italy)

Sodium hydroxide (Carlo Erba Reagenti, Italy)

TEMED (CH₃)₂NCH₂CH₂N(CH₃)₂ (Amresco, USA)

Tris-(hydroxyl methyl)-aminomethane (Fluka, Switzerland)

Triton X-100 (Merck, Germany)

Tween 20 (Bio-RAD Laboratories, USA)

2.1.5 Enzymes

DNA polymerase, large (Klenow) fragment (New England Biolabs, Inc., USA)

DyNAzyme II DNA polymerase (Finnzymes, Finland)

Glucose-6-phosphate dehydrogenase from baker's yeast (Sigma Chemical Co., USA)

Restriction endonucleases: *Sall*, *HindIII* (Fermentas, Inc., USA),
NdeI, *VspI* (New England Biolabs, Inc., USA)

T4 DNA ligase (New England Biolabs Inc., USA)

Taq DNA polymerase (Fermentus, Inc., USA)

Vent DNA polymerase (New England Biolabs Inc., USA)

2.1.6 Kits and Plasmids

Expression vector: pET21a(+) (Merck, Germany)

Gel/PCR DNA fragments extraction kit (Geneaid, Taiwan)

High-speed plasmid mini kit (Geneaid, Taiwan)

pTZ57R/T cloning vector (Fermentus, Inc., USA)

2.1.7 Radioactive

Tran-³⁵S-Label methionine (1175 Ci/mmol) (MP Biomedicals, USA)

2.1.8 Antibiotics

Ampicillin (Sigma Chemical Co., USA)

2.1.9 Oligonucleotide primers

The oligonucleotide primers were synthesized by Operon, Germany.

2.1.10 Microorganisms

Escherichia coli

strain Rosetta(DE3)pLysS

strain Rosetta-gami

strain XL1-Blue: MRF'

2.1.11 Software

BlastX (<http://www.ncbi.nlm.nih.gov/blast/Blast.cgi>)

ClustalW (<http://www.ebi.ac.uk/Tools/clustalw2/index.html>)

ExPASy ProtParam (<http://au.expasy.org/tools/protparam.html>)

GENETYX version 7.0 program (Software Development Inc.)

SECentral (Scientific & Educational Software)

2.2 Bacterial growth medium

Luria-Bertani broth (LB medium) (Maniatis *et al.*, 1982)

LB medium containing 1% peptone, 0.5% NaCl and 0.5% yeast extract was prepared and pH adjusted to 7.2 with NaOH. For agar plates, it was supplemented with 1.5% (w/v) agar. The medium was autoclaved for 20 minutes at 121° C, 1.2 kg/cm². If needed, the medium was then supplemented with a selected antibiotic drug.

2.3 Methods

2.3.1 Quantitative method for determination of DNA concentration

The concentration of DNA was determined by measuring the absorbance at 260 nm (A_{260}) and estimated in $\mu\text{g/ml}$ using the equation: $[\text{DNA}] (\mu\text{g/ml}) = A_{260} \times \text{dilution factor} \times 50$ as an absorbance at 260 nm of 1.0 corresponds to 50 $\mu\text{g/ml}$ of DNA (Sambrook *et al.*, 1989).

2.3.2 Sequence analysis

Sequences of the cDNA clones encoding putative NADKs (designated *NADK1* and *NADK2*) were obtained from the rice databases via the Rice Genome Annotation Project (<http://rice.plantbiology.msu.edu/>) and the Rice Annotation Project Database (RAP-DB) at the NIAS (<http://rapdb.dna.affrc.go.jp/>). Sequencing of the cDNA clones was carried out at Macrogen, Korea. Multiple sequence alignment was performed using ClustalW (<http://www.ebi.ac.uk/clustalw>).

2.3.3 Cloning of the NAD kinase genes into cloning vector (pTZ57R/T)

2.3.3.1) Primer design

The genes (and their GenBank Accession numbers) used were as follows: *NADK1* (AK099730) and *NADK2* (AK065215). Based on the cDNA sequences encoding the *NADK1* and *NADK2* genes, a pair of oligonucleotide primers for amplifying the coding region of each *NADK* gene was designed using the SECentral program (Scientific & Educational Software) with *NdeI* and *Sall* restriction sites engineered at the 5' and 3' ends, respectively. They were checked for minimal self-priming and primer dimer formation. The sequences and the length of the all oligonucleotide primers are shown in Table 2.1.

Table 2.1 The sequences and the length of oligonucleotide primers used for cloning of the NAD kinase genes

Gene	Primer	Sequence	Length
<i>NADK1</i>	Forward	5' -GCCCATATGTCGCTCGACGAGCTTCCGCAC- 3'	30
	Reverse	5' -CTGGTCGACATCACGCGGGCCGTCGAATGA- 3'	30
<i>NADK2</i>	Forward	5' -TGCCATATGCTCGCCGTCTGCGCGCGGCAC- 3'	30
	Reverse	5' -TAAGTCGACTAATGCCTTCTGGTCCAGTCG- 3'	30

2.3.3.2) PCR amplification

The coding regions of *NADK1* and *NADK2* genes were amplified using their respective *NADK* cDNA clones, which were obtained from DNA Bank of the National Institute of Agrobiological Science (NIAS), as template. For *NADK1*, the amplification reaction was performed in a 25- μ l reaction that contained 1X NEB ThermoPol buffer, 2.5 mM MgCl₂, 50-100 ng of DNA template, 200 μ M each of dATP, dCTP, dGTP and dTTP, 1 μ M of each primer and 5 units of *Vent* DNA polymerase (New England Biolabs, Inc., USA). PCR amplification was performed as follows: pre-denaturation at 94 °C for 5 minutes, 30 cycles of denaturation at 94°C for 1 minute, annealing vary 69-72°C for 1 minute and extension at 72°C for 1 minute. In the final extension step, 5 units of *Tag* DNA polymerase (Fermentus, Inc., USA) were added and incubated at 72 °C for 10 minutes to add a dA at the 3' end. For *NADK2*, the amplification reaction was performed in a 50- μ l reaction that contained 1X DyNAzyme II DNA polymerase buffer, 2.5 mM MgCl₂, 50-100 ng of DNA template, 200 μ M each of dATP, dCTP, dGTP and dTTP, 1 μ M of each primer and 5 unit of DyNAzyme

II DNA polymerase (Finnzymes, Finland). PCR amplification was performed as follows: pre-denaturation at 94 °C for 5 minutes, 30 cycles of denaturation at 94°C for 30 seconds, annealing at 60°C for 30 seconds and extension at 72°C for 1 minute. The final extension step performed at 72 °C for 10 minutes. PCR products were separated by agarose gel electrophoresis and visualized by ethidium bromide staining.

2.3.3.3) Agarose gel electrophoresis

Standard agarose gel electrophoresis method was used to separate, identify, and purify DNA fragments. The concentration of agarose gel used varied with the size of the DNA fragments to be separated. The DNA samples were run on an agarose gel in Tris-acetate-EDTA (TAE) buffer. Before loading into an agarose gel, DNA samples were mixed with 10% (v/v) DNA gel loading buffer (0.1M EDTA/NaOH pH 7.5, 50% (v/v) of glycerol, 1% (w/v) of SDS, 0.5 (w/v) of xylene cyanol FF, and 0.5 (w/v) of Bromophenol blue). Electrophoresis was performed at a constant voltage of 100 volts until the bromophenol blue dye migrated to an appropriate distance through the gel. After electrophoresis, the gel was stained with ethidium bromide solution (5-10 µg/ml in distilled water) for 5 minutes and destained with distilled water for 10 minutes. DNA fragments on the agarose gel were visualized on UV light transilluminator and photographed. The concentration and molecular weight of DNA fragments was determined by comparison of the band intensity and the relative mobility with those of the standard λ /*Hind*III DNA markers.

2.3.3.4) Extraction of DNA fragments from agarose gel

The amplification products generated by PCR were purified from agarose gel using Geneaid gel extraction protocol (Geneaid, Taiwan). After electrophoresis, the desired DNA fragment was excised as gel slice from an agarose gel using a scalpel and transferred to a microcentrifuge tube. Five hundred μl of DF buffer was added and the mixture was incubated for 10 minutes at 55-60°C or until the gel slice has been completely dissolved. During incubation, the tube was inverted every 2-3 minutes. The mixture was then transferred into a DF column and the column was centrifuged at 12,000 rpm for 1 minute. The flow through solution was discarded. Then 400 μl of W1 buffer was added and the column was centrifuged at 12,000 rpm for 1 minute. The flow through was discarded and 600 μl of Wash buffer was added to the DF column. The column was let standing for 1 minute and centrifuged at 12,000 rpm for 1 minute, then the flow through solution was discarded. The DF column was centrifuged again for 3 minutes to remove a trace element of the Wash buffer. The DF column was then placed into a sterile 1.5 ml microcentrifuge tube. DNA was eluted by an addition of 15-50 μl of sterilized water to the center of the DF column. The column was let standing for 2 minutes, and then centrifuged at 12,000 rpm for 2 minutes to elute the DNA. The DNA concentration was determined by agarose gel electrophoresis.

2.3.3.5) Ligation of PCR products to pTZ57R/T

After the PCR products were purified from the agarose gel, they were ligated to the pTZ57R/T vector (see in Appendix A). A suitable molecular ratio

between vector and inserted DNA in a mixture of cohesive-end ligation is usually 1:3. To calculate the appropriate amount of the PCR product (insert) used in a ligation reaction, the following equation was used:

$$\frac{\text{ng of vector} \times \text{kb size of insert}}{\text{kb size of vector}} \times \text{insert : vector molar ratio} = \text{ng of insert}$$

The 20 μl of ligation mixture, which contained appropriate amounts of the vector DNA and the gene fragment, 1x ligation buffer and 10 U of T4 DNA ligase, was incubated overnight at 16°C.

2.3.3.6) Transformation of ligated products to *E. coli* host cells by CaCl_2 method

a) Preparation of *E. coli* competent cells

Competent *E. coli* strain XL1-Blue was prepared according to the method of Sambrook *et al.* (1989). Three ml of LB broth (1% (w/v) tryptone, 0.5% (w/v) yeast extract, and 1% (w/v) NaCl, pH 7.2) was inoculated with a single colony of *E. coli* strain XL1-Blue and incubated at 37 °C with shaking at 250 rpm overnight. Fifty ml of LB medium was then inoculated with two percents of the starting culture and the culture was incubated at 37 °C with shaking at 250 rpm for 3-4 hours until the optical density at 600 nm (OD_{600}) of the culture reached 0.45-0.55. The culture was chilled on ice slurry for 15-30 minutes and the cells were harvested by centrifugation at 8,000 xg at 4 °C for 10 minutes. The supernatant was decanted and the cell pellet was washed with 25 ml of fresh ice-cold 150 mM CaCl_2 , resuspended by gently mixing and centrifuged at 8,000 xg at 4 °C for 10 minutes. The supernatant was discarded. The cells were resuspended

with 25 ml of fresh ice-cold 150 mM CaCl₂ and incubated on ice for 30 minutes, then centrifuged at 8,000 xg at 4 °C for 15 minutes. The supernatant was discarded and finally, the cells were resuspended in 1 ml of fresh ice-cold 150 mM CaCl₂ and incubated on ice for 1 hour. These cells were used as freshly prepared competent cells.

b) Transformation by CaCl₂ method

In this study, competent cells were transformed with the recombinant plasmids by CaCl₂ method. Sixty microliters of competent cells were mixed well with 10 µl of the ligation mixture and then placed on ice for 30 minutes. The cells were heat-shocked for 90 seconds in a waterbath set to 42 °C and quickly incubated on ice for 5 minutes. Five hundred µl of LB medium was added then the cell suspension was incubated at 37 °C with shaking at 250 rpm for 1 hour and the cells were spun down to retain 200 µl. Finally, the cell suspension was spread onto LB agar plates containing 100 µg/ml ampicillin, 10 µl of 0.1 M Iso-1-thio-β-D-thiogalactopyranoside (IPTG), and 50 µl of 20 mg/ml 5-Bromo-4-chloro-3-indole-beta-D-galactopyranoside (X-gal) (on a plate with the diameter of 10 cm) and incubated at 37 °C overnight. The recombinant clones containing the inserted DNA were white while those without inserted DNA were blue. The white colonies which potentially contained recombinant plasmids were selected and analyzed by restriction enzyme digestion.

2.3.3.7) Analysis of recombinant plasmids

a) Plasmid DNA isolation by alkaline lysis method

A single colony of recombinant cells was selected and grown in 5 ml of LB broth (1% (w/v) tryptone, 0.5% (w/v) yeast extract, and 1% (w/v) NaCl) containing 100 µg/ml of ampicillin overnight at 37 °C with shaking at 250 rpm. The cells were spun in a microcentrifuge at 8000×g for 10 minutes at 4 °C. The cells were resuspended in 300 µl of Lysis buffer (50 mM of Tris base, 10 mM of Na₂EDTA.H₂O and 100 µg/ml of RNaseA) and mixed by vortexing. The suspension was allowed to stand for 5 minutes at room temperature, then 300 µl of Alkaline-SDS solution (200mM NaOH and 1% SDS) was added and the suspension was inverted gently several times to mix and allowed to stand on ice of 5 minutes. Three hundred µl of High salt solution (3M of potassium acetate) was then added to the mixture. The suspension was mixed gently and allowed to stand for 10 minutes on ice. The insoluble salt-genomic DNA precipitate was then removed by centrifugation at 14,000 rpm at 4°C for 15 minutes. The supernatant was transferred to a fresh microcentrifuge tube and the nucleic acid was precipitated by adding 480 µl (0.6 volumes) of isopropanol. The sample was mixed thoroughly and immediately centrifuged for 20 minutes to collect the precipitated DNA. The DNA pellet was resuspended in 90 µl of sterile water and the suspension was vortexed gently. Ten µl of 3 M sodium acetate, pH 7 and 300 µl of cold absolute ethanol were added to the DNA solution, then mixed and chilled on ice for 30 minutes. The DNA was collected by centrifuging at 14,000×g for 20 minutes at 4 °C. The pellet was rinsed with 300 µl of 70% ethanol and allowed to dry for 10-15 minutes. The plasmid DNA was resuspended with 30 µl of sterile water and stored at -20 °C.

b) Restriction enzyme analysis

The recombinant plasmids isolated by the alkaline lysis method were analyzed for the presence of the interested cloned fragments by digestion with appropriate restriction endonucleases. All restriction digestion was performed in the conditions recommended by the enzyme manufacturer. The *NADK* recombinant plasmids were digested with *NdeI* and *SalI*. Each of the reactions was carried out in a 10 µl-mixture at 37 °C. The DNA products were analyzed by 1% agarose gel electrophoresis. The size of DNA fragments was determined by comparing with those of the λ / *HindIII* marker.

2.3.4 Cloning of *NADK* genes into expression vector pET21a(+)

2.3.4.1) Vector DNA preparation

The *E. coli* XL-1 Blue, which contained pET21a(+) plasmids was grown in 5 ml LB medium containing 100 µg/ml ampicillin at 37°C with shaking at 250 rpm for 16 hours. The pET21a(+) vector was extracted using Alkaline lysis method as described above. The expression vector pET21a(+) was linearized with *NdeI* and *SalI* digestion using the conditions recommended by the enzyme manufacturer. The reaction was incubated at 37°C for 3-4 hours. The linearized pET21a(+) was harvested from agarose gel using Geneaid gel extraction protocol.

2.3.4.2) Preparation of *NADK* gene fragments

After the *NADK* genes were cloned into pTZ57R/T and the recombinant clones were checked with restriction enzyme digestion. The recombinant

plasmids that containing *NADK* genes were extracted by using Alkaline lysis method as described above. The *NADK* genes were digested with *NdeI* and *Sall* using the conditions recommended by the enzyme manufacturer. The reaction was incubated at 37°C overnight. The *NADK* gene fragments were harvested from agarose gel using Geneaid gel extraction protocol.

2.3.4.3) Ligation of *NADK* gene fragments to pET21a(+)

To clone *NADK* genes into the pET21a(+) expression vector, the prepared gene fragments were ligated to the linearized vector. A suitable molecular ratio between vector and inserted DNA in a mixture of 1:5 was used. The 20 µl of ligation mixture containing appropriate amounts of the vector DNA and the gene fragment, 1x ligation buffer and 10 U of T4 DNA ligase, was incubated overnight at 16°C.

2.3.4.4) Transformation of *E. coli* XL-1Blue cell by CaCl₂ method

Competent cells were prepared as described above. To transform the *E. coli* cells, the ligation mixtures were added to the the competent cell and then placed on ice for 30 minutes. The mixture was heat-shocked for 90 seconds in a water bath set to 42 °C and the cells were quickly incubated on ice for 5 minutes, 500 µl of LB medium was then added the cell suspension and the suspension was incubated at 37 °C with shaking at 250 rpm for 1 hour and the cells were spun down to retain 200 µl. Finally, the cell suspension was spread onto the LB agar plates containing 100 µg/ml ampicillin and the plates were incubated at 37 °C

overnight. The recombinant clones which contained the pET21a(+) vector could growth on LB agar plates containing ampicillin. A single colony was selected and analyzed by restriction enzyme digestion.

2.3.4.5) Analysis of recombinant plasmids

A single colony of recombinant cells was selected and grown in 5 ml of LB broth (1% (w/v) tryptone, 0.5% (w/v) yeast extract, and 1% (w/v) NaCl) containing 100 µg/ml of ampicillin overnight at 37 °C with shaking at 250 rpm. The recombinant plasmids were extracted using alkaline lysis method. The recombinant plasmids were digested with *NdeI* and *SalI*. The reaction was incubated at 37°C overnight and the products were analyzed by 1% agarose gel electrophoresis. The size of the DNA insert was determined by comparing with those of the λ / *HindIII* marker.

2.3.5 Sequence analysis

The recombinant plasmids were extracted by High Speed plasmid Mini kit (Geneaid, Taiwan) and nucleotide sequences of the inserts were determined. DNA sequencing was carried out at Macrogen, Korea. The sequencing primers used were the same as the primers for PCR amplification.

2.4 Expression of the *NADK1* and *NADK2* genes

To produce recombinant proteins, the *NADK1* and *NADK2* genes cloned in the expression vector pET21a(+) were expressed in *E.coli* Rosetta (DE3) and

Rosetta-gami, respectively. Both proteins were expressed in *E.coli* as described below.

2.4.1 Preparation of cell expression

The recombinant pET21a(+) plasmids containing *NADK* genes were transformed into *E.coli* strain Rosetta (DE3) or Rosetta-gami cells by heat shock method. The competent cells were prepared as described above. The recombinant plasmids were mixed with the competent cells and then placed on ice for 30 minutes. The cells were heat-shocked for 90 seconds in a water bath set to 42 °C and quickly incubated on ice for 5 minutes, 500 µl of LB medium was added, then the cell suspension was incubated at 37 °C with shaking at 250 rpm for 1 hour. Finally, fifty µl of the cell suspension was spread onto the LB agar plates containing 100 µg/ml ampicillin and incubated at 37 °C overnight.

2.4.2 Optimization for *NADK* genes expression

A single colony of recombinant cells was grown overnight at 37°C for 16 hours in 5 ml of LB medium, pH 7.0, containing 100 µg/ml ampicillin. The starter was diluted 1:100 into the same medium and cultured at 37°C with shaking for 3 - 4 hours until the optical density at 600 nm (OD₆₀₀) of the culture reached 0.6. Protein production was induced by adding IPTG to the final concentration of 0.1 mM for *NADK1* and 0.6 mM for *NADK2* and the incubation was continued at 37°C for 3 hours. The cells were harvested by centrifugation at 8000xg for 15 minutes, and then the cell pellets were washed twice in cold wash

buffer (50 mM Tris-HCl, pH 7.5) and the cells were collected again by centrifugation. The cell pellet was stored at -80°C until it was sonicated. In crude extract preparation, the cell pellet was resuspended in cold lysis buffer (50 mM Tris-HCl, pH 7.5, 1 mM EDTA, and 1 mM DTT), incubated on ice for 30 minutes and then broken by sonication on ice. Unbroken cells and cell debris were removed by centrifugation at $27000\times g$ for 30 minutes. The supernatant was kept at 4°C until it was used.

2.4.3 Determination of protein concentration

Protein concentration was determined by the modified method of Bradford, M. M. (1976). The reaction mixture contained $100\ \mu\text{l}$ of the protein sample and 1 ml of Bradford solution, which was prepared as described in (Appendix B). The combined solution was mixed by vortexing. Protein concentration of the sample was determined by measuring the absorbance at 595 nm after letting the mixture stand at room temperature for 5 minutes but before 1 hour. The concentration was calculated using the standard curve of protein standards ($0\text{-}20\ \mu\text{l}$ of 1 mg/ml BSA).

2.4.4 SDS-polyacrylamide gel electrophoresis

The SDS-PAGE system was performed according to the method of Bollag *et al.*, 1996. The slab gel system contained 0.1% SDS (W/V) and consisted of 12% separating gel and 3.9% stacking gel. Tris-glycine (25 mM Tris, 192 mM glycine and 0.1% SDS), pH 8.3 was used as electrode buffer. The gel preparation was described in (Appendix B). The protein samples were mixed

with 5x sample buffer (60 mM Tris-HCl pH 6.9, 79% glycerol, 2% SDS, 0.1% bromophenol blue and 14.4 mM β -mercaptoethanol) by the ratio of 5: 1 and boiled for 10 minutes before loading to the gel. The electrophoresis was run from the cathode towards the anode at a constant current of 20 mA per gel at room temperature. The molecular weight marker proteins containing β -galactosidase (116,000 Da), bovine serum albumin (66,200 Da), ovalbumin (45,000 Da), lactate dehydrogenase (35,000 Da), restriction endonuclease Bsp98I (25,000 Da), β -lactoglobulin (18,400 Da) and lysozyme (14,400 Da) were used.

2.4.5 Protein staining

The gel was transferred to a box containing Coomassie staining solution (0.25% Coomassie Blue R-250, 50% methanol, and 7% glacial acetic acid) The gel was stained for 1 hour at room temperature with gentle shaking. After staining, the stain solution was poured off, the gel was briefly rinsed with water and incubated with the Coomassie destaining solution (10% methanol and 7% glacial acetic acid). The gel was gently destained for several times until protein bands were readily visible.

2.5 Purification of the *NADKI* proteins

2.5.1 Crude extract preparation

For the large scale protein expression, a single colony of recombinant cells was grown overnight at 37 °C for 16 hours in 25 ml of LB medium, pH 7.0, containing 100 μ g/ml ampicillin. Then, 1,000 ml of the same medium was inoculated with 2.0% of the starter culture and was cultured at 37 °C with shaking

for 3-4 hours until the optical density at 600 nm (OD_{600}) of the culture reached 0.6. Protein production was induced by adding IPTG to the final concentration of 0.1 mM and the incubation was continued at 37 °C for 4 hours. The cells were harvested by centrifugation at 8,000xg for 15 minutes, then the cell pellet was washed twice in cold wash buffer (20 mM Phosphate buffer, pH 7.5) and collected again by centrifugation. The cell pellet was stored at -80 °C until it was sonicated. In crude extract preparation, the cell pellet was resuspended in 50 ml of cold lysis buffer (20 mM Phosphate buffer, pH 7.5, 1 mM EDTA, and 1 mM DTT), incubated on ice for 30 minutes and then broken by sonication on ice. Unbroken cells and cell debris were removed by centrifugation at 20,000xg for 30 minutes. The supernatant was kept at 4 °C until it was used.

2.5.2 *NADKI* protein purification by Nickel Sepharose column

The high performance Ni sepharose was packed into a small column and washed with 5 column volumes of distilled water and 5-10 column volumes of binding buffer (20 mM phosphate buffer, pH 7.4, containing 25 mM imidazole), respectively. The soluble protein fraction was loaded into the column at room temperature. The flow through was collected by a gravity flow. The column was washed with the binding buffer followed by wash buffer (20 mM phosphate buffer pH 7.4 containing 25 mM imidazole) to remove unbound proteins. After washing, the protein was eluted with elution buffer (20 mM phosphate buffer, pH 7.4, containing 200 mM imidazole). The presence and purity of the purified protein was evaluated by SDS-polyacrylamide gel electrophoresis as described above. The imidazole was

removed by dialysis for at least 4 hours at 4 °C against 20 mM phosphate buffer, pH 7.4 twice.

2.6 Western blot detection of the His-tagged protein

After running the SDS-PAGE, the SDS-gel slab was removed from the glass plates. The membrane, gel and filter paper were soaked in transfer buffer (25 mM Tris base, 150 mM glycine and 20% methanol) for 30 minutes before they were consequently laid on the Trans-Blot® SD (Bio-Rad) membrane. The filter paper was placed on the platform, followed by the membrane, the gel and the filter paper, respectively, as shown in Figure 2.1.



ศูนย์วิทยทรัพยากร
จุฬาลงกรณ์มหาวิทยาลัย

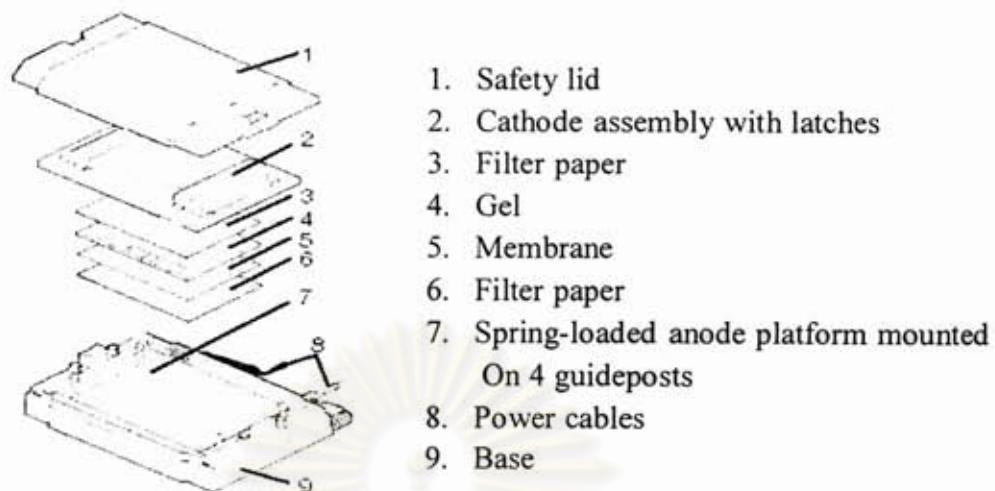


Figure 2.1 Exploded view of the Trans-Blot[®] SD (Bio-Rad).

ศูนย์วิทยทรัพยากร
จุฬาลงกรณ์มหาวิทยาลัย

Protein transfer was performed at a constant current of 90 mA from the cathode towards the anode for 90 minutes. After transferring the proteins from the gel to the membrane, the orientation of the gel was marked on the membrane. The membrane was then transferred to an appropriate container (petri dish) and incubated in blocking buffer (1× PBS buffer [10 mM phosphate buffer, 150 mM NaCl, pH 7.4, 0.05% (v/v) Tween™-20 and 5% (w/v) non-fat dry milk]) at room temperature overnight with gentle shaking. The membrane was washed 3 times for 10 minutes each in washing buffer (PBS-Tween buffer [1× PBS buffer (10 mM phosphate buffer, 150 mM NaCl, pH 7.4, 0.025% (v/v) Tween™-20) and incubated in an anti-His antibody solution (1 : 3000 dilution) in the washing buffer containing 1% (w/v) non-fat dry milk, at ambient temperature with gentle mixing for 3 hours. Then, the membrane was washed 3 times for 10 minutes each in washing buffer and then incubated in a secondary antibody solution (1 : 2500 dilution) in the washing buffer containing 1% (w/v) non-fat dry milk with agitation for 1 hour. The membrane was washed 3 times for 10 minutes each in washing buffer at room temperature. The bound antibody was detected by color development using NBT/BCIP (Fermentas) dissolved in 100 mM Tris- HCl, 100 mM NaCl and 50 mM MgCl₂, pH 9.5 as substrate.

2.7 NAD kinase assay

2.7.1 In-gel activity staining

The native polyacrylamide gel using 7% separating gel and 4% stacking gel was prepared as described in (Appendix B). Electrophoresis was performed

on 100 μg of crude extract proteins at 4 $^{\circ}\text{C}$ using Tris-glycine (25 mM Tris, 192 mM glycine), pH 8.3 containing 1 mM DTT and 0.1 mM ATP. After electrophoresis, NAD kinase activity was detected by incubating the gel at 37 $^{\circ}\text{C}$ in a 10-ml staining mixture containing 2.25 ml of nitroblue tetrazolium (NBT; 2 mM), 150 μl of phenazine methosulfate (2.7 mM), 300 μl of G6P (0.1 M), 25 μl of G6PDH (0.5 units/ μl), 500 μl of ATP (60 mM), 300 μl of MgCl_2 (100 mM), and 1.0 ml of Tris-HCl (1.0 M; pH 7.5) with or without 250 μl NAD^+ (100 mM).

2.7.2 Measurement of NAD kinase activity

NADK activity was measured (150 μL final volume) in a microtiter plate or a quartz cuvette. The standard assay mixture, unless otherwise specified, contained 50 mM Tris-Cl (pH 7.9), 4 mM ATP, 4 mM NAD^+ , 6 mM MgCl_2 , 1 mM CaCl_2 , and 300 mM recombinant rice CaM1 (Appendix B). The reaction was initiated with up to 15-30 μL of protein extract and allowed to proceed for 30 minutes at room temperature. The reaction was stopped by boiling for 5 minutes followed by centrifugation to remove the denatured protein. The NADP^+ formed was detected by adding 50 μL of the NADK assay mixture to the cycling assay (250 μL final volume), which contained 50 mM Tris-HCl (pH 7.5), 17.7 mM Glc-6P, 1 mM EGTA, 0.1 units of yeast Glc-6-P dehydrogenase, 1 mg/ml 2,6-dichlorophenolindophenol (DCIP), and 1 mg/ml methyphenazinium methylsulfate (PMS). Reduction of DCIP was monitored at 600 nm using the microtiter plate reader or the spectrophotometer.

2.8 Partial purification of NAD kinase from rice *Oryza sativa* L. cultivar Khao Dok Ma Li 105 (KDML105)

2.8.1 Preparation of rice seedlings

Seeds of the Khao Dok Ma Li 105 (KDML105) indica rice cultivar *Oryza sativa* L. were obtained from Kasetsart University. Healthy rice seeds were rinsed with deionized water and soaked for 20 minutes in 2.1% sodium hyperchlorite with shaking, then extensively washed with deionized water for at least 3 times. Washed seeds were germinated in NB medium, which was prepared as described in (Appendix B) for 7 days under a 16-hr light/8-hr dark photoperiod. After 7 days, germinated seeds were transferred to 1X Limpinuntana's nutrient solution (Limpinuntana, 1978) (Appendix B) and grown for 2 weeks under a 16-hr light/8-hr dark photoperiod. To determine the effect of NaCl, 3-week old seedlings were treated with 150 μ M NaCl in 1X Limpinuntana's nutrient solution for 0, 3, 6, 9, 12 or 24 hours.

2.8.2 Preparation of soluble extract

All steps were carried out at 0 °C to 4 °C. Leaves from the 3 week-old seedlings were collected, immersed in liquid nitrogen and ground in liquid nitrogen using chilled mortars and pestles. The plant material was kept frozen and ground to a fine powder. Then buffer A (50 mM Tris-Cl, pH 7.5, 200 mM KCl, and 3 mM MgCl₂), 1 mM EGTA, 0.5 mM EDTA, 1 mM dithiothreitol (DTT), 1 mM phenyl methyl sulfonyl fluoride (PMSF), 1 mM benzamidine, 50 μ M leupeptin, and 1X Protease inhibitor mix was added. The homogenate was filtered and centrifuged at 15,000xg for 20 minutes. The supernatant was then

dialyzed against buffer B (50 mM Tris-Cl, pH 7.5, 100 mM KCl, 3 mM MgCl₂, 1 mM EGTA, 0.5 mM EDTA, and 1 mM DTT).

2.8.3 Partial purification of NAD kinase

The crude protein in buffer B was applied to a column (25 mL) of DEAE-Toyoparl (TOSOH, Japan). The non-binding protein eluate, which contained NADK activity, was collected and brought to 3.5 M NaCl. The sample was clarified by centrifugation at 15,000xg for 10 minutes and applied (3 ml/min) to a column (10 ml) of Butyl-Toyoparl (TOSOH, Japan). The column was washed with buffer C (50 mM Tris-Cl, pH 7.5, 3.5 M NaCl, 3 mM MgCl₂, and 1 mM DTT) until the A_{280} decreased to the baseline. The adsorbed proteins were eluted with a linear gradient (150 mL) of 0% to 100% buffer D (50 mM Tris-Cl, pH 7.5, 30% [v/v] ethanediol, 100 mM KCl, 3 mM MgCl₂, and 1 mM DTT). NADK activity was eluted as a single peak of activity at approximately 95% buffer D. Fractions (7 mL) were collected and those containing greater than 20% peak NADK activity were pooled, dialyzed and frozen in liquid nitrogen. NADK activity was assayed as described above.

2.9 ³⁵S-recombinant CaM binding assay

³⁵S-Labeled recombinant CaM was prepared using a rice *Cam* (*OsCam1-1*) cloned into the pET21a(+) expression vector. Samples of NAD kinase proteins were separated by SDS-polyacrylamide gel electrophoresis (SDS-PAGE) and electrotransferred onto nitrocellulose membrane (whatman, USA). Following the transfer, the membrane was blocked by immersing in blocking solution (3% (w/v)

skim milk in 1X TBS-Tween-20 [20 mM Tris-HCl, 150 mM NaCl, pH 7.5, 0.05% (v/v) Tween-20], 5 mM CaCl₂) at room temperature for 2 hours with gentle shaking. The membrane was then washed in 1X TBS, 5 mM CaCl₂ once and incubated with probe solution (1X TBS-Tween-20, 5 mM CaCl₂, 1% (w/v) gelatin, 200 nM ³⁵S-labeled recombinant OsCaM1) for 2 hours. The membrane was washed twice with 1X TBS, 5 mM CaCl₂ and let dry at room temperature overnight. Then, the membrane was exposed to an X-ray film for 3 days to 1 week.



ศูนย์วิทยทรัพยากร
จุฬาลงกรณ์มหาวิทยาลัย

CHAPTER III

RESULTS

3.1 NAD kinase sequence analysis

Database searches for NAD kinase (*NADK*) genes identified two putative *NADKs* in the rice (*Oryza sativa* L.) genome. We have named these genes *OsNADK1* and *OsNADK2*. The primary structures of *OsNADK1* and *OsNADK2* proteins were compared with those of *NADK1* and *NADK2* from Arabidopsis. Based on pairwise alignments, *OsNADK1* and *OsNADK2* share 65% and 56% amino acid identities, respectively with their Arabidopsis counterparts. Multiple sequence alignment of all proteins was performed and the result excluding the diverged N-terminal regions is shown in Figure 3.1. Within these conserved C-terminal regions, two highly conserved and functionally important motifs, which have been identified within the NAD kinase family: a GGDG motif (XXX-XXGGDG-XL) and a Gly-rich motif (DGXXX-TPTGSTAY), where X represents a hydrophobic residue, are largely conserved in both *OsNADK1* and *OsNADK2*. The GGDG motif is well conserved in four kinase families including NAD kinases, sphingosine kinases, eukaryotic diacylglycerol kinases, and phosphofructokinase. In the N-terminal extension of *OsNADK2*, a CaM-binding domain was predicted by comparison with *NADK2* from Arabidopsis, which is conserved among putative homologs in other plants (Figure 3.2).


```

CeNADK2  -MLAVCARHGF--AKLPPPPFPPLAGERAAAANVVG-----RWWWRPAAAGRRGVVAA 48
AtNADK2  MFLCFCPCCHVPIMSRLSPATGISSRLRFBIGLSSDGRLIPFGFRFRNDVPFKRRLRFVI 60
      :*..* * * :*:.. : * : : . * : .. ** ..

CeNADK2  RASF---FSSRIGLESQNVHTRDLSQLLWVGFVPGDIAEIEAYCRIFRAEQLHTAVMSA 105
AtNADK2  RAQLSEAFSPDLGLDSQAVKSRDTSNLPWIGFVPGDIAEVEAYCRIFRSAERLHGALMET 120
      **: : ** :***** :** :* :*****:*****:*** ***:

CeNADK2  LCDPETGECFVRVDVQTEDLPVLEDKVAAVLGCMLALLNRRGRKEVLSGRSGVASAFQGSE 165
AtNADK2  LCNFVTGECRVFYDFSSPEEKPLLEDKIVSVLGCILSLLNKRKEILSGRSSMNSFNLDD 180
      **** **** * ..: :*****:*****:*****:*****. :*: :

CeNADK2  D-STMDKIPPLALFRGDLKRCCESMQVALASYLVSEARGLDIWRKLQRLKNACYDAGFF 224
AtNADK2  VGVAAESLPPPLAVFRGEMKRCCESLHIALENYLTDDERSGIVWRKLQKLNVCYDAGFF 240
      : :*****:*****:*****:*** ***: : * :*****:***:*****

CeNADK2  RADGHPCPTLFANWFFVYFSTVPEDELSDELEVAFWRGGQVSEEGLEWLLKGFKTIVDL 284
AtNADK2  RSDNYPCQTLFANWDFIYSSNIKEDIDSYESEIAFWRGGQVTQEGLKWLIENGFKTIVDL 300
      *:*:* ***** :* .. :* * * :*****:*****: :*****

CeNADK2  REEDVHDDLVLSAIHEAVSLGKIEVWNLFEVIGTAPSAEQVQRFAEIVSDSAKKPIYLHS 344
AtNADK2  RAEIVKDTFYQIALDDAISLGTKITVWQIPIDVPMAPKAEQVELFASIVSDSSKRPIYVHS 360
      * * ** :* :*:***** :*: : : ** :***** :** :*****:*****

CeNADK2  QEGISRTSAMVSRWKQYVTRAERLATQNRSLNGNGKHWVNDQTEQLTNSPGFSSEGSSENG 404
AtNADK2  KEGVWRISAMVSRNKQYNT---RSLTKELFVSEESKREVSSEIKLGSN-----AVVSGKG 412
      :*: ***** : * : : : : * : : : : * : : * :

```

Figure 3.2 Sequence comparison of the N-terminal region containing a predicted CaM-binding domain from OsNADK2 and AtNADK2. The solid line indicates positions of the putative CaM-binding domains; identical residues on the same column are indicated by an asterisk (*); conserved substitutions sequences are indicated by a colon (:), semi-conserved sequences are indicated by a dot (.); and a gap introduced for alignment purposes is indicated by a dash (-).

3.2 Molecular cloning of the NAD kinase genes

The complete coding region for *NADK1* and *NADK2* was amplified by PCR using their respective full-length cDNA clone as a template and a pair of oligonucleotide primers designed by the SECentral program. For *NADK1*, the sequence of the forward primer, designated as NADK1-F was 5'- **GCCCATATGTCGCTCGACGAGCTTCCGCAC** -3', which contains an *NdeI* restriction site (in bold letters) at its 5' end. The sequence of the reverse primer, designated as NADK1-R was 5'- **CTGGTCGACATCACGCGGGCCGTCGAATGA** -3', which contains a *SalI* restriction site (in bold letters) at its 5' end. For *NADK2*, the sequence of the forward primer, designated as NADK2-F was 5'- **TGCCATATGCTCGCCGTCTGCGCG** CGGCAC -3', which contains an *NdeI* restriction site (in bold letters) at its 5' end. The sequence of the reverse primer, designated as NADK2-R was 5'- **TAAGTCGACTAATGCCT** TCTGGTCCAGTCG -3', which contains a *SalI* restriction site (in bold letters) at its 5' end. After PCR amplification, PCR products were separated by agarose gel electrophoresis and visualized by ethidium bromide staining (Figure 3.3).

The *NADK1* and *NADK2* fragments were purified from agarose gel using the Geneaid gel extraction kit. The purified *NADK1* and *NADK2* fragments were then ligated into pTZ57R/T vector. After the competent *E. coli* strain XL1Blue cells were transformed with the ligation mixtures, the transformants were selected by blue/white colony screening on ampicillin agar plates containing X-gal and IPTG. White colonies were randomly picked and cultured in LB broth containing 100 µg/ml of ampicillin at 37 °C overnight and the cultures were subjected to plasmid extraction. To confirm insertion of the PCR product into the vector by restriction

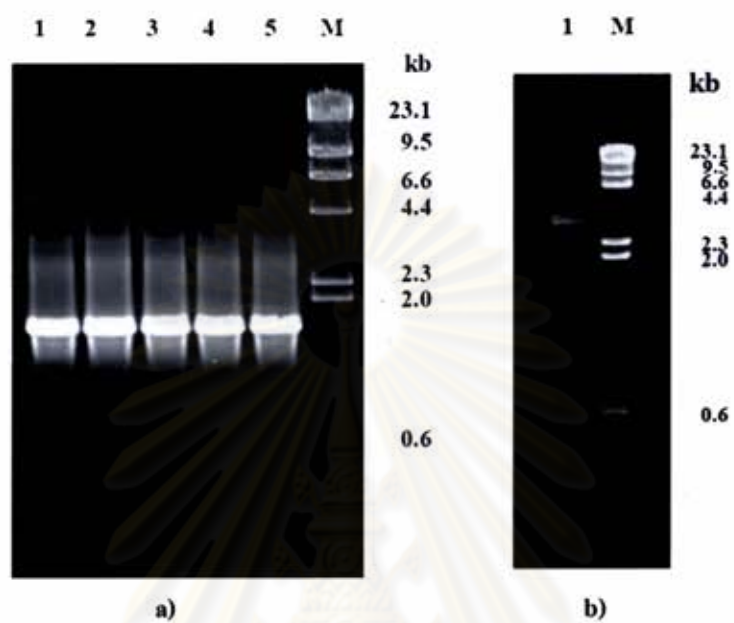


Figure 3.3 Ethidium-bromide stained 1% agarose gels of the PCR products amplified from the *NADK1* and *NADK2* cDNAs. a) Lane 1-5 *NADK1* fragments from varying annealing temperatures between 69-72 °C and b) *NADK2* fragment from the annealing temperature of 60 °C. Lanes M: λ /HindIII marker.

ศูนย์วิทยทรัพยากร
จุฬาลงกรณ์มหาวิทยาลัย

analysis, potential recombinant plasmids were digested with *NdeI* and *SalI* for *NADK1* and *NdeI*, *SalI* and *VspI* for *NADK2*, and incubated at 37 °C overnight. These reactions were then analyzed by 1.0% agarose gel electrophoresis. The results in Figure 3.4 showed that DNA fragments of approximately 1.6 and 3.0 kb for *NADK1* and *NADK2*, respectively, were obtained. The length of these gene fragments was as expected.

3.3 Expression of the recombinant NADK1 and NADK2

The *NADK1* and *NADK2* were inserted into pET21a(+) at the 5'-*NdeI* and 3'-*SalI* sites in frame with the C-terminal His6 tag. The resulting recombinant plasmids, which were named pET21a/*NADK1* and pET21a/*NADK2*, were checked for insertion by digesting them with *NdeI* and *SalI* from which the results were obtained as shown in Figures 3.5 and 3.6, respectively. All of the subcloned fragments were verified by DNA sequencing. The recombinant proteins were then expressed in an *Escherichia coli* system strain Rosetta (DE3) pLysS and Rosetta-gami for *NADK1* and *NADK2*, respectively.

Based upon the cDNA and sequencing data, the amino acid sequences for both recombinant *NADK1* and *NADK2* were deduced as presented in Figure 3.7 and 3.8, respectively. The recombinant genes were predicted to encode the recombinant proteins of 547 residues and 996 residues corresponding to molecular masses of approximately 60.6 kD and 110.3 kD for *NADK1* and *NADK2*, respectively.

To produce the recombinant proteins, a single colony containing pET21a/*NADK1* and pET21a/*NADK2* was cultured in LB medium containing 100 mg/ml ampicillin at 37 °C until the OD600 reached 0.6. Isopropyl-b-D-thiogalactoside (IPTG) was added to the final concentration of 0, 0.1, 0.3 and 0.5 mM

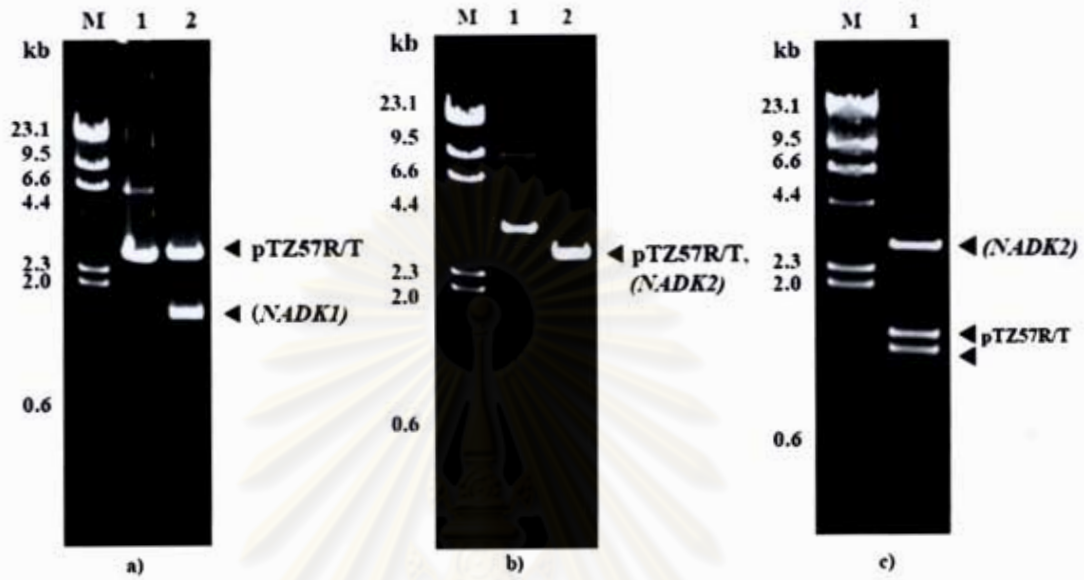


Figure 3.4 Analyses of the recombinant plasmid pTZ57R/T with *NADK1* or *NADK2* inserted by digesting with restriction enzymes followed by separation by 1% agarose gel electrophoresis. a) and b) Lane 1: pTZ57R/T with fragments of *NADK1* and *NADK2* inserted, respectively without digestion and lane 2: the respective plasmids digested with *NdeI* and *SalI*. The digested *NADK2* clone generated a single band, which consisted of both pTZ57R/T and *NADK2* fragments; and c) pTZ57R/T with the inserted *NADK2* digested with *NdeI*, *SalI* and *VspI*. Two bands under the *NADK2* band were the digested fragments of pTZ57R/T. Lane M: λ HindIII marker.

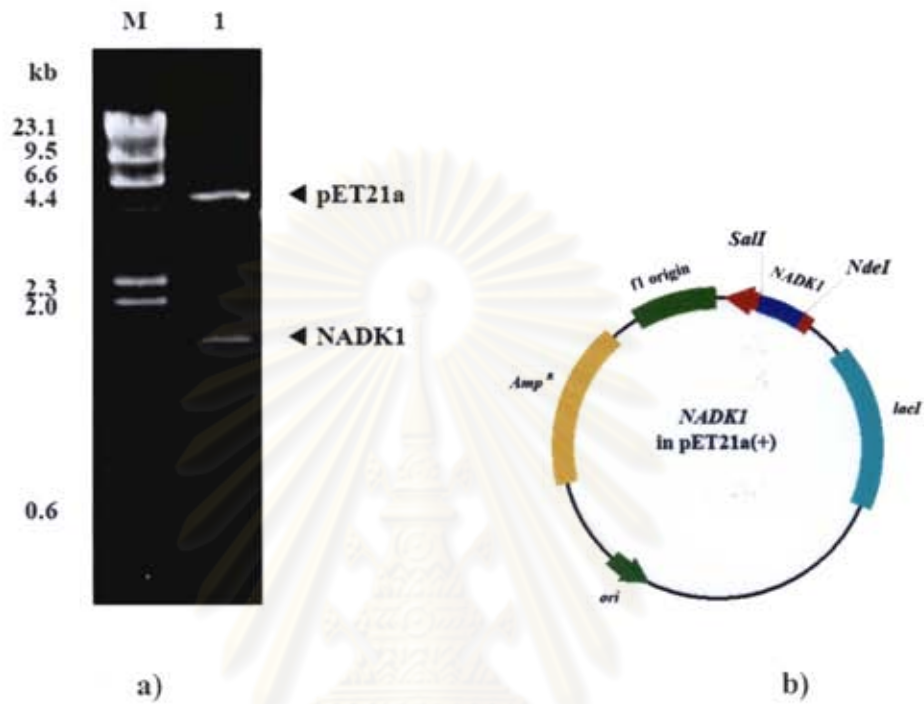


Figure 3.5 Restriction analysis of the recombinant pET21a/*NADK1* on 1.0 % agarose gel.

a) Lane M: λ *Hind*III marker

Lane 1: pET21a/*NADK1* digested with *Nde*I and *Sal*I

b) Schematic diagram of the recombinant pET21a(+) containing *NADK1*

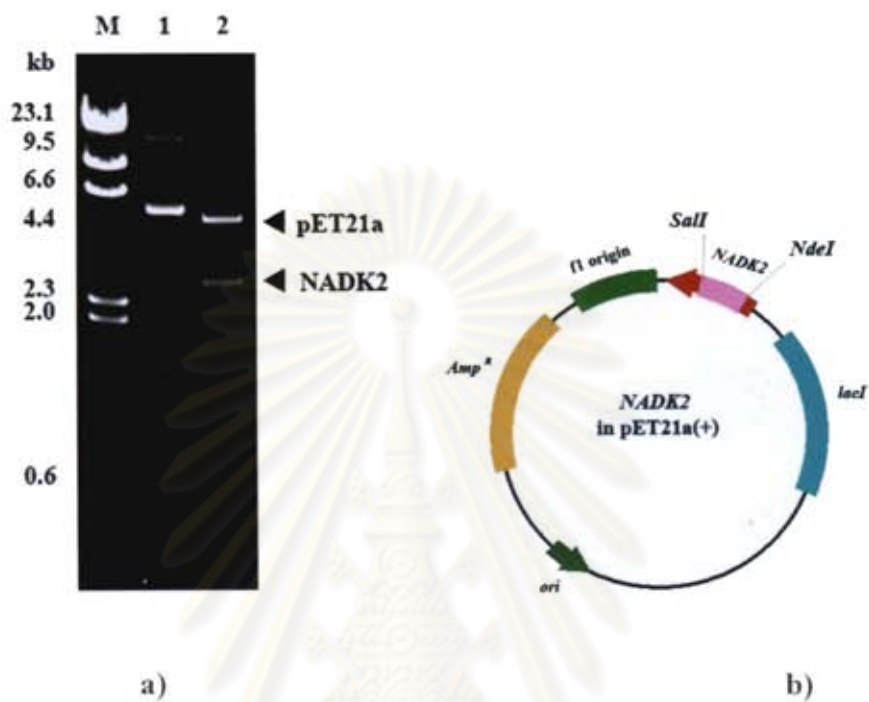


Figure 3.6 Restriction analysis of the recombinant pET21a/*NADK2* on 1.0 % agarose gel.

a) Lane M: λ HindIII marker

Lane 1: pET21a/*NADK2* without digestion

Lane 2: pET21a/*NADK2* digested with *NdeI* and *SalI*

b) Schematic diagram of the recombinant pET21a(+) containing *NADK2*

ATGTCGCTCGACGAGCTTCCGCACAAGGTTTCTGATGAGAGAGTAAACCATGATACTGTG	60
M S L D E L P H K V S D E R V N H D T V	20
ACCTCACATGAAAGTGAAATTGGGTCTGGGTCCATCTCCACAGTTAGCTCAACAGTTAGT	120
T S H E S E I G S G S I S T V S S T V S	40
TCAGTAGAATCAGAGAAAGCAGCTTATGAATTCCTTGCTCAAACCTCCTATCAAGTCAACC	180
S V E S E K A A Y E F L A Q T P I K S T	60
GATGCACACCTTGTTGAGTTTTCAGAAGCTATGAGAACTGTTGCAAAAGCATTGCGACGA	240
D A H L V E F S E A M R T V A K A L R R	80
GTTGCAGAAGGGAAAGCTGCTGCTCAAGCTGAGGCGGAAGAGTGGAGGCGTAAATATGAA	300
V A E G K A A A Q A E A E E W R R K Y E	100
TTAGAGATGGCACACAAACAGCAGAGAAAAATCAAAGGCTATGGCAGTTGTGCCAATAAT	360
L E M A H K Q Q R K I K G Y G S C A N N	120
GAATTAGAAAAGTTGGCCAGCCAACTAACACTGGAGACGCCTGCATCTGATCAAGCGGGA	420
E L E K L A S Q L T L E T P A S D Q A G	140
TGTTGTGGAAATCATGGTATATGTTACATGAGGTTCTTCAGGATGAAAGTCCTGGTCCT	480
C C G N H G I C S H E V L Q D E S P G P	160
AACCCCGATCTAGTCACAAGCTGGTGAGTAGAAAGGCATCATTTAGACTTTCATGGGGA	540
N P R S S H K L V S R K A S F R L S W G	180
TGCAATGGGGATAAAAAACGGCCAGCACAAGCATGATTTTGTATCATTGAAAAGGGAGAT	600
C N G D K N G Q H K H D F V S F E K G D	200
ATAACAACAGCAGAGCGCAGCAACAAGCAGATTTTGCTGAAATGGGAATCCTCGCCACAA	660
I T T A E R S N K Q I L L K W E S S P Q	220
ACTGTTCTTTTCATAACCAAACCTAATTCTAACTCCGTGCATGTTCTTTGTGCTGAAATG	720
T V L F I T K P N S N S V H V L C A E M	240
GTCAGATGGCTTAAGGAACATAAAAAAGATAAATGTTGTTGTAGAGCCACGTGTTAGCAAG	780
V R W L K E H K K I N V V V E P R V S K	260
GAACTCTTAACAGAAGATTCCTACTACAATTTTCATCCAAACATGGGATGATGATGAGGAG	840
E L L T E D S Y Y N F I Q T W D D D E E	280
AAAAAGATGTTGCACACAAAGGTTGATCTCATTGTAACCTTGGTGGTGGTGGACTGTT	900
K K M L H T K V D L I V T L G G D G T V	300
TTATGGGCTGCGTCTTTGTTCAAAGGGCCAGTTCCTCCGGTTGTTGCTTTCTCCCTAGGA	960
L W A A S L F K G P V P P V V A F S L G	320
TCACTGGGATTCATGACACCTTTCCCAAGTGAGCAATATCGTGATTGTCTGGACAATGTG	1020
S L G F M T P F P S E Q Y R D C L D N V	340
CTGAATGGACCATTTAGCATCACATTGAGAAACCGTCTACAGTGCCATGTAATCCGTGAT	1080
L N G P F S I T L R N R L Q C H V I R D	360
GCAGCAAAGGATGAACTTGAGACTGAGGAGCCAATTTTAGTGTTAAACGAAGTCACAATT	1140

A A K D E L E T E E P I L V L N E V T I	380
GACCGTGGAAATATCATCTTACCTTACCTACTTGGAAATGCTACTGTGATAGTTCTTTCGTT	1200
D R G I S S Y L T Y L E C Y C D S S F V	400
ACATGTGTACAAGGGGATGGACTGATCATATCAACAACATCTGGAAGCACGGCATATTCA	1260
T C V Q G D G L I I S T T S G S T A Y S	420
TTGGCAGCTGGAGGATCCATGGTTCATCCACAGGTCCCAGGAATCCTATTACGCCGATC	1320
L A A G G S M V H P Q V P G I L F T P I	440
TGCCCGCATTCCCTGTCATTCAGGCCTTTGATACTGCCTGAATATGTGACCCTGCGCGTA	1380
C P H S L S F R P L I L P E Y V T L R V	460
CAAGTGCCACATAACAGCAGGGGCCAAGCTTGGGCATCATTCGATGGCAAAGATCGGAAG	1440
Q V P H N S R G Q A W A S F D G K D R K	480
CTGCTGTCACCCGGGGATGCTCTCATCTGCAGCATTCTCCATGGCCTGTGCCACGGCT	1500
L L S P G D A L I C S I S P W P V P T A	500
TGCCTGGTGGATTCAACAACCGATTTCTTACGCAGCATCCACGAGGGTCTCCACTGGAAC	1560
C L V D S T T D F L R S I H E G L H W N	520
CTGAGGAAGTCCCAGTCATTCGACGGCCCGCGTGATGTCGACAAGCTTGC GGCCGCACTC	1620
L R K S Q S F D G P R D V D K L A A A L	540
GAGCACCACCACCACCACCACTGA •	1644
E <u>H H H H H H</u> *	548

Figure 3.7 Nucleotide and deduced amino acid sequences of *NADK1* gene in the recombinant plasmid. The underlined amino acid sequence is a His₆ tag and the stop codon is marked with an asterisk (*).

ศูนย์วิทยุทรัพยากร
จุฬาลงกรณ์มหาวิทยาลัย

ATGCTCGCCGCTCTGCGCGCGGCACGGGCCCCGGAAGCTTCCGCCGCCGCCGCCGCCGCTC	60
M L A V C A R H G P A K L P P P P P P L	20
GCCGGGAGCGGGCGGCCGCATGGGTCTGTCGGGAGGTGGTGGTGGAGGCCGGCGGGCG	120
A G E R A A A W V V G R W W W R P A A A	40
GGCGGGCGGGCGTCTGTCGCCGCGGGGCGTCTTCTCAGCTCGCGGATCGGGCTCGAC	180
G R R G V V A A R A S F F S S R I G L D	60
TCCCAGAATTATCACACAAGGGACCTGTCCCAACTGTTGTGGGTGGGTCCGGTGCCCGGC	240
S Q N Y H T R D L S Q L L W V G P V P G	80
GACATTGCAGAGATTGAGGCATACTGCCGCATATTCGGTGCAGCTGAGCAGCTCCACACT	300
D I A E I E A Y C R I F R A A E Q L H T	100
GCGGTCATGTCTGCACTCTGTGATCCAGAGACAGGGGAGTGCCTGTCCGCTATGATGTG	360
A V M S A L C D P E T G E C P V R Y D V	120
CAAACCGAGGACCTGCCAGTACTGGAGGACAAGGTCTGCTGCCGTGCTCGGATGCATGCTG	420
Q T E D L P V L E D K V A A V L G C M L	140
GCATTGCTGAACCGGGGCCGAAAGAGGTGCTCTCAGGTGATCAGGTGTTGCGAGTGCA	480
A L L N R G R K E V L S G R S G V A S A	160
TTTCAGGGATCTGAGGACAGCACAATGGATAAGATTCCACCTCTCGCCTTGTTCGGTGGG	540
F Q G S E D S T M D K I P P L A L F R G	180
GATTTGAAGCGATGCTGTGAGAGTATGCAGGTTGCACTTGCCAGCTACCTTGTGCCAAGT	600
D L K R C C E S M Q V A L A S Y L V P S	200
GAGGCCCGAGGGTTGGATATATGGAGGAAGCTGCAGAGGCTGAAGAATGCCTGCTATGAT	660
E A R G L D I W R K L Q R L K N A C Y D	220
GCAGGTTTTCCAAGGGCTGATGGTCATCCTTGTCCAACCTTTATTTGCGAATTGGTTTTCCG	720
A G F P R A D G H P C P T L F A N W F P	240
GTGTACTTTTTCAACTGTGCCAGATGATTCATTATCAGATGAGTTAGAGGTTGCATTCTGG	780
V Y F S T V P D D S L S D E L E V A F W	260
AGGGGAGGGCAAGTCAGTGAGGAGGGACTGGAATGGTTATTGTTGAAGGGATTCAAACT	840
R G G Q V S E E G L E W L L L K G F K T	280
ATTGTTGATCTACGGGAGGAAGATGTTAAAGATGATTTGTACCTTTCAGCAATTCATGAA	900
I V D L R E E D V K D D L Y L S A I H E	300
GCTGTCTCATTGGGAAAGATAGAGGTGGTGAATTTGCCTGTTGAGATTGGGACTGCGCCC	960
A V S L G K I E V V N L P V E I G T A P	320
TCTGCTGAACAGGTTTCAGCGATTCGCGGAAATTGTGTCTGATAGTGCGAAGAAACCCATT	1020
S A E Q V Q R F A E I V S D S A K K P I	340
TATCTTCATAGCCAGGAAGGGATTAGTAGGACATCTGCGATGGTTTTCGAGATGGAAGCAG	1080
Y L H S Q E G I S R T S A M V S R W K Q	360

TACGTCACTCGTGCTGAGAGACTGGCTACTCAGAACC GTTCATTAATGGGAATGGTAAG	1140
Y V T R A E R L A T Q N R S L N G N G K	380
CATGTGAGGAATGATCAAACAGAACAGCTCACAAACAGCCCAGGTTTCTCCTCAGAAGGT	1200
H V R N D Q T E Q L T N S P G F S S E G	400
AGCGAAAACGGTACACCTCTGGAATCCGATAGAACCATGGAGGGGGAAAACATGTGACATA	1260
S E N G T P L E S D R T M E G E T C D I	420
GACATTGAAACAGCACGTCATAATCTGGAAATCACTAATTCCTTCCAGTGAACAAAGT	1320
D I E T A R H N L E I T N S L P S E Q S	440
ACTGAACAAGGTGAACTGCATGGCACCAGGACAGAACTTCAGTCAAAC TTTAGACTAGAG	1380
T E Q G E L H G T R T E L Q S N F R L E	460
AGTAATCCTCTTAAGGCACAATTTCTTCTTGATGTTTTCTCCAAAAAGGGGATGACT	1440
S N P L K A Q F P S C D V F S K K G M T	480
GACTTTTTTAGAAGCAAAAAGGTATATCCAAAATCTGTTTTAAACCCTCGGAGACGGTGC	1500
D F F R S K K V Y P K S V L N P R R R S	500
AATAGCTTGTGGTCTCAAGGAGAAAACAAAGTCTCAGTGCTGAACAAAAATGGAGCCATT	1560
N S L L V S R R K Q S L S A E Q N G A I	520
GACTATGAAGCAGCCGAATTTAAAGTTCTAAAAAGTTCGAATGGAGCATCGTTCCGATAAT	1620
D Y E A A E F K V L K S S N G A S F D N	540
GATTATATTCTATCAGTTGCTTCAGGTATTACTAATGGAAAACCATCCAACAATGGAGCC	1680
D Y I L S V A S G I T N G K P S N N G A	560
TCCACATCTGTTGAGGACAGGGAAATGGAAACCTCAGTTGTAACAGTTGATCCTAGAACA	1740
S T S V E D R E M E T S V V T V D P R T	580
TCTGATACCAGCAATTCTAATGGCAATGCTCCACTTGGATCACAAAAATCTGCTGAAAGG	1800
S D T S N S N G N A P L G S Q K S A E R	600
AACGGTTCCTTTATGTGGAGAGAGAAAGATCAGATCATGTTGATGGAAATATGTGTGCA	1860
N G S L Y V E R E R S D H V D G N M C A	620
TCTGCAACTGGTGTGTTAGACTTCAGTCAAGAAGAAAAGCAGAGATGTTTCTAGTACGC	1920
S A T G V V R L Q S R R K A E M F L V R	640
ACTGATGGATTTTCTGTACAAGAGAAAAAGTAACTGAATCATCTCTGGCTTTTACGCAT	1980
T D G F S C T R E K V T E S S L A F T H	660
CCTAGCACCCAGCAGCAGATGCTTATGTGGAAATCTCCTCCAAAGACTGTCCTACTATTG	2040
P S T Q Q Q M L M W K S P P K T V L L L	680
AAGAAATTAGGTGATGAGCTCATGGAAGAAGCTAAAGAGGTTGCTTCATTTCTGCATCAT	2100
K K L G D E L M E E A K E V A S F L H H	700
CAAGAAAAGATGAATGTTCTAGTGGAGCCTGATGTTTCATGATATATTTGCTAGGATTCCT	2160
Q E K M N V L V E P D V H D I F A R I P	720

GGTTATGGTTTTGTGCAGACCTTCTATACTCAGGATACCAGCGACCTTCATGAGAGAGTT	2220
G Y G F V Q T F Y T Q D T S D L H E R V	740
GATTCGTTGCTTGCCTGGGTGGAGATGGCGTCATTCTGCATGCGTCAAATTTATTTAGA	2280
D F V A C L G G D G V I L H A S N L F R	760
ACTTCTGTACCACCTGTTGTCTCTTTCAATCTTGGATCTCTTGGATTCTGACTTCACAC	2340
T S V P P V V S F N L G S L G F L T S H	780
AATTCGAAGGTTTCAGACAAGACTTGAGGGCTGTCATCCATGGGAACAATACACTTGGA	2400
N F E G F R Q D L R A V I H G N N T L G	800
GTTTATATAACCCTTAGAATGCGTGTACGATGTGAGATCTTTCGCAATGGAAAAGCAATG	2460
V Y I T L R M R V R C E I F R N G K A M	820
CCTGGAAGATATTTGATGTGCTAAATGAAGTTGTTGTTGATCGGGGTTCTAATCCTTAC	2520
P G K V F D V L N E V V V D R G S N P Y	840
CTGTCCAAAATTGAATGCTATGAGCATAACCATTTAATCACAAAGGTTCAAGGTGATGGG	2580
L S K I E C Y E H N H L I T K V Q G D G	860
GTGATAGTAGCAACACCGACTGGCAGTACAGCATACTCTACTGCAGCAGGAGGCTCAATG	2640
V I V A T P T G S T A Y S T A A G G S M	880
GTCCATCCAAATGTCCCGTGTATGCTGTTTACTCCAATCTGCCCGCACTCGCTATCATT	2700
V H P N V P C M L F T P I C P H S L S F	900
AGACCTGTCATCCTTCTGATTCTGCTCGTCTTGAATTGAAGATTCCAGATGATGCAAGA	2760
R P V I L P D S A R L E L K I P D D A R	920
AGTAACGCCTGGGTATCATTGATGGCAAAGGAGGCAGCAATTATCAAGGGGAGACTCT	2820
S N A W V S F D G K R R Q Q L S R G D S	940
GTTCAAATATCCATGAGTCAGCACCCGCTCCCAACAGTTAATAAATCTGACCAAACCTGGT	2880
V Q I S M S Q H P L P T V N K S D Q T G	960
GACTGGTTCCGCAGCTTGATCAGGTGCCTGAACTGGAACGAGCGACTGGACCAGAAGGCA	2940
D W F R S L I R C L N W N E R L D Q K A	980
TTAGTCGACAAGCTTGCGGCCGCACTCGAGCACCACCACCACCACCCTGA	2991
L V D K L A A A L E <u>H H H H H H</u> *	997

Figure 3.8 Nucleotide and deduced amino acid sequences of *NADK2* gene in the recombinant plasmid. The underlined amino acid sequence is a His₆ tag and the stop codon is marked with an asterisk (*).

for the recombinant NADK1 and 0, 0.2, 0.4 and 0.6 mM for the recombinant NADK2 to induce the expression. The cells were harvested at 2 hours after IPTG induction and then analyzed by 18% SDS-PAGE.

For NADK1, the SDS-PAGE results showed that the recombinant protein expression could not be detected in the soluble protein fraction (Figure 3.9) but was detected in the inclusion bodies (Figure 3.10) after 0.1, 0.3 and 0.5 mM IPTG induction. For NADK2, no over-expressing band was detected in either soluble protein fraction (Figure 3.9) or inclusion bodies (Figure 3.10) after induction by varying concentrations of IPTG.

3.4 NAD kinase assay of the recombinant NADK1 and NADK2

3.4.1 Measurement of NAD Kinase Activity

NAD kinase activity in cell lysates was measured by a two-step procedure described previously with minor modifications. First, 15 μ l of cell lysate was added to a 150- μ l reaction mixture containing 50 mM Tris-Cl (pH 7.9), 4 mM ATP, 4 mM NAD⁺, 6 mM MgCl₂, 1 mM CaCl₂ followed by incubation for 30 minutes at room temperature. The reaction was stopped by boiling for 5 minutes followed by centrifugation to remove the denatured protein. The amount of NADP⁺ produced was then determined, using a cycling assay, by transferring the mixture into 200 μ l of 50 mM Tris-HCl (pH 7.5), 17.7 mM Glc-6P, 1 mM EGTA, 0.1 units of yeast Glc-6-P dehydrogenase, 1 mg/ml 2,6-dichlorophenolindophenol (DCIP), and 1 mg/ml methylphenazinium methylsulfate (PMS). Reduction of DCIP was monitored at 600 nm. In the inclusion bodies from *E. coli* expressing NADK2, after the proteins were solubilized in 8M urea and refolded by 50 mM Tris-HCl (pH 7.5), 0.1 mM DTT and 0.2 mM EDTA, no NAD kinase activity was detected. On the contrary, NAD kinase

activity was found in the soluble proteins from both *E. coli* Rosetta (DE3) pLysS harboring *NADK1* and *E. coli* Rosetta-gami harboring *NADK2*. NAD kinase specific activity of the crude proteins extracted from *E. coli* expressing *NADK1* was highest when the culture was not induced by IPTG and decreased when induced with higher concentrations of IPTG (Figure 3.11). For *NADK2*, NAD kinase specific activity of the crude proteins extracted from *E. coli* expressing *NADK2* was highest when the culture was induced by 0.6 mM of IPTG (Figure 3.12). From the results above, 0.1 mM IPTG for *NADK1* and 0.6 mM IPTG for *NADK2* were further used for inducing production of the recombinant proteins. because of 0 mM IPTG was no detected the *NADK1* band

3.4.2 In-gel activity staining

The soluble proteins extracted from *E. coli* Rosetta (DE3) pLysS harboring *NADK1* and Rosetta-gami harboring *NADK2* were separated in native electrophoresis using 7% separating gel and 4% stacking gel. Electrophoresis was performed on 100 µg of the crude extracts at 4 °C. NAD kinase activity was detected by incubating the gel at 37 °C in a 10 ml staining mixture containing 2.25 ml of nitroblue tetrazolium (NBT; 2 mM), 150 µl of phenazine methosulfate (2.7 mM), 300 µl of G6P (0.1 M), 25 µl of G6PDH (0.5 units/µl), 500 µl of ATP (60 mM), 300 µl of MgCl₂ (100 mM), and 1.0 ml of Tris-HCl (1.0 M; pH 7.5) with or without 250 µl of NAD⁺ (100 mM). As a result, the purple precipitate appeared in the crude extracts from *E. coli* cells harboring the recombinant plasmids only in the presence of NAD⁺, which marked the position of NAD kinase activity (Figure 3.13). The result shows that the crude protein extracts of both recombinant *NADK1* and *NADK2* appear to have activity of NAD kinase.

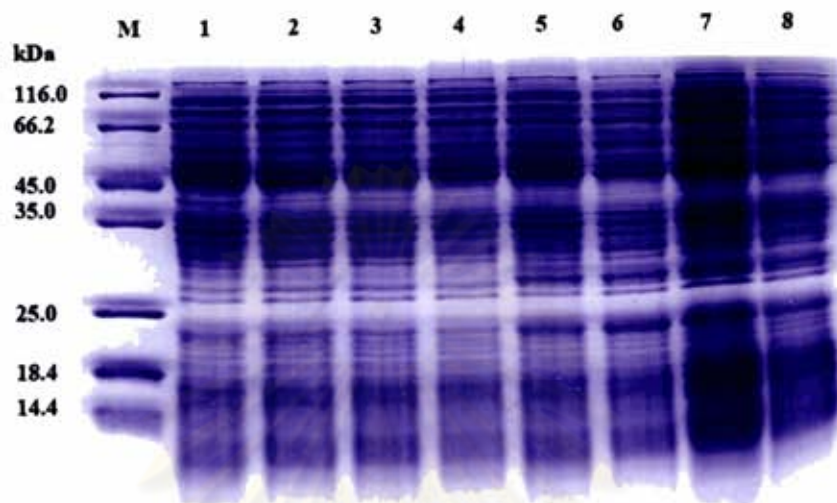


Figure 3.9 SDS-PAGE analysis of the soluble protein fractions from *E. coli* Rosetta (DE3) pLysS harboring pET21a/*NADK1* and Rosetta-gami harboring pET21a/*NADK2* after induction by various IPTG concentrations.

Lane M: protein marker (Fermentas)

Lane 1: soluble proteins of cells carrying pET21a/*NADK1* uninduced

Lane 2: soluble proteins of cells carrying pET21a/*NADK1* induced by 0.1 mM IPTG

Lane 3: soluble proteins of cells carrying pET21a/*NADK1* induced by 0.3 mM IPTG

Lane 4: soluble proteins of cells carrying pET21a/*NADK1* induced by 0.5 mM IPTG

Lane 5: soluble proteins of cells carrying pET21a/*NADK2* uninduced

Lane 6: soluble proteins of cells carrying pET21a/*NADK2* induced by 0.2 mM IPTG

Lane 7: soluble proteins of cells carrying pET21a/*NADK2* induced by 0.4 mM IPTG

Lane 8: soluble proteins of cells carrying pET21a/*NADK2* induced by 0.6 mM IPTG

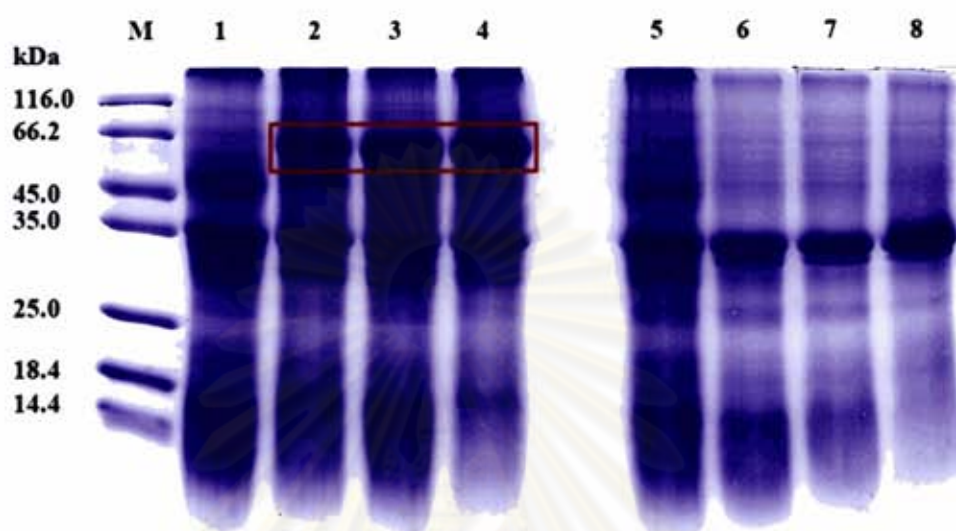


Figure 3.10 SDS-PAGE analysis of the inclusion bodies from *E. coli* Rosetta (DE3) pLysS harboring *NADK1* and Rosetta-gami harboring *NADK2* after induction by various IPTG concentrations. The red box shows bands of the recombinant *NADK1* with the molecular mass of approximately 60.6 kD.

Lane M: protein marker (Fermentas)

Lane 1: inclusion bodies of cells carrying pET21a/*NADK1* uninduced

Lane 2: inclusion bodies of cells carrying pET21a/*NADK1* induced by 0.1 mM IPTG

Lane 3: inclusion bodies of cells carrying pET21a/*NADK1* induced by 0.3 mM IPTG

Lane 4: inclusion bodies of cells carrying pET21a/*NADK1* induced by 0.5 mM IPTG

Lane 5: inclusion bodies of cells carrying pET21a/*NADK2* uninduced

Lane 6: inclusion bodies of cells carrying pET21a/*NADK2* induced by 0.2 mM IPTG

Lane 7: inclusion bodies of cells carrying pET21a/*NADK2* induced by 0.4 mM IPTG

Lane 8: inclusion bodies of cells carrying pET21a/*NADK2* induced by 0.6 mM IPTG

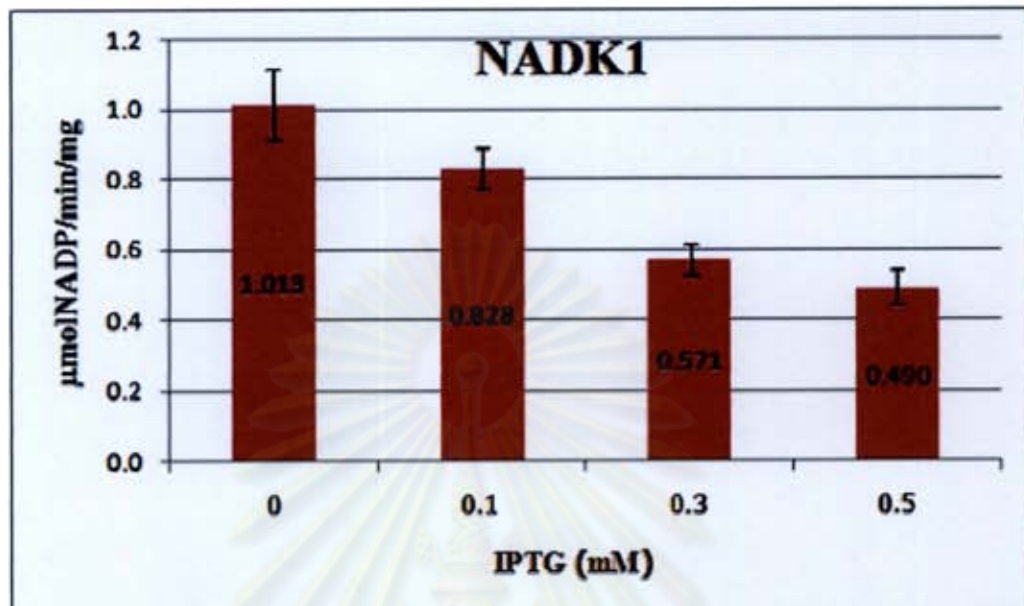


Figure 3.11 Induction of recombinant NADK1 at various IPTG concentrations.

The recombinant vector pET21a/NADK1 was expressed in *E. coli* Rosetta (DE3) pLysS.

ศูนย์วิทยทรัพยากร
จุฬาลงกรณ์มหาวิทยาลัย

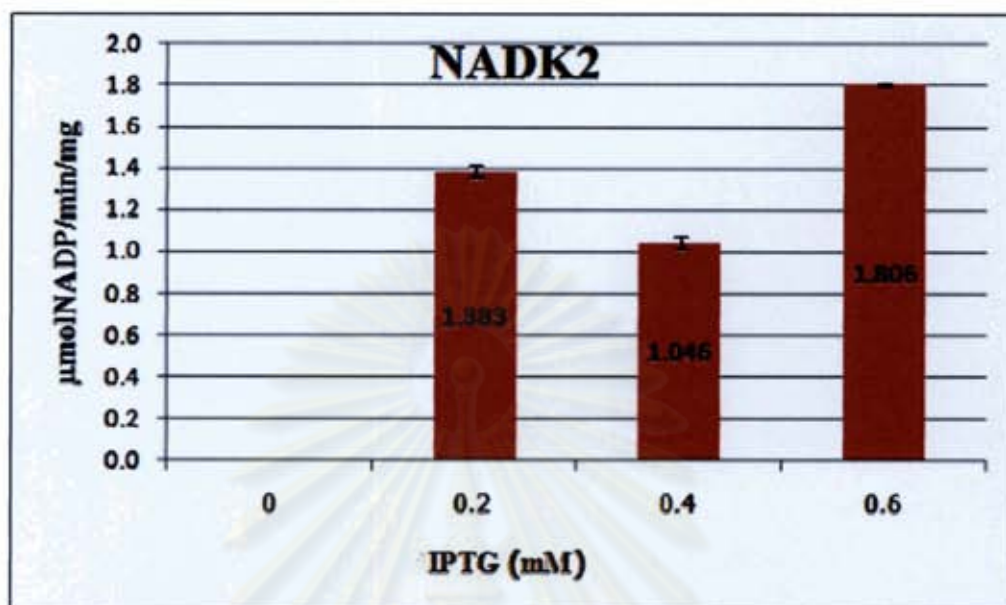


Figure 3.12 Induction of recombinant NADK2 at various IPTG concentrations.

The recombinant vector pET21a/NADK2 was expressed in *E. coli* Rosetta-gami.

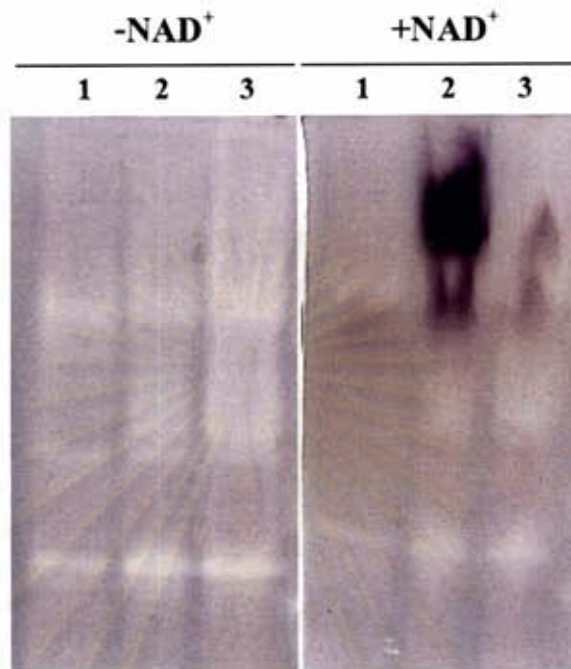


Figure 3.13 In-gel activity staining of soluble proteins extracted from *E. coli* Rosetta (DE3) pLysS harboring *NADK1* and Rosetta-gami harboring *NADK2*. NAD kinase activity was assayed by incubating the gel with (+NAD⁺) or without (-NAD⁺) the substrate NAD⁺.

Lanes 1: soluble proteins of cells carrying pET21a(+) (control)

Lanes 2: soluble proteins of cells carrying pET21a/*NADK1*

Lanes 3: soluble proteins of cells carrying pET21a/*NADK2*

3.5 Purification and characterization of the recombinant NADK1 protein

Both recombinant proteins produced were expected to contain a His₆ tag, which consists of six consecutive histidine residues, at their carboxyl terminal end, therefore a Ni Sepharose was used to purify the proteins based on the principle that poly-His-fusion proteins bind to nickel ions. For the recombinant NADK1 protein, insoluble proteins from the inclusion bodies was dissolved with buffer containing 8 M urea and 25 mM imidazole and left overnight at room temperature with shaking. After centrifugation at 10,000xg, the supernatant was applied to the Ni Sepharose high performance column at room temperature. The flow through was collected by a gravity flow and the column was washed with the binding buffer containing with 25 mM imidazole to remove unbound proteins. After washing, the NADK1 was eluted with the elution buffer containing 200 mM imidazole. Proteins obtained from each step of purification were analyzed for the identity and purity by 18% SDS-PAGE (Figure 3.14).

Even though, no recombinant NADK1 protein was observed in the soluble protein fraction by SDS-PAGE, NAD kinase activity was detected in this fraction. Therefore, purification of the soluble NADK1 protein was attempted using a Ni Sepharose high performance column following the methods described above. All steps were performed at 4 °C. Proteins obtained from each step of purification were analyzed for the identity and purity on 18% SDS-PAGE (Figure 3.15).

To verify the presence of a His₆ tag within the recombinant NADK1 protein, western blot analysis using an anti-His₆ tag antibody was conducted. After proteins of interest were separated by SDS-PAGE and transferred from the gel to the PVDF membrane, detection of His₆-tagged proteins was carried out with the

Anti-His primary antibody (anti – His antibody: mouse anti – His Ab from mouse ascites fluid; product code 27-4710-01, Amersham Biosciences) with the dilution of 1:3000, followed by the secondary antibody, alkaline phosphatase (AP)-conjugated rabbit anti-mouse IgG (Jackson ImmunoResearch) with the dilution of 1:2500. The result was visualized by assaying the alkaline phosphatase activity using NBT/BCIP (Figure 3.16).

Data describing the purification of the recombinant protein NADK1 from the soluble protein fraction were obtained as presented in Table 3.1. Overall, through the Ni Sepharose high performance column, a 23-purification fold was obtained. To examine the kinetic properties of the purified NADK1, the substrate saturation curves of NADK1 were generated and plotted as shown in Figure 3.17. Initial velocities of NADK1 were measured in the presence of a saturating concentration of one of the substrates, NAD^+ or ATP, for varying concentrations of the other. Figure 3.17a shows the saturation curve for NAD^+ generated in the presence of 4 mM ATP and 0.6 mM Mg^{2+} for different concentrations of NAD^+ (0.2-6 mM). Figure 3.17b shows the saturation curve for ATP generated in the presence of 4 mM NAD^+ for different concentrations of ATP (0.2-6 mM). Mg^{2+} concentration was adjusted to be 2 mM higher than each ATP concentration used to ensure that at least 90% of ATP existed as MgATP^{2-} (Delumeau, 1998) and free calcium concentration was reduced to 0.1 mM to limit CaATP^{2-} formation. The Lineweaver-Burk plots or the inverted substrate saturation curves were constructed (Figure 3.18a, b). V_{\max} is expressed in mol NADP^+ formed $\text{h}^{-1} (\text{mg protein})^{-1}$. The calculated V_{\max} ($\text{unit mg}^{-1}\text{protein}$) and K_m (mM) are 0.35 and 0.79 for NAD^+ and 2.32 and 0.29 for ATP.

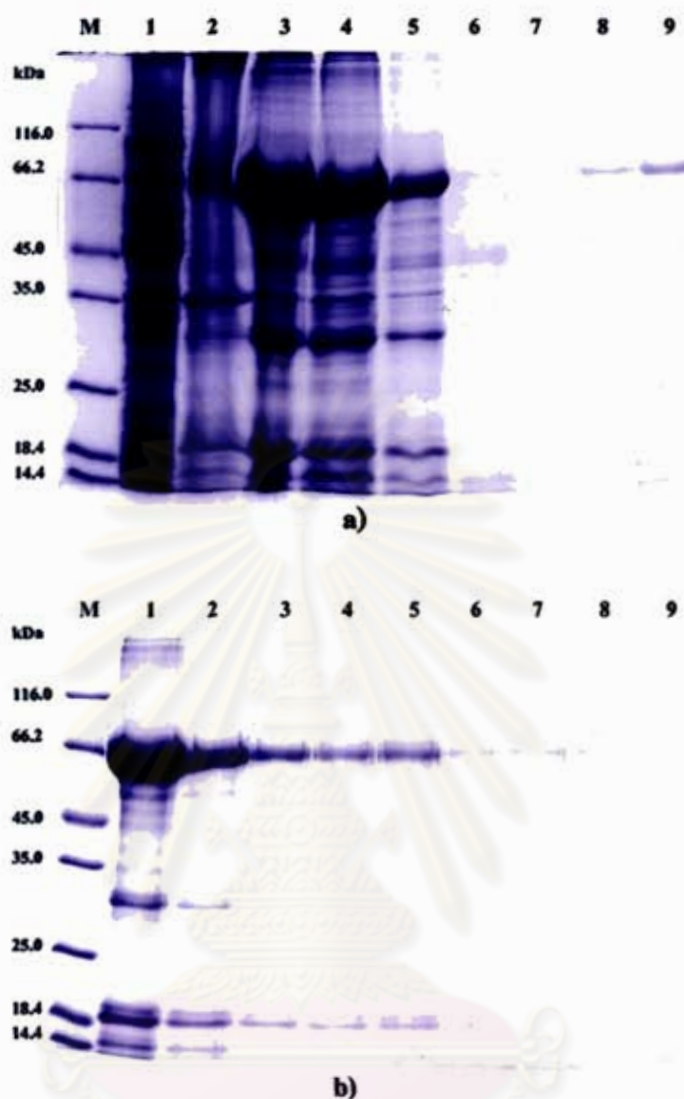


Figure 3.14 Purification of recombinant NADK1 from the inclusion bodies.

a) Lane M: protein marker (Fermentas)

Lane 1: insoluble proteins

Lane 2: insoluble proteins dissolved with 8 M urea

Lane 4-5: flow-through

Lane 6-7: fractions washed with buffer containing 8 M urea and 25 mM imidazole

Lane 8-9: fractions eluted with buffer containing 8 M urea and 50 mM imidazole

b) Lane M: protein marker (Fermentas)

Lane 1-3: fractions eluted with buffer containing 8 M urea and 200 mM imidazole

Lane 4-9: fractions eluted with buffer containing 8 M urea and 500 mM imidazole

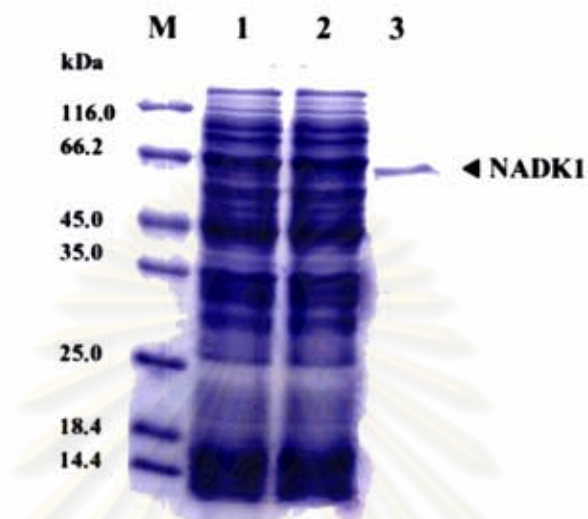


Figure 3.15 Purification of recombinant NADK1 from the soluble protein fraction.

Lane M: protein marker (Fermentas)

Lane 1: soluble proteins

Lane 2: flow-through

Lane 3: fraction eluted with 200 mM imidazole, in which a protein band with the molecular weight of approximately 60.6 kD was obtained

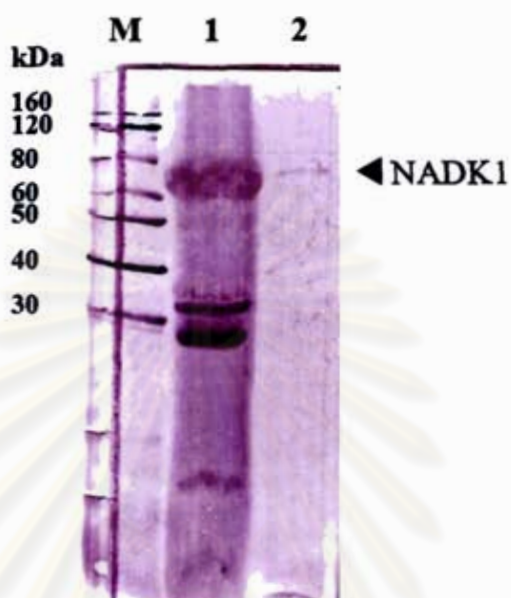


Figure 3.16 Western blot analysis of the recombinant protein from *E. coli*

Rosetta (DE3) pLysS harboring *NADK1*.

Lane M: Marker Benchmark His-tagged

Lane 1: inclusion bodies

Lane 2: *NADK1* purified by Ni-Sepharose from the soluble protein
fraction

Table 3.1 The purification table of the recombinant NADK1 by Ni-Sepharose column chromatography.

NADK1	Total volume (ml)	Protein content (mg/ml)	Total protein (mg)	Specific Activity $\mu\text{molNADPmin}^{-1}\text{mg}^{-1}$	Total Activity $\mu\text{molNADPmin}^{-1}$	Purification fold
Crude	25	5.34	133.53	1.39	185.72	1
purified	5	0.08	0.38	31.33	11.84	22.53

ศูนย์วิทยทรัพยากร
จุฬาลงกรณ์มหาวิทยาลัย

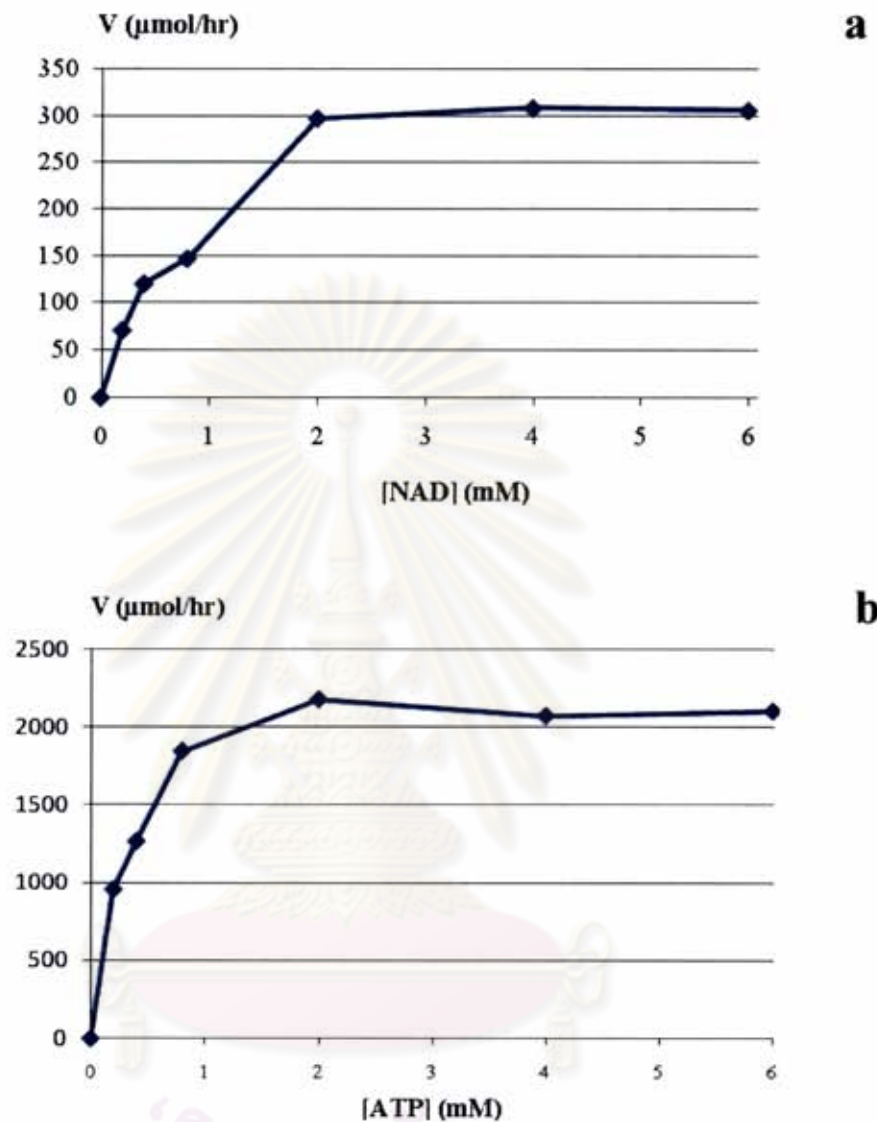
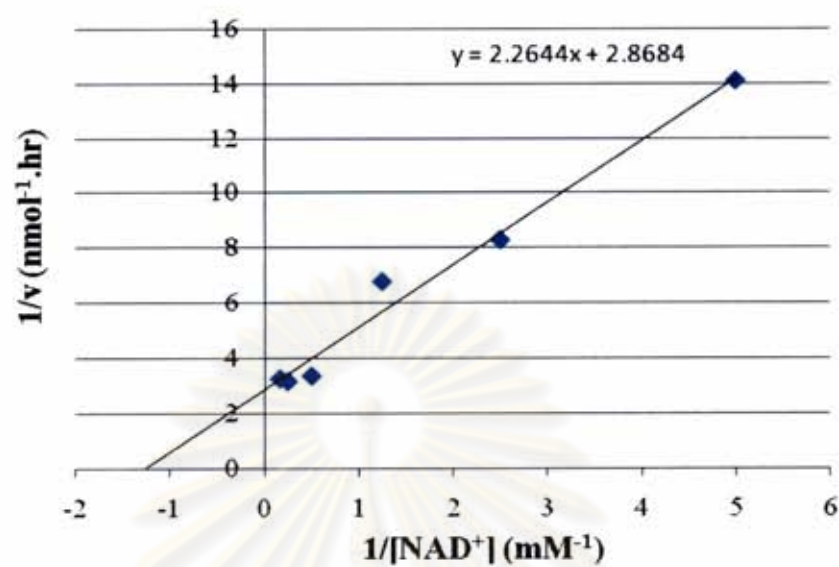


Figure 3.17 Substrate saturation curves of the recombinant NADK1.

- a) In the presence of saturating concentration of ATP (4 mM) for varying NAD^+ concentrations (0.2, 0.4, 0.8, 2, 4 and 6 mM).
- b) In the presence of saturating concentration of NAD^+ (4 mM) for varying ATP concentrations (0.2, 0.4, 0.8, 2, 4 and 6 mM).

a



b

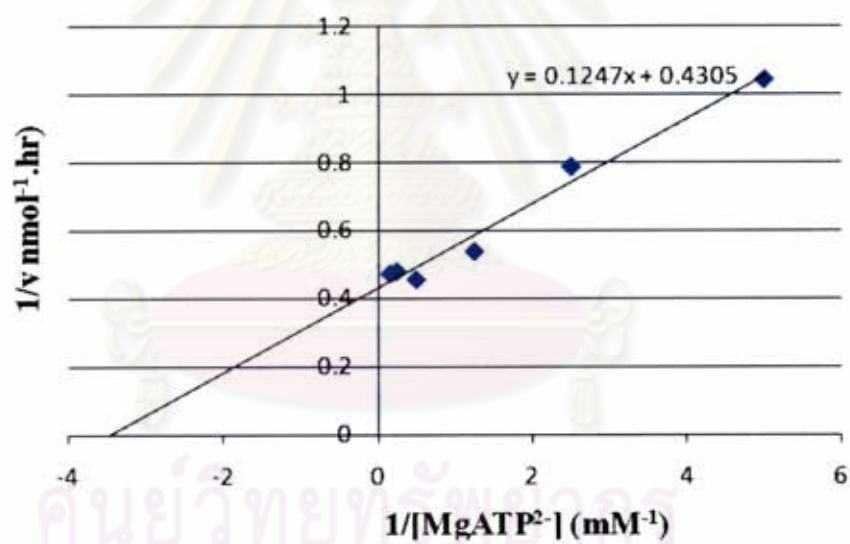


Figure 3.18 Lineweaver-Burg plots of NAD kinase. a) plot of $1/v$ against $1/NAD^+$ for different concentrations of ATP. b) plot of $1/v$ against $1/MgATP^{2-}$ for different concentrations of NAD^+ . Initial velocities are expressed in μmol of $NADP^+$ formed $h^{-1} \text{mg}^{-1}$.

3.6 NAD kinase activity of rice (*Oryza sativa* L.) cultivar Khao Dok Ma Li 105 (KDML105).

3.6.1 Measurement of NAD kinase activity in rice under salt stress.

NAD kinase activity was assayed in the crude extracts from leaves of KDML105 rice seedlings grown under salt stress. After 1 week of germination, rice seedlings were transferred to 1X Limpinuntana's nutrient solution and grown for 2 weeks under a 16-hr light/8-hr dark photoperiod. Then, the 3-week old seedlings were treated with 150 mM NaCl in 1X Limpinuntana's nutrient solution for 0, 3, 6, 9, 12 or 24 hours. Figure 3.19 shows that, after 3 hours, NAD kinase activity remained the same as the control at 0 hr but a decrease was observed after 6 hours of salt stress treatment. The NAD kinase activity in the rice seedlings then continued to decline until after 24 hours of salt stress.

3.6.2 Partial purification of NAD kinase from rice (*Oryza sativa* L.) cultivar Khao Dok Ma Li 105 (KDML105).

Khao Dok Ma Li 105 (KDML105) rice seeds were germinated in NB medium. After 7 days, germinated seeds were transferred to 1X Limpinuntana's nutrient solution (Limpinuntana, 1978) and grown for 2 weeks under a 16-hr light/8-hr dark photoperiod. Leaves from the 3 week-old seedlings were collected and ground in liquid nitrogen using chilled mortars and pestles. The plant material was kept frozen, ground to a fine powder, and proteins were extracted according to the methods described above. Rice crude protein extract was then precipitated with 0-30%, 30-50% and 50-70% saturated ammonium sulfate. Proteins obtained from each step of purification were analyzed for the identity and purity on 18% SDS-PAGE compared with the recombinant NADK1

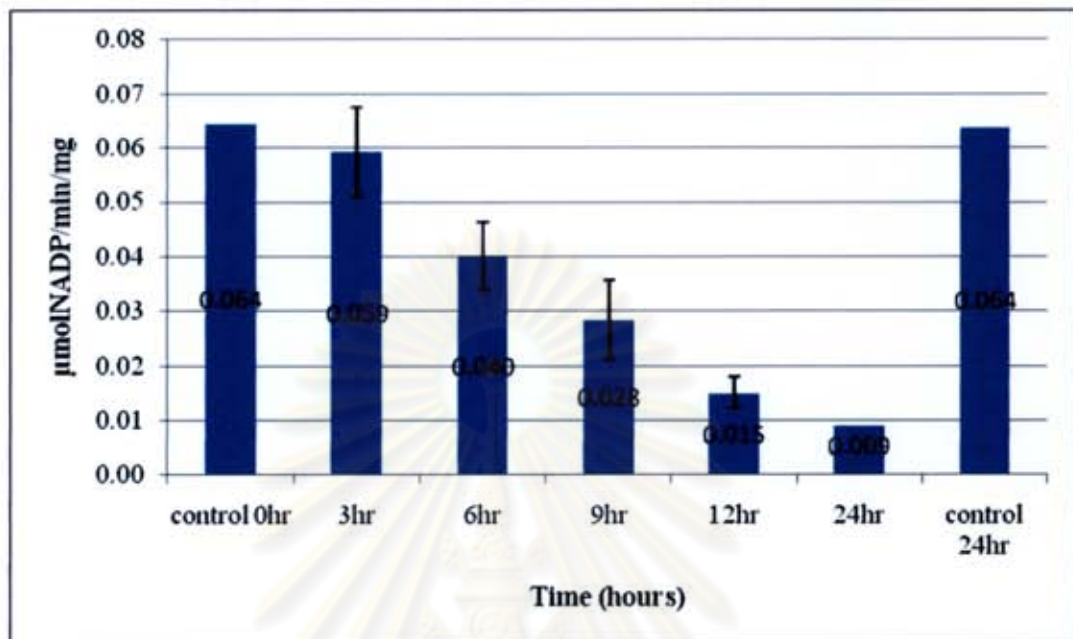


Figure 3.19 NAD kinase activity of the crude extracts from 3-week old KDML105 rice seedlings after salt stress. Controls were plants grown in 1X Limpinuntana's nutrient solution collected at the beginning (0 hr) and the end (24 hr) of the experiment.

ศูนย์วิทยทรัพยากร
จุฬาลงกรณ์มหาวิทยาลัย

and NADK2 proteins (Figure 3.20, 3.21). For the rice protein extract, proteins precipitated with 0-30% saturated ammonium sulfate had the highest NAD kinase activity (Figure 3.22), which is similar to the recombinant protein NADK2 (Figure 3.24). In contrast, the recombinant NADK1 had the highest NAD kinase activity when precipitated with 30-50% saturated ammonium sulfate (Figure 3.23). The samples with the highest specific activity would be used to assay regulation of NAD kinase by calmodulin from rice as described below.

To achieve better purification, crude protein extract was dialyzed and applied to a column (25 ml) of DEAE-Toyopearl (TOSOH, Japan). The non-binding protein eluate, which contained NADK activity, was collected and brought to 3.5 M NaCl. The sample was then applied (3 ml/min) to a column (10 ml) of Butyl-Toyopearl (TOSOH, Japan). The column was washed and eluted with a linear gradient (150 mL) of 0% to 100% buffer D (50 mM Tris-Cl, pH 7.5, 30% [v/v] ethanediol, 100 mM KCl, 3 mM MgCl₂, and 1 mM DTT). NADK activity was eluted as a single peak of activity at approximately 95% buffer D. Fractions (7 ml) were collected and those containing greater than 20% peak NADK activity were pooled, dialyzed in buffer contained 50 mM Tris-Cl, pH 7.5, 100 mM KCl, 3 mM MgCl₂, and 1 mM DTT. Proteins obtained from each step of purification were analyzed for the identity and purity on 18% SDS-PAGE (Figure 3.25). Data describing the partial purification of NAD kinase from the 3-week old rice seedlings were obtained as shown in Table 3.2. Overall, DEAE-Toyopearl and Butyl-Toyopearl column chromatography gave a purification fold of 11.76.

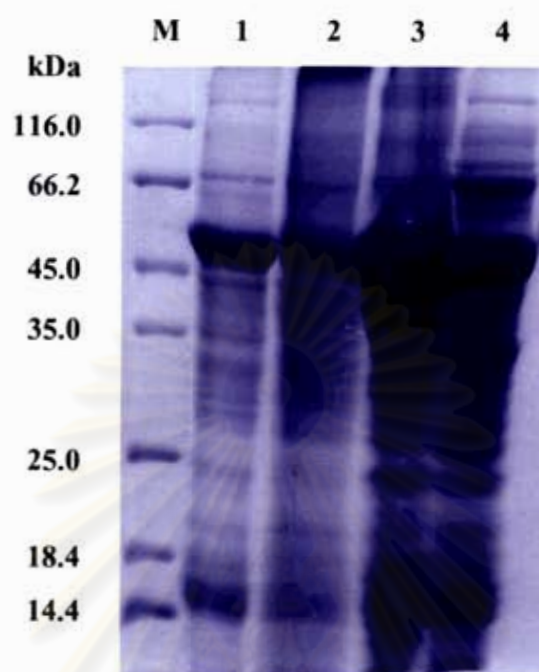


Figure 3.20 SDS-PAGE analysis of the rice protein crude extract precipitated with saturated ammonium sulfate.

Lane M: protein marker (Fermentas)

Lane 1: crude extract

Lane 2: crude extract precipitated with 0-30% saturated ammonium sulfate

Lane 3: crude extract precipitated with 30-50% saturated ammonium sulfate

Lane 4: crude extract precipitated with 50-70% saturated ammonium sulfate

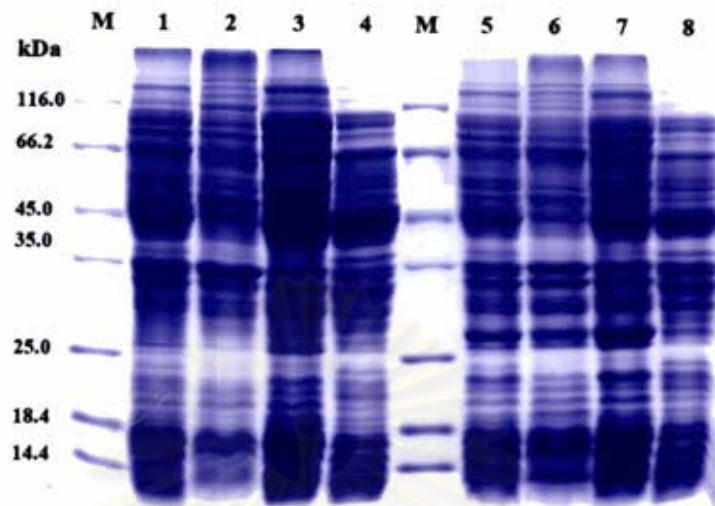


Figure 3.21 SDS-PAGE analysis of the protein crude extract from *E. coli* expressing NADK1 and NADK2 precipitated with saturated ammonium sulfate.

Lanes M: protein marker (Fermentas)

Lane 1: crude extract from *E. coli* expressing NADK1

Lane 2: crude extract from *E. coli* expressing NADK1 precipitated with 0-30% saturated ammonium sulfate

Lane 3: crude extract from *E. coli* expressing NADK1 precipitated with 30-50% saturated ammonium sulfate

Lane 4: crude extract from *E. coli* expressing NADK1 precipitated with 50-70% saturated ammonium sulfate

Lane 5: crude extract from *E. coli* expressing NADK2

Lane 6: crude extract from *E. coli* expressing NADK2 precipitated with 0-30% saturated ammonium sulfate

Lane 7: crude extract from *E. coli* expressing NADK2 precipitated with 30-50% saturated ammonium sulfate

Lane 8: crude extract from *E. coli* expressing NADK2 precipitated with 50-70% saturated ammonium sulfate

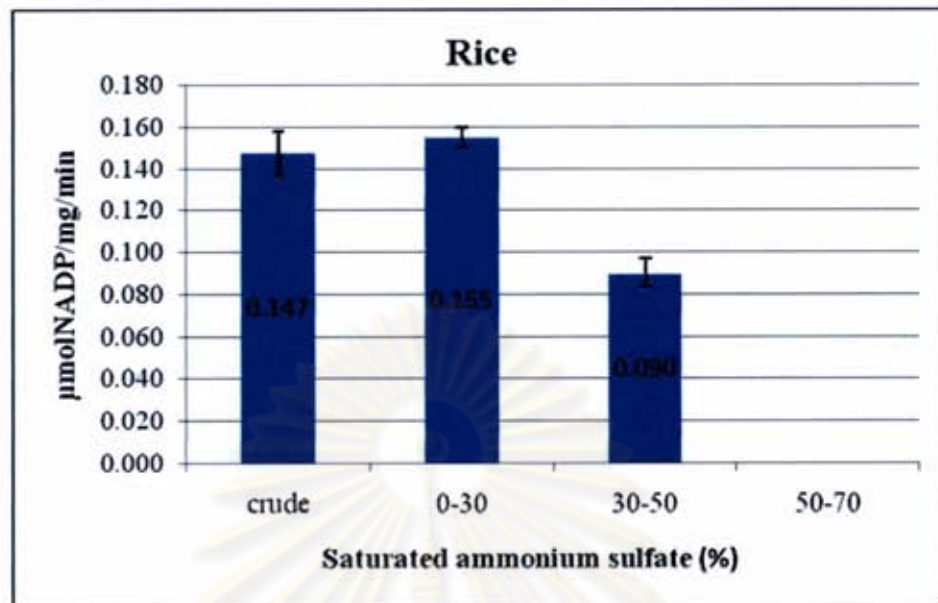


Figure 3.22 NAD kinase specific activity of rice extracts precipitated in various concentrations of saturated ammonium sulfate.

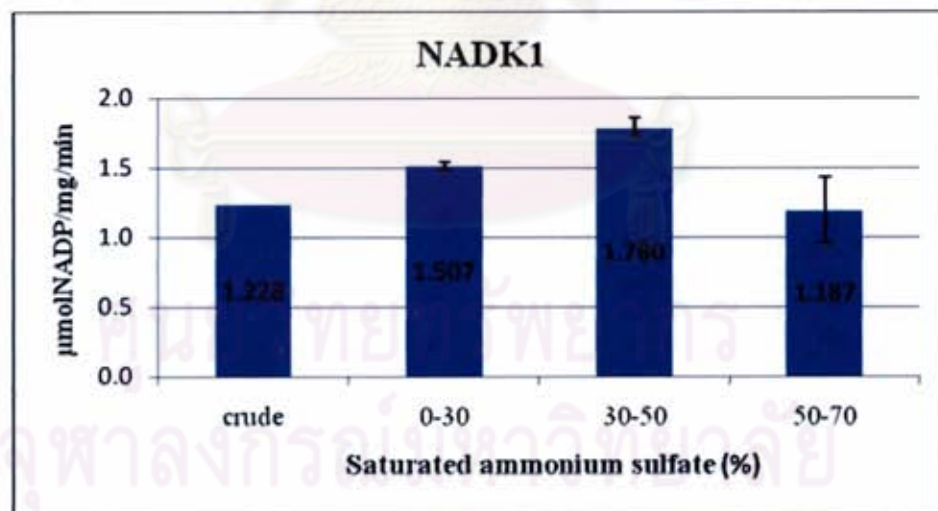


Figure 3.23 NAD kinase specific activity of crude extracts from *E. coli* expressing NADK1 precipitated in various concentrations of saturated ammonium sulfate.

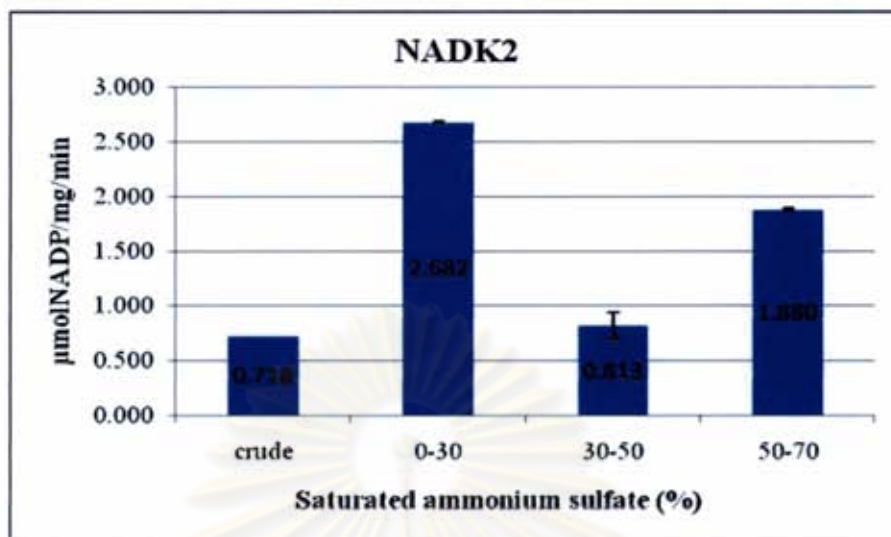


Figure 3.24 NAD kinase specific activity of crude extract from *E. coli* expressing NADK2 in various concentrations of saturated ammonium sulfate.

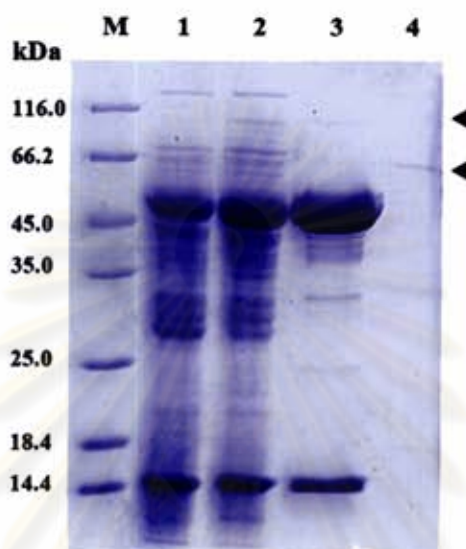


Figure 3.25 SDS-PAGE analysis of the partially purified native NAD kinase from 3-week old rice seedlings.

Lane M: protein marker (Fermentas)

Lane 1: crude extract of rice

Lane 2: unbound fraction from DEAE-Toyopearl

Lane 3: eluted fraction from Butyl- Toyopearl

Lane 4: purified recombinant NADK1

Table 3.2 The purification table of native NADK from 3-week old rice seedlings.

Sample	Total volume (ml)	Protein content (mg/ml)	Total protein (mg)	Specific Activity $\mu\text{molNADP}/\text{min}/\text{mg}$	Total Activity $\mu\text{molNADP}/\text{min}$	Purification fold
crude extract	15	1.77	26.55	0.06	1.72	1
DEAEunbound	4.5	0.057	0.258	0.416	0.107	6.93
Butyl-Toyopearl	2.5	0.045	0.113	0.700	0.079	11.67

ศูนย์วิทยทรัพยากร
จุฬาลงกรณ์มหาวิทยาลัย

3.7 Regulation by calmodulin

3.7.1 Effect of CaM on NAD kinase activity

Protein production in *E. coli* strain BL21 harboring the *OsCam1-1* in pET21a(+) was induced with 0.1 mM IPTG for 3 hours. Proteins were extracted and applied to a Phenyl-Sepharose column followed by washing and eluting the column as described above. The proteins in each step during the purification were analyzed by SDS-polyacrylamide gel electrophoresis (Figure 3.26). The fractions containing OsCaM1-1 protein were pooled and dialyzed against sufficient EGTA to remove calcium ions. All proteins were concentrated using Centrifugal Filters (10000 Daltons molecular weight cut-off) (Amicon) before protein concentration was determined by Bradford solution. The effect of OsCaM1-1 on NAD kinases was examined by measuring their activity as described earlier. The results are shown in Figures 3.27, 3.28 and 3.29 for the purified recombinant NADK1, the 0-30% saturated ammonium sulfate precipitate from *E. coli* expressing NADK2 and the rice crude extract. For both recombinant proteins, the presence of OsCaM1-1 did not cause the activation of NAD kinase. On the contrary, NAD kinase activity tended to decrease when the Ca^{2+} concentration was increased, especially in NADK2. For the rice crude extract, Ca^{2+} also negatively affected the activity of NAD kinase. However, OsCaM1-1 appeared to reduce the effect of Ca^{2+} in all concentrations.

3.7.2 ^{35}S -recombinant CaM binding assay

To determine whether NADK1 and NADK2 were target proteins of a calmodulin, calmodulin-binding assay using ^{35}S -labeled recombinant calmodulin as a probe was performed. ^{35}S -Labeled recombinant CaM was prepared using the rice *Cam*

(*OsCam1-1*) cloned into the pET21a(+) expression vector. Samples of NAD kinase (recombinant NADK1, recombinant NADK2 and rice protein extract) were separated by SDS-polyacrylamide gel electrophoresis (SDS-PAGE) and electro-transferred onto nitrocellulose membrane (whatman, USA). Following the transfer, the membrane was blocked and incubated with the probe solution containing 200 nM ³⁵S-labeled recombinant OsCaM1-1 protein for 2 hours. The membrane was washed and exposed to an X-ray film for 1 week. Figure 3.30 shows that while no signal was detected in the recombinant NADK1 and in any protein fractions from rice *Oryza sativa* L., OsCaM1-1 specifically detected the recombinant protein NADK2, which appeared as two major bands. However, none is the expected size of NADK2 (approximately 110 kDa).

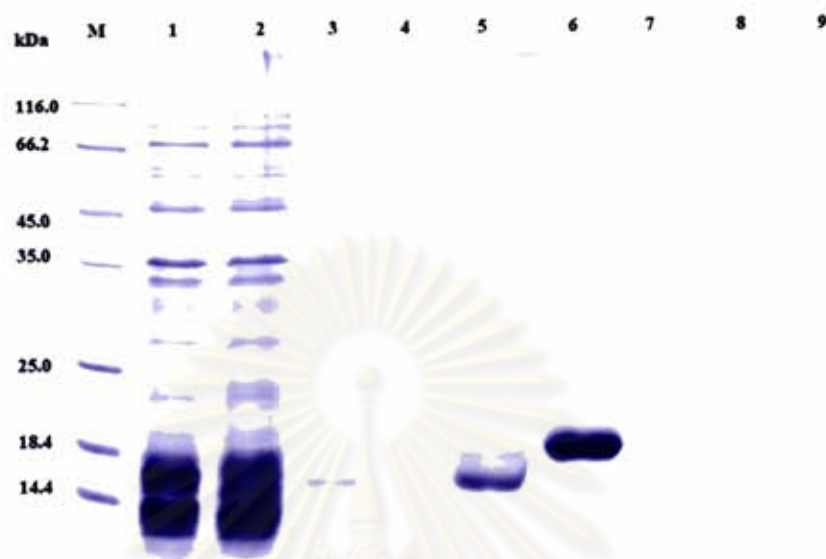


Figure 3.26 SDS-PAGE analysis of the purification of recombinant OsCaM1-1 protein by Phenyl-Sepharose.

Lane M: marker protein

Lane 1: crude protein

Lane 2: flow through

Lane 3-4: washed fraction with buffer containing 1 mM CaCl_2 and 200 mM NaCl

Lane 5-9: eluted fraction with buffer containing 5 mM EGTA

จุฬาลงกรณ์มหาวิทยาลัย

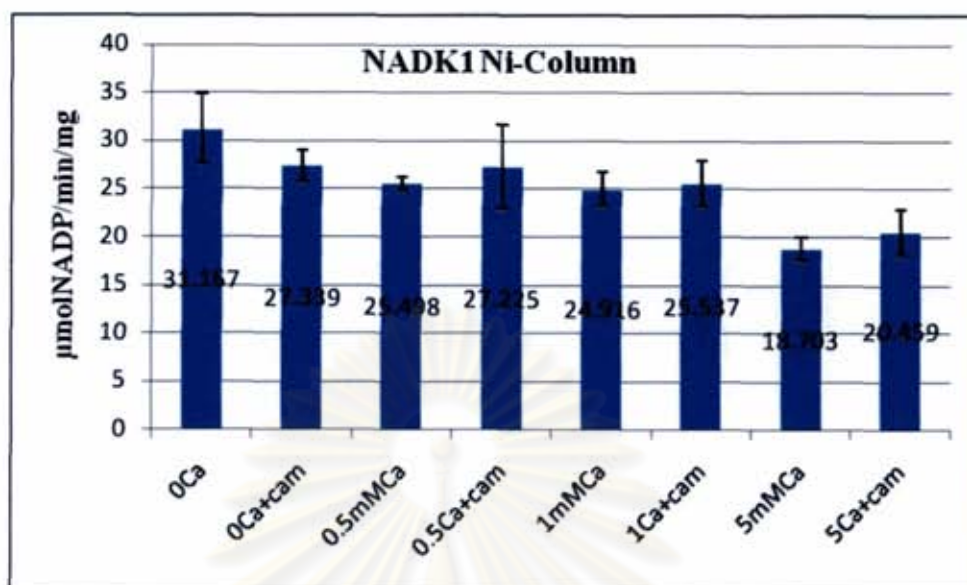


Figure 3.27 NAD kinase specific activity of the purified recombinant NADK1 in the presence of various calcium concentrations and 300 nM OsCaM1-1.

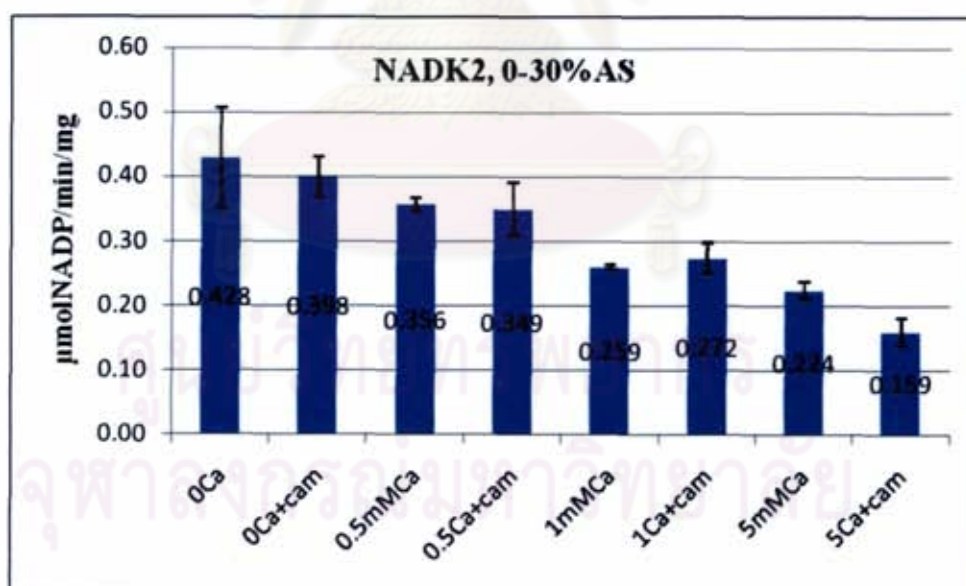


Figure 3.28 NAD kinase specific activity of the 0-30% saturated ammonium sulfate precipitate from *E. coli* expressing NADK2 in the presence of various calcium concentrations and 300 nM OsCaM1-1.

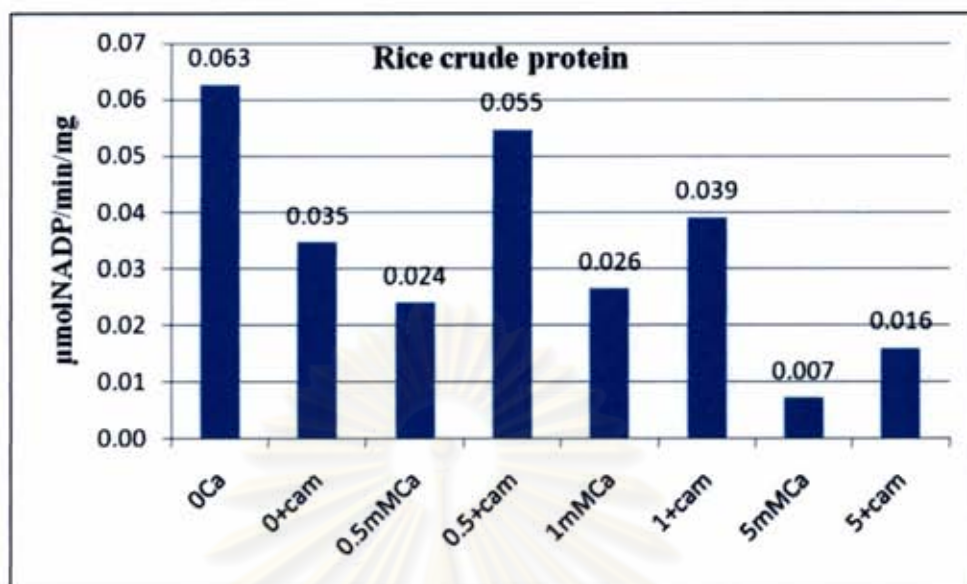


Figure 3.29 NAD kinase specific activity of the rice protein crude extract in the presence of various calcium concentrations and 300 nM OsCaM1-1.



Figure 3.30 ^{35}S -recombinant CaM binding assay. Proteins were subjected to SDS/PAGE and transferred onto a nitrocellulose membrane. The membrane was incubated with 200 mM ^{35}S -recombinant OsCaM1-1. Arrows indicate positive signals.

Lane M: protein marker (Fermentus)

Lane 1: rice crude protein extract

Lane 2: unbound DEAE-Toyopearl fraction of rice crude protein

Lane 3, 5, 6: eluted fraction of Butyl-Toyopearl of rice crude protein

Lane 4: 0-30% saturated ammonium precipitate of rice crude protein

Lane 7: purified recombinant NADK1 protein

Lane 8: insoluble protein fraction from *E. coli* expressing NADK1

Lane 9: soluble protein fraction from *E. coli* expressing NADK2

CHAPTER IV

DISCUSSION

4.1 Amino acid sequences of NAD kinase from rice *Oryza sativa* L.

We have identified, cloned, and characterized cDNAs encoding two distinct NADK isoforms, denoted NADK1 (OsNADK1) and NADK2 (OsNADK2) (Figure 3.1). The sequence similarity between the predicted proteins for *NADK1* and *NADK2* is restricted to the C-terminal region. The motifs, XXX-XXGGDG-XL and GDXXX-TPTGSTAY, where X represents a hydrophobic residue, have been reported in NADKs (Turner *et al.*, 2004 and Liu *et al.*, 2005). Both motifs were found to be conserved in both OsNADK1 and OsNADK2. The conserved GGDG motif of NADKs has been suggested to be catalytically important and to be involved in nucleotide binding (Shirakihara, *et al.*, 1988) or in phosphate transfer (Pignot, *et al.*, 2000).

The recombinant protein encoded by *NADK1*, with a predicted mass of roughly 60 kD, is similar to the size predicted for an Arabidopsis NADK (Turner *et al.*, 2004) and a tomato CaM-independent NADK (Delumeau *et al.*, 2000). We found no evidence of CaM binding to NADK1 or effect of CaM on its activity suggesting that OsNADK1 is also a CaM-independent NADK. CaM-independent NADKs have been described in a number of higher plant species including pea, spinach, oat and tomato (Simon *et al.*, 1982, 1984; Gallais *et al.*, 2001; Delumeau *et al.*, 1998). Sequence analysis (sequence homology searches) of NADK2, which has 996 residues and a predicted molecular mass of about 110.3 kD, revealed the long N-terminal extension that shares a strong sequence similarity (about 60% identity) to AtNADK2 from Arabidopsis (Figure 3.2). This region was reported to contain a CaM-binding

domain, of which the presence appears to be unique to plant NADKs. Widespread distribution of putative NADK2 homologues in other higher plants (e.g. arabidopsis, canola, soybean, lettuce, sorghum, wheat, and others) has been reported.

A number of different physiological roles have been proposed for NADKs in plants. Having multiple, differentially regulated NADKs may afford additional metabolic flexibility in coordinating cellular NAD to NADP ratios. An important consideration, however, and one which merits additional research, is the subcellular localization of NADK isoforms in plants given the importance of NADP in different organelles. There has been substantial debate as to where CaM-dependent and -independent isoforms are localized within plant cells, and the issue remains unresolved. CaM-dependent NADK activity has been observed in mitochondrial fractions (Dieter *et al.*, 1984; Sauer *et al.*, 1985; Pou De Crescenzo *et al.*, 2001), chloroplastic fractions (Muto *et al.*, 1981; Jarrett *et al.*, 1982; Simon *et al.*, 1984), and the cytosolic fraction (Simon *et al.*, 1982; Gallais *et al.*, 2000; Pou De Crescenzo *et al.*, 2001). By comparison, CaM-independent NADK activity in plant cells has been observed in the cytosolic fraction of cells (Gallais *et al.*, 2000; Pou De Crescenzo *et al.*, 2001) and in the chloroplast (Simon *et al.*, 1984). The roles of these isoforms remain unclear, although it has been suggested that chloroplastic NADK might participate in the light-stimulated conversion of NAD to NADP (Jarrett *et al.*, 1982).

4.2 Cloning and expression of NAD kinase genes

The complete cDNA for NADK1 and NADK2 was amplified by PCR using the full-length cDNA as a template. The sense primer contained *NdeI* site, while the antisense primer consisted of *SalI* site for further cloning purpose. Vent DNA

polymerase was used for amplification of *NADK1* because of its high fidelity derived in part from an integral 3'→5' proofreading exonuclease activity not possessed by *Taq*. The fidelity of Vent DNA polymerase (New England Biolabs Inc., USA) is 5-15-fold higher than that observed for *Taq* DNA polymerase. For *NADK2*, DyNzyme DNA polymerase (Finnzymes, Finland), which can amplify long PCR fragments up 4.0 kb, was used because of its improvement on the amplification of GC rich sequences or regions containing long complementary areas.

DNA fragments of NAD kinase from Rice *Oryza sativa* L. *NADK1* and *NADK2* were ligated into a TA vector, pTZ57 R/T and introduced by transformation into *E. coli* XL1-Blue. The *lacZ* reading frame is interrupted resulting in the appearance of white colonies. The *NADK* gene fragments were ligated with the *NdeI-SalI* sites of pET-21a in frame with the sequence encoding a 6x His tag to produce a fusion protein. pET system has been developed for tightly-regulated expression of recombinant proteins in *E. coli* cells. The approach to control basal expression is the use of vectors that contain what is termed a *T7lac* promoter (Studier *et al.*, 1990; Dubendorff *et al.*, 1991). These plasmids contain a *lac* operator sequence just downstream of the T7 promoter. They also carry the natural promoter and coding sequence for the *lac* repressor (*lacI*), oriented so that the *T7lac* and *lacI* promoters diverge. When this type of vector is used in DE3 lysogens, the *lac* repressor acts both at the *lacUV5* promoter in the host chromosome to repress transcription of the T7 RNA polymerase gene by the host polymerase and at the *T7lac* promoter in the vector to block transcription of the target gene by any T7 RNA polymerase that is made. For protein production under this system control, addition of IPTG to a growing culture of the lysogen induces T7 RNA polymerase production, which in turn transcribes the

target DNA in the plasmid.

For NADK1, the recombinant plasmid was transformed into *E. coli* Rosetta (DE3) pLysS, derivative of BL21, which was designed for expression of eukaryotic proteins that contain rare codons. For NADK2, *E. coli* Rosetta-gami, an Origami derivative, which combines the enhanced disulfide bond formation with the Rosetta characteristics resulting from the *trxB/gor* mutations with enhanced expression of eukaryotic proteins. Analyzed by SDS-PAGE, only expression of NADK1 in the inclusion bodies was observed. The result indicates that *NADK1* was highly expressed but the protein might not be folding properly causing the insoluble aggregates while *NADK2* was not expressed or expressed at a very low level if any. However, by measurement of NAD kinase activity, it was found that both genes were expressed as soluble proteins in all concentrations of IPTG used for NADK1 and in 0.2- 0.6 mM IPTG for NADK2, though at the level that could be detected by SDS-PAGE. For *NADK1*, it was expressed at the highest level (1.0 $\mu\text{molNADP}/\text{min}/\text{mg}$) in the absence of IPTG while in the presence of IPTG, the level of NAD kinase specific activity was lower and continuously decreased at higher concentrations of IPTG. Expression in the absence of IPTG can occur because there is some expression of T7 RNA polymerase gene under control of the *lacUV5* promoter from the *E. coli* genome (Novagen, USA). At higher IPTG concentrations, it is possible that the overexpressed protein may result in an accumulated misfolding protein leading to formation of inactive aggregates. For *NADK2*, NAD kinase specific activity was highest at 0.6 mM IPTG concentration (1.8 $\mu\text{molNADP}/\text{min}/\text{mg}$). However, the expressed protein could not be detected by SDS-PAGE.

The ability of NADK to produce NADP^+ in the presence of ATP was employed to obtain an activity band in the in-gel activity staining method. With the aid of the appropriate substrate and NADP^+ -dependent enzyme (G6PDH), the resulting NADPH transfer of reducing power from NADPH to NBT, by PMS, results in the formation of a blue-purple formazan precipitate at the site where the enzyme is immobilized. Results from the in-gel activity staining indicate that both recombinant proteins: NADK1 and NADK2 were produced as soluble proteins.

4.3 Purification and characterization of recombinant NAD kinase

After the host *E.coli* cells were collected and the cell wall was disrupted by ultrasonication, proteins were extracted in extraction buffer containing ethylenediamine tetraacetic acid (EDTA) to inhibit metalloproteases by chelating the divalent cations necessary for their activity. Addition of a reagent containing a thiol group such as dithiothreitol (DTT) and also a chelating agent such as EDTA in the extraction buffer will minimize the oxidation damage (Bollag *et al.*,1996). The recombinant NADK1 was successfully purified by Ni-sepharose column chromatography from the solubilized inclusion bodies and the soluble protein fraction. Western blot analysis using an anti-His₆ tag antibody confirmed identity of the recombinant proteins produced by the pET expression system. When NAD kinase activity was measured by the reactions involved reduction of DCIP, the solubilized and refolded proteins from the inclusion bodies did not show any activity. However, NAD kinase activity was detected in the soluble protein fraction from *E.coli* expressing NADK2. Unlike NADK1, the recombinant NADK2 protein could not be purified by Ni-sepharose or detected in western blot analysis (data not show) and

could barely be detected by in-gel activity staining suggesting that production level of the recombinant NADK2 was low.

Overall, through the Ni Sepharose high performance column, a 23-purification fold was obtained for the purification of the recombinant NADK1. Subsequently, the kinetic properties of the recombinant NADK1 were examined. All NAD kinase activities were linear with respect to time and protein concentration (data not shown). The calculated V_{\max} (unit mg^{-1} protein) and K_m (mM) are 0.35 and 0.79 for NAD^+ and 2.32 and 0.29 for ATP, respectively. Considerable variability between plant species has been reported for the $V_{\max}^{\text{Mg}^{2+}\text{ATP}}$ 11.1 (unit mg^{-1} protein) and K_m (mM) are 0.52 for NAD^+ and 0.73 for ATP from arabidopsis recombinant AtNADK1 (Turner *et al.*, 2004).

4.4 NAD kinase activity of rice (*Oryza sativa* L.) cultivar Khao Dok Ma Li 105 (KDML105).

Salt stress has been shown to have an effect on seed germination and growth of rice seedlings. Germination of rice seeds was remarkably decreased when NaCl concentration was increased. At 150 mM NaCl concentration the germination frequency was decreased up to 8-fold as compared to the non-stressed (0 mM NaCl) rice seeds. In addition, high level of NaCl also inhibited rice growth and caused injury on rice plants such as rolling of rice leaves, necrosis and death of rice seedlings. Beside germination and growth of rice seedlings, salt stress also had an effect on protein synthesis (Tanonkeow *et al.*, 2004). In this study, NAD kinase activity was assayed in the crude extracts from leaves of KDML105 rice seedlings grown under salt stress. It was decreased after 6 hours of salt stress treatment and continued to

decline until after 24 hours of salt stress. In contrast to the increase in NAD kinase activity observed after aluminium stress in monocotyledons (Slaski *et al.*, 1989) and after cold treatment in *Brassica napus* (Maciejewska, 1990), our study indicates that a NaCl treatment induces a large decrease in this enzymatic activity in the rice (*Oryza sativa* L.) cultivar Khao Dok Ma Li 105 (KDML105). A decrease in NAD kinase activity had already been reported in the salt-tolerant tomato *L. pimpinellifolium* under salt stress (Delumeau *et al.*, 2000) and in wheat after a water stress (Zagdanska *et al.*, 1990). The alterations of NAD kinase activity seem to be dependent on the nature of the stress and, from previous reports, the redox state of the NAD kinase seems to be an important modulator of its activity. Such a decrease in NAD kinase activity was unexpected in response to salt stress. This is because NAD kinases have been shown to play important roles to protect the cell against oxidative stress and, studies have already demonstrated that salt stress induces oxidative stress and changes in the anti-oxidant enzymatic defenses (Comba *et al.*, 1998; Gosset *et al.*, 1994).

In addition, our experiments indicate that a relationship exists between the external Ca^{2+} availability and the relative extent of NAD kinase inhibition. Displacement of the Ca^{2+} from the plasma membrane by NaCl had already been proposed to be a primary response to salt stress, and increases in cytosolic Ca^{2+} have also been recorded (Cramer *et al.*, 1985; Lynch *et al.*, 1987; Lynch *et al.*, 1988; Lynch, *et al.*, 1989). This could explain the decrease in NAD kinase activity observed whatever the nature of the ionic stress applied to the cells.

Solubility differences in salt are frequently exploited to separate proteins in the early stages of purification protocols. Ammonium sulfate was the salt of choice and was used in this work because it combined many useful features such as **salting**

out effectiveness, pH versatility, high solubility, low heat of solution and low price (Bollag *et al.*, 1996 and Creighton, 1993). Preliminary experiment on ammonium sulfate precipitation was also done in this work. Rice crude protein extract precipitated by 0-30% saturated ammonium sulfate had the highest NAD kinase activity (Figure 3.22), which is similar to the recombinant protein NADK2 (Figure 3.24). In contrast, the recombinant NADK1 had the highest NAD kinase activity when precipitated with 30-50% ammonium sulfate. For further purification, most protocols involve some forms of chromatography, which has become an essential tool in protein purification. Ion exchange chromatography separates proteins with differences in charge to give a very high resolution with high sample loading capacity. The difference in charge properties of protein is often considerable. Ion exchange chromatography is capable of separating species with very minor differences in properties, such as two proteins differing by only one amino acid. DEAE-Toyopearl is an anion exchanger which separates charged counter-ions. It is widely used in the purification of NAD kinase from other sources. After purification by DEAE-Toyopearl, the non-binding protein eluate contained NADK activity with a 7-fold purification. The next step of purification was the hydrophobic interaction chromatography (HIC). HIC takes advantage of the hydrophobicity of proteins promoting its separation on the basis of reversible hydrophobic interaction between immobilized hydrophobic ligands on chromatographic medium and non-polar regions on the surface of proteins (Queiroz *et al.*, 2001). Butyl-Toyopearl, which butyl groups are chemically bonded on the surface of hydrophilic resin was used. Adsorption of proteins to a HIC adsorbent is favored by a high salt concentration in the mobile phase. The elution of solute is accomplished by decreasing the salt concentration with

increasing hydrophobicity. In this work, the enzyme was eluted from Butyl-Toyopearl column using linear gradient 30% [v/v] ethanediol. From this step, NADK activity was obtained with a 12-purification fold. From SDS-PAGE (figure 3.25), the bands at approximately 56 and 14 kDa were likely the Rubisco large and small subunits, respectively (Ma *et al.*, 2009). We suggested that the upper band in the fraction eluted from Butyl-Toyopearl of approximately 110 kDa might be OsNADK2 and that OsNADK1 which has CaM-independent activity was undetectable following DEAE chromatography (Turner *et al.*, 2004). However, we noticed that NAD kinase activity of the purified enzyme as well as of the crude extract was lost very quickly, after 5 days at 4°C. These results indicated a low stability of NAD kinase, which has also been reported in Arabidopsis (Turner *et al.*, 2004) and yeast (Bieganowski *et al.*, 2006). One of the explanations is that most of the activators were separated from the enzyme and hence the enzyme was inactivated.

4.5 Regulation by calmodulin

Activity of plant NAD kinases has been reported to be regulated by Ca²⁺/CaM in pea (Muto, 1983, Simon *et al.*, 1984), tomato (Delumeau *et al.*, 1998), oat (Pou De Crescenzo *et al.*, 2001), and maize (Dieter *et al.*, 1984). A Ca²⁺/CaM-dependent membrane-bound NAD⁺ kinase was also described in mitochondria of maize: either linked to the outer membrane (Dieter *et al.*, 1984), or to both outer and inner membranes (Sauer *et al.*, 1985). Such membrane-bound isoform was also reported to increase after dormancy breakage in *Avena* seeds (Gallais *et al.*, 1999). Unlike Arabidopsis, in which the enzyme was fully activated by conserved CaM in the presence of calcium and displayed differential responsiveness to various CaM-like

Arabidopsis proteins (Turner *et al.*, 2004), our results did not show activation of any NAD kinase by $\text{Ca}^{2+}/\text{CaM}$ suggesting that activity of both NAD kinases might not be regulated by $\text{Ca}^{2+}/\text{CaM}$ or the responsiveness of NAD kinase to $\text{Ca}^{2+}/\text{CaM}$ regulation (if there is any) might be lost in the recombinant proteins. In sequence analysis suggests that NADK2 has a CaM-binding domain.

Even though measurement of NAD kinase activity in the presence of OsCaM1-1 did not indicate $\text{Ca}^{2+}/\text{CaM}$ -dependent activation, ^{35}S -recombinant CaM binding assay showed that while no signal was detected in the recombinant NADK1 and in any protein fractions from rice *Oryza sativa* L., OsCaM1-1 specifically interacted with the recombinant protein NADK2, which appeared as two major bands, but none has the expected size of NADK2 (approximately 110 kDa). However, the possibility that the positive bands were derived from the recombinant protein that has been truncated could not be ruled out. Further experiments need to be conducted in order to make a conclusive statement that activity of this NAD kinase isoform is regulated by $\text{Ca}^{2+}/\text{CaM}$.

ศูนย์วิทยทรัพยากร
จุฬาลงกรณ์มหาวิทยาลัย

CHAPTER V

CONCLUSIONS

1. The primary structure of OsNADK1 and OsNADK2 shares 65% and 56% amino acid similarity with NAD kinases from Arabidopsis, AtNADK1 and AtNADK2, respectively, and contains two conserved sequences: the GGDG motif and the Gly-rich motif in their conserved C-terminal region.
2. The *OsNADK1* and *OsNADK2* genes, which encode 547 and 996 amino acids with a predicted mass of roughly 60 kDa and 110 kDa, respectively, were successfully engineered and cloned into pET21a expression vector.
3. NAD kinase activity in the soluble protein fraction from *E. coli* strain Rosetta (DE3) pLysS carrying *OsNADK1* and Rosetta-gami carrying *OsNADK2* was detected by in-gel NAD kinase activity staining, while SDS-PAGE detected protein bands only in the inclusion bodies from the cells expressing *OsNADK1*.
4. The insoluble recombinant OsNADK1 was solubilized with 8 M urea, purified by Ni-column chromatography and refolded but no NAD kinase activity was detected.
5. The soluble recombinant OsNADK1 was purified using Ni-Sepharose with a 23-purification fold and the following kinetic properties: V_{\max} (unit mg^{-1} protein) and K_m (mM) of 0.35 and 0.79 for NAD and 2.32 and 0.29 for ATP, respectively.

6. In leaves of KDML105 rice seedlings grown under 150 mM salt stress, NAD kinase activity in the crude protein extracts was decreased after 6 hours of treatment and continued to decline until after 24 hours.
7. NAD kinase was partially purified from leaves of 3-week old rice seedlings using DEAE-Toyopearl and Butyl Toyopearl column chromatography with an overall 12-purification fold.
8. ^{35}S -recombinant CaM binding assay showed that OsCaM1-1 specifically interacted with the protein bands from crude extract of recombinant NADK2 suggesting that NADK2 might be a target protein of OsCaM1-1.

REFERENCES

- Anderson, J. M., Charbonneau, H., Jones, H. P., McCann, R. O. and Cormier, M. J. (1980). Characterization of the plant nicotinamide adenine dinucleotide kinase activator protein and its identification as calmodulin. *Biochemistry* 19: 3113-3120.
- Babu, Y. S., Bugg, C. E., and Cook, W. J. (1988). Structure of calmodulin refined at 2.2 Å resolution. *J Mol Biol.* 204: 191-204.
- Beckingham, K. (1991). Use of site-directed mutations in the individual Ca²⁺-binding sites of calmodulin to Ca²⁺-induced conformational changes. *J Biol Chem.* 266: 6027-6030.
- Bieganowski, P., Seidle, H. F., Wojcik, M. and Brenner, C. (2006). Synthetic lethal and biochemical analyses of NAD and NADH kinases in *Saccharomyces cerevisiae* establish separation of cellular functions. *J Biol Chem.* 281: 22439-22445.
- Berrin, J. G., Pierrugues, O., Brutesco, C., Alonso, B., Montillet, J. L., Roby, D. and Kazmaier, M. (2005). Stress induces the expression of AtNADK-1, a gene encoding a NAD(H) kinase in *Arabidopsis thaliana*. *Mol Genet Genomics* 27: 10-19.
- Boonburapong B., Buaboocha T. (2007). Genome-wide identification and analyses of the rice calmodulin and related potential calcium sensor proteins. *BMC Plant Biol* 7:4
- Buaboocha, T., and Zielinski, R.E. (2002). Calmodulin. In *Protein-Protein Interactions in Plant Biology*. Edited by McManus, M. T., Liang, W. A. and

- Allen, A. C. Sheffield, UK: Sheffield Academic Press, Roberts, J.A. (Series Editor). *Annu Plant Rev.* 7: 285-313.
- Chai, M. F., Chen, Q. J., An, R., Chen, Y. M., Chen, J. and Wang, X. C. (2005). NADK2, an Arabidopsis chloroplastic NAD kinase, plays a vital role in both chlorophyll synthesis and chloroplast protection. *Plant Mol Biol.* 59: 553-564.
- Chai, M. F., Wei, P. C., Chen, Q. J., An, R., Chen, J., Yang, S. and Wang, X. C. (2006). NADK3, a novel cytoplasmic source of NADPH, is required under conditions of oxidative stress and modulates abscisic acid responses in Arabidopsis. *J Plant.* 47: 665-674.
- Chen, C.W., Yang, Y.W., Lur, H.S., Tsai, Y.G., and Chang, M.C. (2006). A novel function of abscisic acid in the regulation of rice (*Oryza sativa* L.) root growth and development. *Plant Cell Physiol.* 47(1): 1-13
- Dieter, P. and Marme, D. (1984). A Ca^{2+} , Calmodulin-dependent NAD kinase from corn is located in the outer mitochondrial membrane. *J Biol Chem.* 259: 184-189.
- Euler, V. H. and Adler, E. (1938). Enzymic intertransformation of codehydrogenase I and codehydrogenase II. *Z. Physiol Chem.* 252: 41-48.
- Epel, D., Patton, C., Wallace, R. W. and Cheung, W. Y. (1981). Calmodulin activates NAD kinase of sea urchin eggs: an early event of fertilization. *Cell* 23: 543-549.
- Garavaglia, S., Raffaelli, N., Finaurini, L., Magni, G. and Rizzi, M. (2004). A novel fold revealed by *Mycobacterium tuberculosis* NAD kinase, a key allosteric enzyme in NADP biosynthesis. *J Biol Chem.* 279: 40980-40986.
- Gerdes, S. Y., Scholle, M. D., D'Souza M., Bernal A., Baev, M. V., Farrell, M.,

- Kurnasov, O. V., Daugherty, M. D., Mseeh, F., and Polanuyer, B. M. (2002). From genetic footprinting to antimicrobial drug targets: examples in cofactor biosynthetic pathways. *J Bacteriol.* 184: 4555-4572.
- Gilroy, S., Blowers, D. P. and Trewavas, A.J., (1987). Calcium: a regulation system emerges in plant cells. *Development* 100: 181-184.
- Grose, J. H., Joss, L. Velick, S. F., and Roth, J. R. (2006). Evidence that feedback inhibition of NAD kinase controls responses to oxidative stress. *Proceedings of the National Academy of Sciences* 103: 7601-7606.
- Haiech, J., Kilhoffer, M. C., Lukas, T. J., Craig, T. A., Roberts, D. M., and Watterson, D. M. (1991). Restoration of the calcium binding activity of mutant calmodulins toward normal by the presence of a calmodulin binding structure. *J Biol Chem* 266: 3427-3431.
- Hunt, L., Lerner, F. and Ziegler, M. (2004). NAD - new roles in signalling and gene regulation in plants. *New Phytol.* 163: 31-44.
- Kawai, S., Mori, S., Mukai, T., Suzuki, S., Yamada, T., Hashimoto, W. and Murata, K. (2000). Inorganic Polyphosphate/ATP-NAD kinase of *Micrococcus flavus* and *Mycobacterium tuberculosis* H37Rv. *Biochem. Biophys Res Commun.* 276: 57-63.
- Kawai, S., Suzuki, S., Mori, S. and Murata, K. (2001b). Molecular cloning and identification of UTR1 of a yeast *Saccharomyces cerevisiae* as a gene encoding an NAD kinase. *FEMS Microbiol Lett.* 200: 181-184.
- Kobayashi, K., Ehrlich, S. D., Albertini, A., Amati, G., Andersen, K. K., Arnaud, M., Asai, K., Ashikaga, S., Aymerich, S., and Bessieres, P., (2003). Essential *Bacillus subtilis* genes. *Proc Natl Acad Sci USA* 100: 4678-4683.

- Kohler, C., and Neuhaus, G. (2000). Characterisation of calmodulin binding to cyclic nucleotide-gated ion channels from *Arabidopsis thaliana*. *FEBS Lett.* 4710: 133-136.
- Krems, B., Charizanis, C. and Entian, K. D. (1995). Mutants of *Saccharomyces cerevisiae* sensitive to oxidative and osmotic stress. *Curr Genet.* 27: 427-434.
- Kuboniwa, H., Tjandra, N., Grzesiek, S., Ren, H., Klee, C. B., and Bax, A. (1995). Solution structure of calcium-free calmodulin. *Nat Struct Biol.* 2: 768-776.
- Labesse, G., Douguet, D., Assairi, L. and Gilles, A. M. (2002). Diacylglyceride kinases, sphingosine kinases and NAD kinases: distant relatives of 6-phosphofructokinases. *Trends Biochem Sci.* 27: 273-275.
- Lee, S. H., Johnson, J. D., Walsh, M. P., Van Lierop, J. E., Sutherland, C., Xu, A., Snedden, W.A., Kosk-Kosicka, D., Fromm, H., Narayanan, N., and Cho, M. J. (2000). Differential regulation of Ca^{2+} :calmodulin-dependent enzymes by plant calmodulin isoforms and free Ca^{2+} concentration. *Biochem J.* 350: 299-306.
- Lee, S. H., Kim, J. C., Lee, M. S., Heo, W. D., Seo, H. Y., Yoon, H. W., Hong, J. C., Lee, S. Y., Bahk, J. D., Hwang, I., and Cho, J. (1995). Identification of a novel Divergent calmodulin isoform from soybean which has differential ability to activate calmodulin-dependent enzymes. *J Biol Chem.* 270: 21806-21812.
- Lee, S. H., Kim, M. C., Heo, W. D., Kim, J. C., Chung, W. S., Park, C. Y., Park, H. C., Cheong, Y. H., Kim, C. Y., Lee, S. H., Lee, K. J., Bahk, J. D., Lee, S. Y., and Cho, M. J. (1999). Competitive binding of calmodulin isoforms to calmodulin-binding proteins: implications for the function of calmodulin isoforms in plant. *Biochim Biophys Acta.* 1433: 56-67.

- Lee, S. H., Seo, H. Y., Kim, J. C., Heo, W. D., Chung, W. S., Lee, K. J., Kim, M. C., Cheong, Y. H., Choi, J. Y., Lim, C. O., and Cho, M. J. (1997). Differential activation of NAD kinase by plant calmodulin isoforms. The critical role of domain I. *J Biol Chem.* 272: 9252-9259.
- Liu, J., Lou, Y., Yokota, H., Adams, P. D., Kim, R. and Kim, S. H. (2005). Crystal structures of an NAD kinase from *Archaeoglobus fulgidus* in complex with ATP, NAD, or NADP. *J Mol Biol.* 354: 289-303.
- Luan, S., Kudla, J., Rodriguez-Concepcion, M., Yalovsky, S., and Gruissem, W. (2002). Calmodulins and Calcineurin B-like Proteins: Calcium Sensors for Specific Signal Response Coupling in Plants. *Plant Cell.* : 389-400.
- Ma, Z., Cooper, C., Kim, J. H., and Buckner, J. D. (2009). A Study of Rubisco through Western Blotting and Tissue Printing Techniques. *J CBE- Life Sciences Education.* 8: 140-146
- Magni, G., Orsomando, G. and Raffaelli, N. (2006). Structural and functional properties of NAD kinase, a key enzyme in NADP biosynthesis. *Mini Rev Med Chem.* 6: 739-746.
- McGuinness, E.T., and Butler, J.R. (1985). NAD⁺ kinase - A Review. *Int J Biochem.* 17:1-11.
- Montange, P. G., Assairi, L., Arold, S., Pochet, S. and Labesse, G. (2007). NAD kinases use substrate-assisted catalysis for specific recognition of NAD. *J Biol Chem.* 282: 33925-33934.
- Mori, S., Yamasaki, M., Maruyama, Y., Momma, K., Kawai, S., Hashimoto, W., Mikami, B. and Murata, K. (2005b). NAD-binding mode and the significance of intersubunit contact revealed by the crystal structure of *Mycobacterium*

- tuberculosis* NAD kinase- NAD complex. *Biochem Biophys Res Commun.* 327: 500-508.
- Muto, S. and Miyachi, S. (1981). Light-Induced Conversion of Nicotinamide Adenine Dinucleotide to Nicotinamide Adenine Dinucleotide Phosphate in Higher Plant Leaves. *Plant Physiol.* 68: 324-328.
- Noctor, G., Queval, G., and Gakière, B. (2006). NAD(P) synthesis and pyridine nucleotide cycling in plants and their potential importance in stress conditions. *J Exp Bot.* 57: 1603–1620.
- Oganesyan, V., Huang, C., Adams, P. D., Jancarik, J., Yokota, H. A., Kim, R. and Kim, S. H. (2005). Structure of a NAD kinase from *Thermotoga maritima* at 2.3 Å resolution. *Acta Crystallogr Sect F Struct Biol Cryst Commun.* 61: 640-646.
- Outten, C. E. and Culotta, V. C. (2003). A novel NADH kinase is the mitochondrial source of NADPH in *Saccharomyces cerevisiae*. *J EMBO.* 22: 2015-2024.
- Ohyanagi, H., Tanaka, T., Sakai, H., Shigemoto, Y., Yamaguchi, K., Habara, T., Fujii, Y., Antonio, B. A., Nagamura, Y., Imanishi, T., Ikeo, K., Itoh, T., Gojobori, T., and Sasaki, T. (2006). The Rice Annotation Project Database (RAP-DB): hub for *Oryza sativa* ssp. japonica genome information. *Nucleic Acids Res.* 34(Database issue): D741-D744.
- Pollak, N., Dölle, C. and Ziegler, M. (2007). The power to reduce: pyridine nucleotides--small molecules with a multitude of functions. *J Biochem.* 402: 205-218.
- Pou De Crescenzo, M. A., Gallais, S., Leon, A. and Laval-Martin, D. L. (2001). Tween-20 activates and solubilizes the mitochondrial membrane-bound,

- calmodulin dependent NAD⁺ kinase of *Avena sativa* L. *J Membr Biol.* 182: 135-146.
- Raffaelli, N., Finaurini, L., Mazzola, F., Pucci, L., Sorci, L., Amici, A. and Magni, G. (2004). Characterization of *Mycobacterium tuberculosis* NAD kinase: functional analysis of the full-length enzyme by site-directed mutagenesis. *Biochemistry* 43: 7610-7617.
- Rossmann, M. G., Moras, D. and Olsen, K. W. (1974). Chemical and biological evolution of nucleotide-binding protein. *Nature* 250: 194-199.
- Salvemini, F., Franze, A., Iervolino, A., Filosa, S., Salzano, S. and Ursini, M. V. (1999). Enhanced glutathione levels and oxidoresistance mediated by increased glucose-6-phosphate dehydrogenase expression. *J Biol Chem.* 274: 2750-2757.
- Sasseti, C. M., Boyd, D. H. and Rubin, E. J. (2003). Genes required for mycobacterial growth defined by high density mutagenesis. *Mol Microbiol.* 48: 77-84.
- Shi, F., Kawai, S., Mori, S., Kono, E. and Murata, K. (2005). Identification of ATP-NADH kinase isozymes and their contribution to supply of NADP(H) in *Saccharomyces cerevisiae*. *J FEBS.* 272: 3337-3349.
- Shianna, K. V., Marchuk, D. A. and Strand, M. K. (2006). Genomic characterization of POS5, the *Saccharomyces cerevisiae* mitochondrial NADH kinase. *Mitochondrion* 6: 94-101.
- Simon, P., Bonzon, M., Greppin, H. and Marme, D. (1984). Subchloroplastic localization of NAD kinase activity: evidence for a Ca²⁺, calmodulin-

- dependent activity at the envelope and for a Ca^{2+} , calmodulin-independent activity in the stroma of pea chloroplasts. *FEBS Lett.* 167: 332-338.
- Simon, P., Dieter, P., Bonzon, M., Greppin, H. and Marme, D. (1982). Calmodulin-dependent and independent NAD kinase activities from cytoplasmic fractions of spinach (*Spinacia oleracea* L.). *Plant Cell Rep.* 1: 119-122.
- Strand, M. K., Stuart, G. R., Longley, M. J., Graziewicz, M. A., Dominick, O.C. and Copeland, W. C. (2003). POS5 gene of *Saccharomyces cerevisiae* encodes a mitochondrial NADH kinase required for stability of mitochondrial DNA. *Eukaryotic Cell* 2: 809-820.
- Takahashi, H., Watanabe, A., Tanaka, A., Hashida, S. N., Kawai-Yamada, M., Sonoike, K. and Uchimiya, H. (2006). Chloroplast NAD kinase is essential for energy transduction through the xanthophyll cycle in photosynthesis. *Plant Cell Physiol.* 47: 1678-1682.
- Takezawa, D., Liu, Z. H., An, G., and Poovaiah, B. W. (1995). Calmodulin gene family in potato: developmental and touch-induced expression of the mRNA encoding a novel isoform, *Plant Mol Biol.* 27: 693-703.
- Tian, W. N., Braunstein, L. D., Apse, K., Pang, J., Rose, M., Tian, X. and Stanton, R. C. (1999). Importance of glucose-6-phosphate dehydrogenase activity in cell death. *Am J Physiol.* 276: 1121-1131.
- Turner, W. L., Waller, J. C. and Snedden, W. A. (2005). Identification, molecular cloning and functional characterization of a novel NADH kinase from *Arabidopsis thaliana* (thale cress). *J Biochem.* 385: 217-223.
- Turner, W. L., Waller, J. C., Vanderbeld, B. and Snedden, W. A. (2004). Cloning and characterization of two NAD kinases from Arabidopsis. identification of a

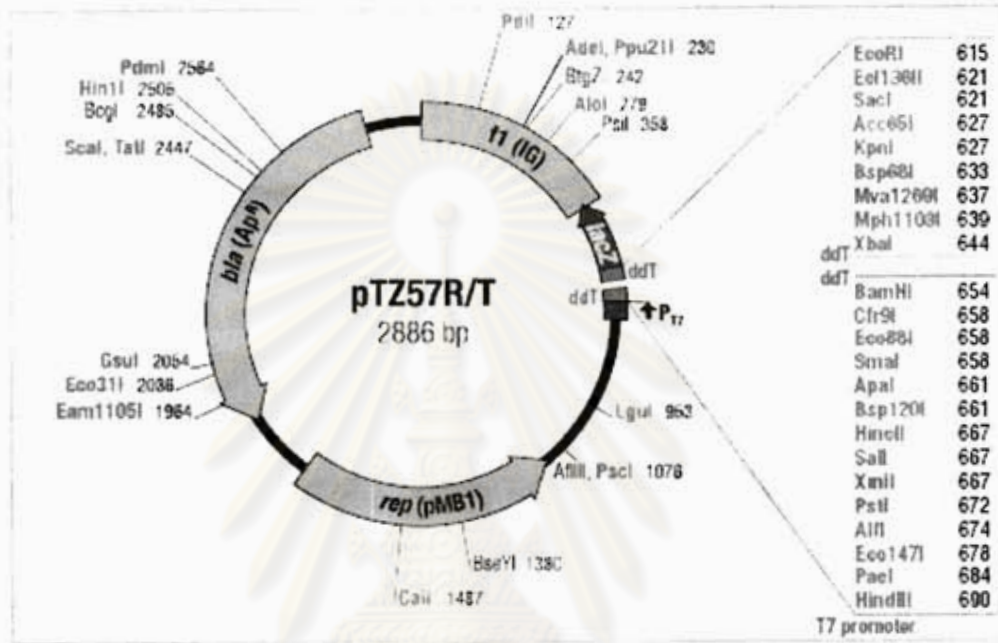
- calmodulin binding isoform. *Plant Physiol.* 135: 1243-1255.
- Valderrama, R., Corpas, F. J., Carreras, A., Gomez-Rodriguez, M. V., Chaki, M., Pedrajas, J. R., Fernandez-Ocana, A., Del Rio, L. A. and Barroso, J. B. (2006). The dehydrogenase-mediated recycling of NADPH is a key antioxidant system against salt-induced oxidative stress in olive plants. *Plant Cell Environ.* 2: 1449-1459.
- Vestin, R. (1937). Enzymic change from codehydrogenase I to codehydrogenase II. *Naturwissenschaften.* 25: 667-668.
- Vetter, S. W. and Leclerc, E. (2003). REVIEW ARTICLE: Novel aspects of calmodulin target recognition and activation. *Eur J Biochem.* 270: 404-414.
- Wikipedia, **Structural features of *Oryza sativa* L.** [online], 21 april 2010.
<http://en.wikipedia.org/wiki/Image:Koeh-232.jpg>
- Williams, M. B. and Jones, H. P. (1985). Calmodulin-dependent NAD kinase of human neutrophils. *Arch Biochem Biophys.* 237: 80-87.
- Zhang, M., Tanaka, T., and Ikura, M. (1995). Calcium-induced conformational transition revealed by the solution structure of apocalmodulin. *Nat Struct Biol.* 2: 758-767.
- Zhu, J. K. (2001). Plant salt tolerance. *Trends Plant Sci.* 6: 66-71.



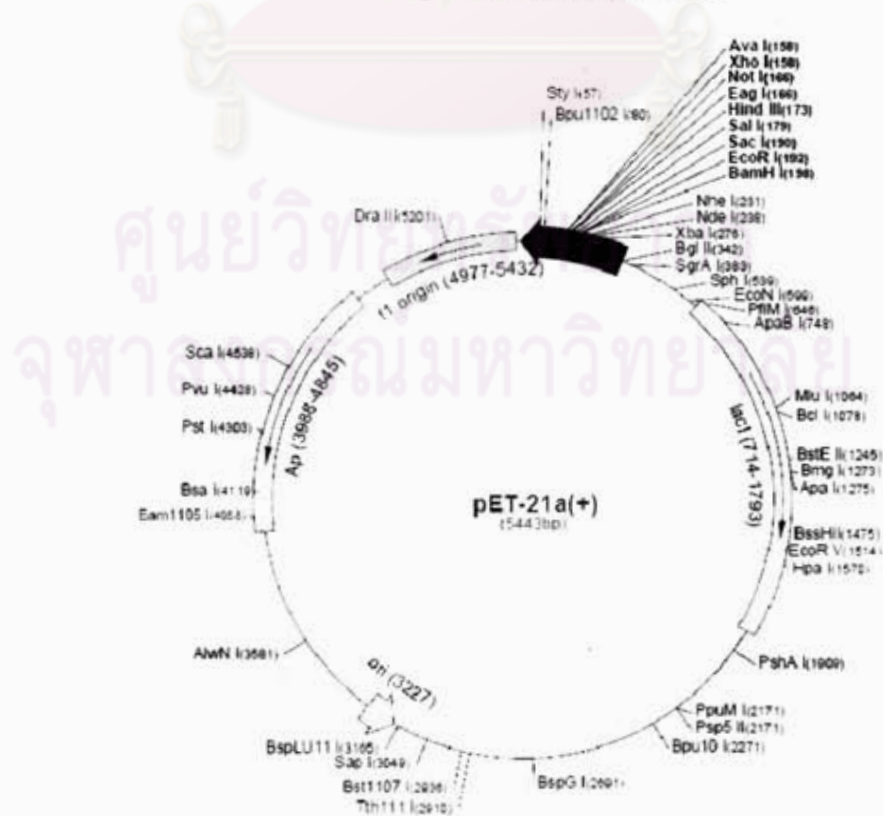
ศูนย์วิทยทรัพยากร
จุฬาลงกรณ์มหาวิทยาลัย

APPENDIX A

Circle map of pTZ57R/T Vector



Circle map of pET21a(+) Vector



APPENDIX B

Chemical solution

1. Determination of protein concentration

Bradford solution:

Coomassie Brilliant Blue (G250) 100 mg

Absolute ethanol 50 ml

Stir in a container protected from light for 2 hours.

Add 100 ml of 85% phosphoric acid.

Mix, and adjust volume to 1 L with dH₂O. Filter through Whatman No.1 pape and store the solution at room temperature in a brown glass bottle (usable for several weeks).

2. SDS-Polyacrylamide Gel Electrophoresis (SDS-PAGE)

2.1. Preparation for polyacrylamide gel electrophoresis

Reagents:

Resolving gel buffer 8X

Tris base 181.7 g

H₂O 250 mL

Adjust pH to 8.8 with conc. HCl.

Add water to a final volume of 500 ml.

Filter through 0.22 µm nitrocellulose.

Store at room temperature.

Stacking gel buffer 4X

Tris base 15.1 g

H₂O 150 mL

Adjust pH to 6.8 with conc. HCl.

Add water to a final volume of 250 ml.

Filter through 0.22 µm nitrocellulose.

Store at room temperature.

Acrylamide, 30% A: 0.8%B

Acrylamide 150 g

Bisacrylamide 4 g

Dissolve in a final volume of 500 ml (in H₂O)

Filter through 0.22 µm nitrocellulose.

Store at 4°C in a dark bottle.

Reservoir buffer 10X

Tris base 60.5 g

Glycine 288 g

Dissolve in a final volume of 2 L in H₂O.

Store at room temperature.

Before use, add 2 g of SDS (0.1% SDS) per 1 L of 1X reservoir buffer

20% (w/v) SDS

Prepare and store in a sterilized container.

Sodium dodecylsulfate 20 g

Dissolve in a final volume of 100 ml in sterile H₂O. Stir rapidly to dissolve completely.

Filter through a 0.22-µm nitrocellulose filter.

Store at room temperature.

Sample buffer 5X

1 M Tris-HCl, pH 6.9	60 μ l (60 mM)
glycerol	790 μ l (79%)
20% (w/v) SDS	100 μ l (2%)
2-mercaptoethanol	50 μ l
Bromophenol blue	1 mg

Store at -20°C in 1-ml aliquots.

Sample buffer 2X

Tris base	150 mg (120 mM)
glycerol	2 ml (20%)
20% (w/v) SDS	2 ml (4%)
2-mercaptoethanol	1 ml (28.8 mM)
H ₂ O	5 ml
Bromophenol blue	~20 mg

Store at -20°C in 1-ml aliquots.

10% (w/v) Ammonium Persulfate

Ammonium persulfate	0.5 g
---------------------	-------

Dissolve in a final volume of 5 ml in H₂O.

Store at 4°C ; prepare fresh every two weeks.

Staining solution

Coomassie Brilliant Blue R250	2.5 g
Methanol	500 ml
Glacial acetic acid	70 ml
H ₂ O	430 ml

Dissolve with rapid stirring.

Store at room temperature

Destaining solution

Methanol 100 ml

Glacial acetic acid 70 ml

H₂O 830 ml

Store at room temperature.

Protocol:

1. Mix the following components listed in the table in a 125-ml flask.

Component	9%	10%	12.5%	15%
Acrylamide, 30%A:0.8%B	12	13.3	16.7	20
Resolving gel buffer 8X	5	5	5	5
20 % SDS	0.1	0.1	0.1	0.1
H ₂ O	22.7	21.7	18	14.7

2. Swirl the flask gently, then add:

10% Ammonium persulfate 200 μ l

TEMED 20 μ l

Swirl the flask gently to mix. Be careful not to generate too many bubbles.

Degas the solution for 1 minute.

3. Pipet the solution into the gel sandwiches to a level about 2 ml below the bottom of the teeth of the gel comb. Overlay the gels with H₂O. A sharp water-gel interface will appear under the H₂O layer when the gel has

polymerized. This step will take about 15-30 min. After the gel has polymerized, pour off the H₂O layer.

4. Prepare the stacking gel solution in a 50-ml flask as follow:

Acrylamide, 30%A:0.8%B	2.6 ml
Stacking gel buffer 4X	5 ml
20% SDS	0.05 ml
H ₂ O	12.3 ml
Swirl the flask gently Mix the components, then add:	
10% Ammonium persulfate	150 µl
TEMED	10 µl

Swirl the flask gently to mix. Be careful not to generate too many bubbles.

Degas the solution for 1 minute.

5. Swirl the flask gently to mix. Fill the tops of the gel sandwiches with the stacking gel mixture. Insert the well-forming combs into the gels. Taking care not to introduce bubbles under the “teeth”. Allow the gels to set for at least 1 hr. They may be stored at 4°C in a plastic bag containing wet pieces of paper before using.
6. These gels should be run at 1 to 2 W (~30-50 V), on the constant power setting until the dye completely enters the stacking gel then increase the power to 3-4 W (~100-120 V). Once the dye completely enters the resolving gel, decrease the power to 2-3 W (50-100 V).
7. At the end of the run, turn off the power supply, remove the gel from the apparatus, and discard the upper reservoir buffer. Gently pry apart the

glass plates, invert the glass plate to which the gel has adhered over a plastic box containing ~100-200 ml of Staining solution, and tease one corner of the gel off the plate. Allow the gel to gently fall off the plate. Cover the box and stain the gel for 1 to 2 hrs at room temperature with gentle shaking.

8. After staining, pour off the used Coomassie blue solution, rinse the gel briefly with water. Then, incubate the gel in several hundred ml of Destaining solution. With gentle shaking, until protein bands are readily visible.

3. Native polyacrylamide gel

3.1. Preparation for polyacrylamide gel electrophoresis

Reagents:

Resolving gel buffer 8X

Tris base	181.7 g
H ₂ O	250 mL

Adjust pH to 8.8 with conc. HCl.

Add water to a final volume of 500 ml.

Filter through 0.22 μ m nitrocellulose.

Store at room temperature.

Stacking gel buffer 4X

Tris base	15.1 g
H ₂ O	150 mL

Adjust pH to 6.8 with conc. HCl.

Add water to a final volume of 250 ml.

Filter through 0.22 μm nitrocellulose.

Store at room temperature.

Acrylamide, 30% A: 0.8%B

Acrylamide 150 g

Bisacrylamide 4 g

Dissolve in a final volume of 500 ml (in H_2O)

Filter through 0.22 μm nitrocellulose.

Store at 4°C in a dark bottle.

Reservoir buffer 10X

Tris base 60.5 g

Glycine 288 g

Dissolve in a final volume of 2 L in H_2O .

Store at room temperature.

3.2. Native-PAGE

7% Separating gel

distilled water 3.487 ml

30% (w/v) Acrylamide solution 1.4 ml

Separated gel buffer 8X 0.75 ml

10% Ammonium persulfate 0.36 ml

TEMED 3 μl

4.0% Stacking gel

distilled water 1.214 ml

30% (w/v) Acrylamide solution 0.27 ml

Stacking gel buffer 4X	0.5 ml
10% Ammonium persulfate	0.015 ml
TEMED	1 μ l

5x Sample buffer

1 M Tris-HCl pH 6.8	0.6 ml
Glycerol	0.5 ml
1% Bromophenol blue	0.1 ml
distilled water	0.2 ml

One part of sample buffer was added to four parts of sample.

3.3. Electrophoresis buffer, 1 litre

(25 mM Tris, 192 mM glycine)

Tris (hydroxymethyl)-aminomethane	3.03 g
Glycine	14.40 g

Dissolve in distilled water to 1 litre. Do not adjust pH with acid or base (final pH should be 8.3). Add 1 mM DTT 0.1 mM ATP before use.

4. NAD kinase assay

Reagents:

The standard assay mixture (1 ml)

	+Ca/-CaM	-Ca/+CaM	+Ca/+CaM	-NAD	Final conc.
1 M Tris-Cl (pH7.9)	50 μ l	50 μ l	50 μ l	50 μ l	(50 mM)
100 mM ATP	40 μ l	40 μ l	40 μ l	40 μ l	(4 mM)
100 mM NAD	40 μ l	40 μ l	40 μ l	-	(4 mM)
1 M MgCl ₂	6 μ l	6 μ l	6 μ l	6 μ l	(6 mM)
10 mM CaCl ₂	110 μ l	-	110 μ l	110 μ l	(2.2 mM)
25 μ M recombinant CaM	-	12 μ l	12 μ l	12 μ l	(300 nM)
H ₂ O	754 μ l	852 μ l	742 μ l	782 μ l	

KNO_3	283.0 g	(2,830 mg/l)
----------------	---------	--------------

100X NB Sulfate stock 1 L

$\text{MgSO}_4 \cdot 7\text{H}_2\text{O}$	18.5 g	(185 mg/l)
$\text{MnSO}_4 \cdot \text{H}_2\text{O}$	1.0 g	(10 mg/l)
$\text{ZnSO}_4 \cdot 7\text{H}_2\text{O}$	200 mg	(2 mg/l)
$\text{CuSO}_4 \cdot 5\text{H}_2\text{O}$	2.5 mg	(0.025 mg/l)

100X NB Halide stock 1 L

$\text{CaCl}_2 \cdot 2\text{H}_2\text{O}$	16.6 g	(166 mg/l)
KI	75.0 mg	(0.75 mg/l)
$\text{CoCl}_2 \cdot 6\text{H}_2\text{O}$	2.5 mg	(0.025 mg/l)

100X NB PBMO stock 1 L

KH_2PO_4	46.0 g	(460 mg/l)
H_3BO_3	300 mg	(3 mg/l)
Na_2MoO_4	25.0 mg	(0.25 mg/l)

100X NB NaFeEDTA stock 1 L

$\text{FeSO}_4 \cdot 7\text{H}_2\text{O}$	2.78 g	(27.8 mg/l)
Na_2EDTA	3.78 g	(37.8 mg/l)

Nicotinic acid stock (1 mg/ml)

Dissolve 100 mg of nicotinic acid in sterilized deionized H₂O, adjust volume to 100 ml. Filter sterilize the solution.

Pyridoxine stock (1 mg/ml)

Dissolve 100 mg of pyridoxine in sterilized deionized H₂O, adjust volume to 100 ml. Filter sterilize the solution.

Thiamine stock (10 mg/ml)

Dissolve 1 g of thiamine in sterilized deionized H₂O, adjust volume to 100 ml. Filter sterilize the solution.

Mix the followings:

		<u>Final concentrations</u>
100X NB Nitrate stock	10 ml	
100X NB Sulfate stock	10 ml	
100X NB Halide stock	10 ml	
100X NB PBMO stock	10 ml	
100X NB NaFeEDTA stock	10 ml	
Myo-inositol	100 mg	(100 mg/l)
Nicotinic acid stock (1 mg/ml)	1 ml	(1 mg/l)
Pyridoxine stock (1 mg/ml)	1 ml	(1 mg/l)
Thiamine stock (10 mg/ml)	1 ml	(10 mg/l)
2,4-D stock (1 mg/ml)	2 ml	(2 mg/l)
Casein hydrolysate	300 mg	(300 mg/l)
L-Proline	500 mg	(500 mg/l)
L-Glutamine	500 mg	(500 mg/l)
Sucrose	30 g	(30 g/l)

Adjust pH to 5.8.

Add H₂O to 1 L.

Autoclave.

6. Limpinuntana's nutrient solution

Growing rice

Reagents:

Limpinuntana's solution

Final concentrations (1X)

300X Solution A (1 L)

KNO ₃	30.333 g	(0.10 g/L)
------------------	----------	------------

Ca(NO ₃) ₂ ·4H ₂ O	47.230 g	(0.16 g/L)
--	----------	------------

300X Solution B (1 L)

MgSO ₄ ·7H ₂ O	12.324 g	(41 mg/L)
--------------------------------------	----------	-----------

NH ₄ H ₂ PO ₄	11.502 g	(38 mg/L)
--	----------	-----------

NaCl	16.577 g	(55 mg/L)
------	----------	-----------

300X Solution C (1 L)

FeSO ₄ ·7H ₂ O	6 g	(20 mg/L)
--------------------------------------	-----	-----------

Na ₂ EDTA	8 g	(27 mg/L)
----------------------	-----	-----------

300X Solution D (1 L)

MnCl ₂ ·4H ₂ O	0.4323 g	(1.44 mg/L)
--------------------------------------	----------	-------------

H ₃ BO ₃	0.342 g	(1.14 mg/L)
--------------------------------	---------	-------------

Na ₂ MoO ₄ ·2H ₂ O	0.0075 g	(0.025 mg/L)
---	----------	--------------

ZnSO ₄ ·7H ₂ O	0.0264 g	(0.088 mg/L)
--------------------------------------	----------	--------------

$\text{CuSO}_4 \cdot 5\text{H}_2\text{O}$ 0.0117 g (0.039 mg/L)

1X Limpinuntana's solution (300 ml)

Mix solution A, B, C and D together (1 ml each), then add deionized water to 300 ml.

Autoclave.



ศูนย์วิทยทรัพยากร
จุฬาลงกรณ์มหาวิทยาลัย

BIOGRAPHY

Miss Thunchanok Dumrisuk was born on December 12, 1983 in Bangkok. She graduated with the degree of Bachelor of Science from the Department of Biology, Faculty of Science, Silpakorn University in 2005. She has studied for the degree of Master of Science at the Department of Biochemistry, Chulalongkorn University since 2006.



ศูนย์วิทยทรัพยากร
จุฬาลงกรณ์มหาวิทยาลัย